EXPERIMENTAL STUDY OF SHEAR FLOWS AND CONVECTIVE HEAT TRANSFER CHARACTERISTICS OF GRANULAR MATERIALS

Thesis by

James Scott Patton

In Partial Fulfillment

of the Requirements for the Degree of

Doctor of Philosophy

Division of Engineering and Applied Science

California Institute of Technology

Pasadena, California 91125

1985

(Submitted May 24, 1985)

To My Mother, Father

and Brother

Acknowledgements

I would like to thank my advisors, Professors Rolf Sabersky and Christopher Brennen for their constant support and encouragement both in my academic work and my personal life. I would also like to thank Union Carbide and the NSF for their financial support of my research.

Several people made contributions to the completion of this work. Fred MacDonald and Elmer Szombathy helped me build the experimental apparatus and gather data. Susan Rosik and Gerald Zeininger both assisted me in the majority of the experimentation. Madeline Haddad, Cecilia Lin and especially Susan Berkley all worked very hard to complete this manuscript. Professors Francis Clauser and James Knowles also contributed valuable input in the course of the investigation. A special thanks is in order for Dr. Charles S. Campbell who encouraged and supported me from the time I entered Caltech.

Several colleagues also helped in the course of this investigation. Eric Matthys, Harri Kytomaa and, Luca d'Agustino were always available to discuss problems related to my work. Steve Toner, Mike Chobatov, Paul Burridge, Jason Wakugawa and Duane Smith also contributed many helpful discussions.

I would also like to thank several of my friends for their help during my years at Caltech. Michael Osborn and Tim Lang were always understanding and supportive of my work. Dean Scammahorn, Angela Gin and Terri and Michael Cowdrey also gave me a great deal of encouragement

and always made me feel good about my studies.

No one was more instrumental in helping me complete my doctorate degree than Melinda P. Lum. I will always be indebted to Melinda for her unselfish caring and encouragement. To her goes my deepest thanks.

I would especially like to thank my Mother, Father, and Brother for their support during my academic studies. Their high ambitions inspired me throughout my life and to them I dedicate my thesis.

ABSTRACT

An experimental study of granular material shear flows and convective heat transfer characteristics are presented in this investigation. A rectangular chute was used to obtain the results. The experiments were conducted with two sizes of glass beads. In addition, some information was obtained on the shear stress of polyethylene pellets.

The bulk flow properties are used to evaluate the wall shear. The development of a method for determining the bulk density allowed for more accurate calculation of the flow quantities. A derivation of a compressible open channel equation is given for determining the wall shear. The wall shear is presented in terms of several forms of the Froude Number and solid fraction. The experimental results show that the friction coefficient (the ratio of the shear stress to the normal stress) is not a constant but increases with the Froude Number. The presentation of the wall shear as a function of a wide range of solid fractions is the first experimental work that can be directly compared to analytical and computational investigations.

The convective heat transfer properties of flowing granular materials were investigated by examining the flow over a flat heating plate. The method for determining the bulk density of the flow also proved revealing for the heat transfer studies. By using this method, a unique curve for each material was produced in terms of a special Nusselt Number and Peclet Number. The results clearly show that the Nusselt Number

reaches a maximum and then decreases for higher values of the Peclet Number. A derivation for convective heat transfer to a flowing granular material is given to predict the heat transfer properties over a wide range of flow conditions.

TABLE OF CONTENTS

LIST OF FIGURES

NOMENCLATURE

b	chute width
c	cohesion between particles
C_f	friction factor
c_p	specific heat
d	particle diameter
f	body force
$f_{ij}(\nu)$	unknown functions of the solid fraction
$f(\lambda)$	unknown function of the linear concentration
Fr^{*2}	square of the Froude Number (referred to as the Froude Number in the text) ; $\frac{U^2}{ghcos(\theta)}$
$Fr^{*2'}$	square of the Froude Number multiplied by $(\frac{d}{h})$
Fr^{*2}_{ν/ν_c}	densinometric Froude Number; $\frac{U^2}{ghcos(\theta)}(\frac{\nu_c}{\nu})$
$(Fr^{*2}_{\nu/\nu_c})^*$	densinometric Froude Number multiplied by $(\frac{d}{L})(\frac{k}{k_g})$
g	gravity
h	depth of flow
h	film coefficient

h_s	film coefficient defined by Sullivan and Sabersky (1975)
k	thermal conductivity
k_g	thermal conductivity of the interstitial fluid
L	length between the two parallel plates in the density gauge
L	length of the heating plate
$\dot{m}$	mass flow rate
M	mass of material captured during a density test
N	Bagnold Number
Nu_L	Nusselt Number based on L; $(\frac{hL}{k})$
$\overline{Nu_d^*}$	granular Nusselt Number; $\frac{hd}{k_g}$
P	normal stress
P	hydrostatic pressure
P_{yy}	normal stress
Pe_L	Peclet Number based on L; $(\frac{UL}{\alpha})$
Pe_L^*	granular Peclet Number; $(\frac{k}{k_g})^2 (\frac{d}{L})^2 \frac{UL}{\alpha}$
Pr_t	"turbulent" Prandtl Number; $\frac{\varepsilon}{\varepsilon_h}$
q''	heat flux

Re	Reynolds Number
S	shear force
St	Stanton Number; $\frac{h}{\rho c_p U}$
T	temperature
T_{11}, T_{22}	normal stresses
U	bulk velocity
u	velocity
$\frac{du}{dy}$	shear rate
α	thermal diffusivity
β	experimental constant accounting for the sidewall contribution to the total shear stress
β	experimental constant in equation 4.3
δ	length
ε	turbulent viscosity
ε_h	turbulent diffusivity
λ	linear solid fraction
μ	interstitial fluid viscosity
μ	friction coefficient

ρ	density
ρ_f, ρ_g	density of the interstitial fluid
τ	shear stress
τ_w	wall shear stress
τ_{xy}	total shear stress
τ_{xy}^{o}	Mohr-Coulomb shear stress
τ_{xy}^{*}	rate-dependent shear stress
σ_{ii}	normal stresses
σ_{ij}	shear stresses
ψ	internal friction angle
ψ_d	dynamic friction angle
θ	chute angle
ν	solid fraction
ν_c	critical solid fraction

Superscripts

$( )'$	fluctuational component
$\overline{( )}$	average value

Subscripts

$( )_w$	evaluated at the wall
$( )_o$	evaluated at y = 0
$( )_\delta$	evaluated at y = delta
$( )_f$	fluid
$( )_p$	evaluated at the plate

Special Notation

$I\!P$	wetted perimeter

CHAPTER 1

INTRODUCTION

The term "granular material" is the name given to a group of particles that are no longer treated as individual entities but are treated as a bulk. This bulk assembly of particles is considered a continuum with its own characteristic properties which might be quite different from the properties of the individual particles. The study of the flow characteristic and convective heat transfer properties of several types of granular materials will be the subject of this thesis. In the shear flows which will be considered any interstitial fluid effects (the effects of the air between the particles to the overall shear) will be neglected, but it will be seen that the interstitial fluid plays a major role in the convective heat transfer of the material.

A granular material may exhibit three distinct states depending on the flow conditions of the material. When a granular material is at rest, the individual particles are in contact with one another and at each point of contact there will be a resistance to both normal and tangential motion. The fact that there is this resistance to motion can make these group of particles act as a single solid. Of course these particles are not capable of sustaining a large tangential stress at these contact points, but certain flow conditions can make the material act as if it were a solid block. Once the material has been forced to the point that the contact resistance between particles is no longer capable of resisting the external force that is causing the added stress throughout the material, the

material will yield. In such a case, the material will develop shear between layers of particles and the equivalent of a liquid shear flow can occur. If the material is even more violently distorted, the individual particles will undergo large fluctuations causing the material to dilate. This type of flow is similar to that of a gas and is, in fact, a compressible flow. Thus, the evaluation of granular material is quite varied in nature. All three of the flow regimes mentioned above will be examined in this paper.

The need for better understanding the flow and convective heat transfer characteristics of a granular material has been motivated by both the academic and the industrial communities. The study of the shear flows of granular materials can help the understanding of the mechanisms that control such physical phenomena as land slides and even the interactions between the rings of Saturn. In the industrial environment, the transportation of granular materials is necessary in the manufacture of plastics and dry chemicals. With a better understanding of the basic flow characteristics of granular materials, more efficient transportation of granular materials can be developed with a savings to the producer and consumer. Many manufacturing processes for granular materials, such as granular detergents, are chemical processes that require elevated temperatures. These materials need to be cooled before they can be packaged. A better understanding of the convective heat transfer to these materials can reduce the time and energy requirements for the cooling process and thus reduce the

manufacturing costs. These are only a few of the examples of the need for further understanding of the characteristics of granular materials.

The present study is divided into two basic parts. First, the flow characteristics of two sizes of glass beads and of polyethylene pellets will be studied. The results of the shear flows of these materials in open channels will be analyzed. Next, the heat transfer of the two sizes of glass beads will be studied and attempts will be made to relate the convective heat transfer of these materials to the flow characteristics. The appendices will include a discussion of possible problems with the measurement techniques used to evaluate the shear, as well as of other experimental errors and possible reasons for the trends in the shear of the materials. An analytical model also will be presented that will attempt to give a correlation between the flow parameters and the heat transfer of a granular material.

CHAPTER 2

REVIEW OF PREVIOUS WORKS

2.1 Bagnold's Contribution to Shear Flows of Granular Materials

The modern study of shear flows of granular materials is attributed to Bagnold (1954, 1956, 1966). His studies were concerned with the flow of both fluid - solid mixtures and dry non-cohesive solids. Bagnold found that the flows could be divided into three distinct regimes. The classification of the flow regime relies on what Hill (1966) named the Bagnold Number which is defined as;

$$N = \frac{\sqrt{\lambda}\rho_f d^2(\frac{du}{dy})}{\mu}$$

where:

N is the Bagnold Number;

λ is the "linear concentration" of particles;

ρ_f is the interstitial fluid density;

d is the solid particle diameter;

$\frac{du}{dy}$ is the shear rate; and,

μ is the interstitial fluid viscosity.

The "linear concentration" may be related to the solid fraction in the following way;

$$\nu = \frac{\nu_m}{(1 + \frac{1}{\lambda})^3}$$

where:

ν_m is the maximum solid fraction (for solid spheres, $\nu_m = .74$);

ν is the solid fraction; and,

λ is the "linear concentration".

Bagnold determined that depending on this non-dimensional number, N, the flow could be considered either macro-viscous, transitional, or grain inertia dominated. The macro-viscous regime is characterized by the dominance of the interstitial fluid and/or low shear rates and, therefore, the shear is linearly related to the shear rate. The grain-inertia regime is generally characterized by high shear rates with minimal interstitial fluid effects. Bagnold determined that if $N < 40$ the flow could be considered "macro-viscous" and if $N > 450$ then the flow could be considered "grain-inertia", otherwise the flow is transitional.

The basic form for the shear and normal force that has been applied to granular material flows also was originally proposed by Bagnold. The form for normal stress is as follows:

$$P = \rho_p f(\lambda) d^2 (\frac{du}{dy})^2 \cos(\psi_d)$$

where:

P is the normal stress;

ρ_p is the particle density;

λ is the linear concentration;

$f(\lambda)$ is an unknown function of λ;

$\frac{du}{dy}$ is the shear rate;

d is the particle diameter; and,

ψ_d is an unknown dynamic friction angle.

The grain shear stress is;

$$\tau = P \tan(\psi_d)$$

where:

τ is the shear stress;

P is the normal stress; and,

ψ_d is an unknown dynamic friction angle.

Bagnold's work has remained the standard in the investigation of shear flows of granular materials. Others have improved on his initial work and theories, but his effort is still regarded as the principal groundwork in the field.

2.2 **Recent Experimental Studies of Granular Flows**

Hoppers have been an important industrial device for generations. Even though hoppers have been widely used, the accurate prediction of simple flow parameters for these devices is still a problem that has not been completely solved. The seemingly simple nature of the flow made theoriticians believe that a hopper should be a good starting point for analyzing the shear flows of granular materials. They soon found that even this simple flow was difficult to model, and further efforts to examine these flows experimentally were undertaken.

Sullivan (1973) used the Jenike and Shield (1959) model to give a general solution to the flows in hoppers. This model is based on the soil mechanical evaluation of the dynamic friction coefficient and is generally represented as follows;

$$|S| = c + P \tan(\psi)$$

where:

S is the shear force;

P is the normal pressure;

c is the cohesion; and,

ψ is the internal friction angle.

Jenike and Shield (1959) used the above condition and assumed no cohesion. This assumption means that the ratio of the shear stress to the

normal stress is directly related by the internal friction angle. The evaluation of the stresses with the above assumptions produced the following relation that had to hold in a flowing medium:

$$\left[\frac{(\sigma_{xx} - \sigma_{yy})^2}{4} + \sigma_{xy}^2\right]^{1/2} \leq \sin(\psi)\{\frac{\sigma_{xx} + \sigma_{xy}}{2}\}$$

where:

σ_{xx} is the normal stress on the xx plane;

σ_{yy} is the normal stress on the yy plane;

σ_{xy} is the shear stress on the xy plane; and,

ψ is the internal friction angle.

Brennen and Pearce (1978) were able to use this expression along with a perturbation technique to predict the mass flow rate in a two-dimensional hopper. Their results compared well with the actual mass flow rate of a small experimental hopper. (However, in a later experimental study with a large industrial two-dimensional hopper the author found the equations set forth by Brennen and Pearce (1978) to be inadequate to predict the proper mass flow rate).

Nguyen, Brennen and Sabersky (1979) expanded the results of Pearce and Brennen to include conical hoppers. The same general form of the stresses was assumed but, Nguyen, et al. wrote the results in cylindrical coordinates. The same perturbation technique was used and similar results as those of Pearce and Brennen were given. Nguyen, et al. also

compared their results to small experimental conical hoppers with good success. Nguyen (1979) did extensive experimental studies of the flow regimes in hoppers. He mapped the regions where the material in the hopper could be considered completely flowing and the conditions when one might expect to find the material against the hopper walls to be stagnant. These stagnant regions should be avoided in practice, especially when the material in the hopper is perishable.

Couette Flow devices have also been used to study the shear flows of granular materials. Savage and Sayed (1982) used an annular shear cell to study the stresses developed during high shear rate experimentation. From these experiments they were able to show a relationship between the shear stress and the solid fraction, and the normal stress and the solid fraction. These experiments were the first detailed works since Bagnold's that took into account the change in the solid fraction as a function of the stresses in a shearing granular material. The annular shear cell that they used for the experimentation had rough walls; thus, the no slip condition could be assumed. They also assumed that the material was shearing throughout the depth of the material which corresponds to a simple shear flow.

Hanes and Inman (1984) performed similar experiments to those done by Savage and Sayed (1982). A Couette flow device was used to study the rapid shearing of both a dry granular material and granular materials with interstitial fluid effects. Hanes and Inman used a talcum

powder on the sidewalls of the Couette Flow device to examine the depth of the shear layer during the dry granular flows. The portion of the flow which did not shear would show no smearing of the talcum and so a more accurate relationship between the shear stress could be determined than in the experiments performed by Savage and Sayed. The results of Hanes and Inman were not very different from Savage and Sayed and the results were presented in a similar manner.

Campbell and Brennen (1985a) used a computer simulation as the means of examining the shear flows of granular materials in a Couette Flow configuration. The assumptions that were used to simulate the flow were that the collisions between particles and collisions of particles with the wall were inelastic. It was further assumed that during a collision, the relative velocities between the contact points were zero. This corresponds to fully rough surfaces. The results that were developed by using this method for investigation gave new insight into the behavior of dry granular materials at very low solid fractions. Campbell and Brennen were able to make movies of the computed flows by allowing the computer to draw the control volume every few seconds and taking single frame pictures of each drawing. This procedure allows the visual examination of the shear flow which gives insight into the mechanisms involved with these granular shear flows.

Theoretical models for the shear flow of cohesionless granular materials are also used to predict the important parameters for these flows.

Savage and Jeffrey (1981) developed a stress tensor in a granular material flow and assumed that binary collisions were the main mechanism for transport of momentum in the flow. The assumption of no-slip, a Maxwellian velocity distribution and a spatial pair distribution was also assumed in their model. The ratio of the characteristic mean shear velocity to the particle fluctuational velocity; R, was a parameter developed for the presentation of their results. When the parameter $R << 1$, the flow may be considered to be a fluidized bed. If $R >> 1$ then the flow may be described as the Bagnold granular-viscous flow and for the case when $R \sim 1$, the flow may be considered a dry granular flow. Scheiwiller and Hunter (1984) attempted to use the equations derived by Jenkins and Savage (1983) to formulate and numerically solve gravity driven flows down chutes.

Lun, Savage, Jeffrey and Chepurniy (1984) developed two models for the rapid shear flow of granular materials. The first model is for the shear flow of granular materials in a Couette flow configuration with an arbitrary coefficient of restitution. This model follows the Savage and Jeffrey (1981) approach and used the results to compare to other theoretical models, the Enskog dense gas theory and experimental results. The second model follows the Chapman-Enskog approach for a dense gas model with the exception that the Boltzman equation for a gas may not be applicable. Lun and Savage (1985) used a similar approach to predict the simple shear flow of rough particles. The results are similar to Lun et al., but not as applicable to direct comparison with

experimental results. Hui and Haff (1984) used the equation of motion with specially derived physical properties, which are dependent upon the fluctuational velocities in the flow field, to determine the flow of granular materials in a vertical channel. The theoretically and numerically derived works presented above all assume a no-slip wall condition. This assumption makes the theoretical work easier to determine but the practical applications usually have a slip condition associated with the flow; thus, the direct comparison between theoretical results and practical problems are limited.

The flows of granular materials in chutes are the most directly applicable to the present work. Takahashi (1937) performed some of the first experimentation with a chute flow. Takahashi used a wooden chute and sands to study the flow characteristics of granular materials. He gives a detailed account of the bulk velocity as a function of the chute angle and made analogies between the laminar and turbulent flow regimes in Newtonian fluids and the flow regimes that are produced in granular material flows. Ishida, Hantano, and Shirai (1980) performed experiments in an aerated inclined chute. Their results included the variations of the flow velocity through the depth of flow. These measurements were made by using a fiber optic probe. Ishida, et al. were able to identify five distinct flow regimes and their results show the effects of the layer height, of different particles, and of the air velocity on the overall flow characteristics. Campbell, Brennen and Sabersky used the open channel equations to interpret the flows of granular materials in a chute. They

were able to characterize the flows as either sub-critical or super-critical depending on the local Froude Number.

Sayed and Savage (1982) developed a shear relationship for the flow down an inclined plane. In their work the shear stress is arbitrarily split into two parts. The first, a rate-independent part of the shear was assumed to follow the Coulomb friction law. The second, a rate-dependent part was selected to be similar to the Bagnold relationship for a dry, cohesionless granular material. These two shear stress terms were simply added together to form the complete shear stress and had the following form for a simple shear flow;

$$\tau_{xy} = \tau^{o}_{xy} + \tau^{*}_{xy}$$

where:

τ_{xy} is the total shear stress;

τ^{o}_{xy} is the Mohr-Coulomb contribution to the shear stress; and

τ^{*}_{xy} is the rate-dependent shear stress.

Sayed and Savage also gave detailed accounts of the sidewall contributions to the total shear stress acting at a given cross-section.

Ridgeway and Rupp (1970) used a horizontal knife-edge to skim off different levels of the flow in a rectangular chute. In this way, they were able to derive the density profile, assuming a uniform velocity profile. Ridgeway and Rupp's experiments were at fairly small depths of flow but even though the depths were small, they found that the density varied

through the depth of flow. They also found that the density decreased as the material moved down the chute. (The present work also shows this trend). Augenstein and Hogg (1974) used the trajectory of the material leaving the chute to determine the velocity and Augenstein and Hogg (1978) determined the velocity distribution and the effects of slip at the surface for different roughnesses. Bailard (1978) combined the experiments performed by Ridgeway and Rupp and Augenstein and Hogg and extensively evaluated the flow for three different diameters of sand. Bailard used the knife-edge technique used by Ridgeway and Rupp to determine the density profile through the depth of flow and the trajectory of the material leaving the chute to determine the velocity profile through the depth of flow as did Augenstein and Hogg. Bailard found that the material reached a uniform state in his chute for a wide variety of flows. (The present work also shows that the flow of glass beads appears to reach a uniform state in the experimental chute).

Campbell and Brennen (1985b) used a computer simulation to model the flow of granular materials in an inclined chute. Campbell and Brennen used the same boundary conditions that were used for their Couette flow simulations which produced uniform flows for all chute angles. The computer simulation produced results of density variations, velocity variations and "temperature" variations for each flow condition. The "temperature" of a granular material is defined as the appropriate sum of all fluctuational velocities. These variables are out of the scope of detailed experimental instrumentation at this point; thus, the computer

simulation used by Campbell and Brennen gives an insight into the flows of granular materials that can not as yet be determined experimentally. Movies were taken of the calculated flows by allowing the computer to draw particles in a fixed control volume every few seconds and taking a single frame exposure of each picture drawn by the computer screen.

An excellent review article on the mechanics of granular material flows was written by Savage (1984). All of the previously mentioned works as well as some which are not included can be found in this review article. The author extensively referred to this review article while working on the shear flows of granular materials and found the work to be both accurate and concise.

2.3 **Heat Transfer to Granular Materials**

There is very little experimental or theoretical work directly related to the convective heat transfer to a granular material. There has been however, a great deal of work done on the heat transfer to a fluidized bed. The extent to which a fluidized bed can be related to the heat transfer to a granular material in an open channel flow is somewhat limited, but some of the general trends that appear in heat transfer in fluidized beds also appear in the heat transfer to granular materials in open channels.

Yoshida, Kunii and Levenspiel (1969) used the results by Toor and Marchello for mass transfer to model the heat transfer of solid-gas mixtures in the granular material. A simple experiment was performed to

test the developed model. The experiment consisted of a tube which was externally heated and contained granular material that could be injected with a gas to produce a fluidized bed. The experimentation showed reasonable results with the predicted values of the heat transfer coefficient from their model. In a similar experiment, Mickley and Trilling (1949) examined the heat transfer conditions at surfaces in contact with a gas-solid mixture when the solid was violently mixing. Mickley and Trilling's data show a general increase in the heat transfer coefficient with slight agitation of the bed, but with increased agitation, a maximum heat transfer coefficient is reached and by agitating the flow further, a decrease in the heat transfer coefficient is observed. Mickley and Trilling also gave the first realistic model for the unsteady heat transfer process by which heat is transfered between a fluidized bed and a heating surface.

Botterill and Williams (1963) produced a model for the unsteady heat transfer between a heated surface and a single particle with an interstitial gas as an active link between the surface and the particle. Botterill, Butt, Cain and Redish (1967) expanded this model to include two layers of particles to more accurately predict the heat transfer between a heating surface and a fluidized bed. Gabor (1970) used two methods to calculate the unsteady heat transfer to both a packed bed and a fluidized bed. The first uses a string of spheres with a general form of the differential equations for both the solid and gaseous phases of the process with some generalized boundary conditions, he then numerically

solves these equations for a particular configuration. The second model developed by Gabor assumes that the heat transfer between the solid and the gaseous phases may be modeled as a series of alternating gas-solid slabs. Both procedures give close agreement with one another and with experimental results.

Kubie and Broughton (1975) developed a model to predict the heat transfer coefficient in the vicinity of a heating plate in a fluidized bed. Their model uses a variation on a penetration theory but the results are not unlike those developed for the original penetration theory. The use of a residence time for a packet of material at the surface is used to quantitatively describe the heat transfer at the surface of the heating plate. The model gives good agreement with the data and in addition does not rely on any physically unrealistic boundary conditions to produce the stated results. Heyed and Klocke (1980) used experimental means to examine the heat transfer between a fluidized bed and a heating or cooling mechanism submerged in the bed. Their results show distinctly that the heat transfer from a heating or cooling element in a fluidized bed is a direct function of the gas velocity causing the fluidization. They determined the gas velocity at which the maximum heat transfer coefficient could be attained in a fluidized bed. (The gas velocity is directly related to the solid fraction since the gas velocity causes the fluidization of the system).

Donskov (1958a) examined the heat transfer from a round cylinder in

a gravity flow of a granular material. Donskov (1958b) extended this work to include bundles of pipes to simulate a granular material heat exchanger. Pearce and Sabersky (1977) performed similar experiments using a cylinder in a gravity device to study the heat transfer of a flowing granular material in a heat exchanger configuration. Syromyatnikov (1971) examined the heat transfer to a plate and a sphere submerged in a fluidized bed. In this study, Syromyatnikov used the standard procedure of assuming a bulk "porosity" for the value of the void fraction next to the immersed body. Tolamchev, Korolev and Syromyatnikov (1971) measured the porosity next to an immersed plate by means of a x-ray device. The results show a more meaningful relation between the heat transfer and the porosity since the actual value of the porosity of the material next to the plate is measured. (This technique could possibly be extended to the shear flows of granular materials to actually measure the solid fraction variations in a shear flow without penetrating the flow).

Muchowski (1980), and Muchowski and Mannchen (1980) examined the heat transfer of vibrated, stirred and packed granular beds at atmospheric pressure and under a vacuum. These papers gave insight into the effects of the interstitial fluid on the overall heat transfer of a granular bed. Their results showed a decrease in the heat transfer with decreases in the pressure.

Wunschmann and Schlunder (1980) used an agitator to study the heat

transfer of several different granular materials. They were also able to develop a theoretical model that proved to be in close agreement with their experimental data by introducing a concept of apparent resting time. Their theory predicted both the packed unagitated heat transfer and the moving packed heat transfer. Bauer and Schlunder (1978a, 1978b) were able to develop a model to determine the radial heat transfer with and without a gas flow. The model was compared to 2500 experiments with good agreement. This model is more versatile for practical applications since heat transfer with particles of different sizes can be predicted. Schlunder (1982) also published a very complete paper on the heat transfer to particles from both a heated plate and from particle to particle heat transfer. Schlunder uses several concepts developed by Martin (1981) to expand the developed results to mixed and fluidized beds.

Sullivan and Sabersky (1975) derived equations for the heat transfer of a flowing granular material. Their experimental set-up made use of a hopper with a submerged heating plate. The addition of an apparent thermal resistance between the heating plate and the granular material was used to modify the single phase convective heat transfer coefficient. By including this additional resistance, they were able to correlate their data with the predicted values from their equation for various granular materials.

The most directly applicable experimentation relating to the present

work was performed by Spelt, Brennen and Sabersky (1982). Spelt, et al. used the flow of a granular material in an open channel to test Sullivan and Sabersky's correlation for the heat transfer of a flowing granular material at much higher flow rates than were performed in the hopper used by Sullivan and Sabersky. Spelt, et al. found that the Sullivan and Sabersky's correlation fit the data well for the slow packed flows but was unable to predict the trends of the heat transfer when the flows became rapid. Spelt, et al. noted that the heat transfer began to decrease once a certain velocity had been reached and any additional increase in the velocity would cause further decrease in the heat transfer coefficient. Spelt, et al. were able to correlate their data in groups, each group corresponding to a different depth of flow.

CHAPTER 3

EXPERIMENTAL STUDY OF SHEAR FLOWS OF GRANULAR MATERIAL

3.1 General Comments

The study of the flows of granular materials is not unique to the academic environment. In fact, as mentioned earlier, much study of granular material flow has been motivated by industry since many materials are handled in granular form. In order to design effective equipment for this purpose it has become evident that there is a need for better understanding the basic relationships which govern these flows. It was this need which motivated both industry and academia to examine more closely the shear flows of granular materials.

Hoppers and chutes are the two basic types of gravity flow devices used to transport granular materials (see figure 3.1). Hoppers are characterized by tapered walls which funnel to an outlet point. Generally, a bin sits on top of a hopper and serves as an extra volume for holding more material than can be placed in the hopper alone. The hopper-bin configuration is generally used to store a material until transportation of the material is desired. A chute, which may be either enclosed (such as a pipe) or opened to the atmosphere (such as an open channel), is used to transport material from one point to another but is rarely used for storing material.

Since hoppers and chutes are widely used in industry, both have been studied rather extensively. Hopper flows are generally characterized by

low velocities and low shear rates. This makes the analysis of hopper flows a problem of Mohr-Coulomb friction rather than shear rate dependent friction. Although one might suspect that such a flow should be easily modeled, intrinsic properties of granular materials make this type of flow more difficult than might first be suspected. Several theoretical models have been developed making use of the Mohr-Coulomb yield criterion and many experimental studies of hoppers have been performed in an effort to understand these flows. A major drawback of the hopper as an instrument for understanding granular material flows is that the obtainable shear rates and variations of solid fractions are generally small. Even though these high density and low shear rate flows are important, it would be desirable to study flows which could cover a wider range of these parameters. In a chute flow on the other hand, it is relatively easy to obtain a wide variety of flow regimes. A low shear rate and high density flow may be accomplished by slip on the chute wall and a plug flow velocity profile through the material. In addition, many shear rates and densities are possible in a chute flow by varying simple quantities such as the mass flow rate or chute inclination angle. For this reason, a chute is preferable to a hopper for the study of a wider range of flow conditions of any granular material.

The chute allows a wider variety of flow regimes to be examined; however, with this versatility also comes several problems not experienced in hopper flows. The most obvious complication comes with the addition of an extra length scale corresponding to the depth of the flow. A hopper is

a device where all length scales are fixed for each experiment. Any variation in a hopper, such as exit diameter or hopper angle, are performed between tests. A chute may have a variation in the depth of flow as the material accelerates or decelerated down the length of the chute. Although this can be measured easily, control of this variable is quite limited. Another problem which arises in a rectangular chute that does not exist in a conical hopper is the addition of sidewall friction. Since the flow in a conical hopper is axisymmetric, the wall shear at any cross-section is uniform. However, a rectangular chute has an added sidewall friction which varies over the perimeter. This variation cannot be predicted accurately at present and, in fact, the general relationship between the friction and the flow quantities is not yet understood. Even though these complications pose a problem in the analysis of chute flows, the variety of flow regimes which may exist in a chute still makes it a desirable experimental apparatus for the basic study of the shear of granular material.

The use of a chute to study the shear flows of granular materials is not unique to this investigation A number of papers, including those by Augenstein and Hogg (1974), and Campbell (1982), as mentioned earlier, use chutes as the basis for their studies. The use of either rough or smooth walls is a consideration that must be examined. If, as done by Savage and Jeffrey (1981), one uses rough walls, it may be argued that a no-slip condition exists at the wall. A no-slip condition is desirable in the theoretical analysis of the flow. When a no-slip condition exists at the

wall, the shear rate becomes closely proportional to the average bulk velocity at a given cross-section. It is not obvious, however, a rough wall would result in shearing through the entire depth of flow. The existence of a stagnation region next to the wall is enhanced by a rough wall and so one can not be certain that shear is occurring at the wall. The smooth wall will have slip at the wall even though there may not be shear through the material. The smooth wall is the common configuration in most practical practical applications and smooth walls have been used in this study.

3.2 **Description of Apparatus**

The purpose of this paper is to add to the basic understanding of the flow and heat transfer characteristics of a granular material, and also to provide data which could be directly helpful to the designer. With these two goals in mind, a chute was chosen for all the experimental work presented in this paper.

The chute was made completely from aluminum, including the sidewalls. The reason for aluminum sidewalls rather than a transparent material, such as glass or lucite, was to minimize the electrostatic effects of the flow. Both Campbell (1982) and Spelt (1982) used lucite sidewalls so that the shearing region could be observed. By using lucite, however, they found that the only way to obtain repeatable results was to spray the lucite sidewalls with an anti-static glass cleaner. As their experiments were repeatable after the use of the cleaner, the effects of

static charge buildup by particle-particle and particle-wall shearing could not be ignored. Rather than constantly using a anti-static cleaner to suppress these electostatic effects, aluminum was chosen for all components of the chute to allow free flow of current through the device. In addition, all components of the experiment were grounded to a hot water line in the laboratory to assure no buildup of electrical potential by any component of the device due to the flow of the granular material.

The present experimental facility included a mechanical conveyor which constituted a major improvement over earlier installations. This conveyor allowed extended and undisturbed observations of the flow. Previous experimental works by Campbell, Savage, and others were limited to the amount of time it took to discharge their feed hoppers. This in general, meant the use of "small" chutes to assure that a steady flow had been achieved for their experimentations and to allow sufficient time for all the experimental data to be recorded before the material in their supply hopper had been exhausted. In the present work, the chute is 12 feet long and 1/2 foot wide (not small even by industrial standards) and the material in the feed hopper was continually replenished by the conveyor so that flows could be examined as long as needed. The use of a large chute also is more directly applicable to industry, because the scaling of these devices is not well documented.

The actual experimental facility is shown in figure 3.2. As previously mentioned, the chute is 12 feet long and 1/2 foot wide and has sidewalls

which measure 3/4 feet, all made from aluminum. The base of the chute was made by taking a channel beam and turning it upside down. A schematic of the chute is shown in figure 3.3. The channel beam base which served as the base of the chute was highly polished to remove any grooves or nicks caused by manufacturing and handling. The sidewalls (initially 1 foot high but 1/4 foot was used for fastening) were bolted to the channel beam and four spacers were placed 2 feet apart along the top of the sidewalls to assure a constant 1/2 foot cross-section throughout the entire width of the chute. The spacers also added rigidity to the chute configuration. A small chute intake hopper was designed to fit on the top of the chute at the inlet point. This chute intake hopper was designed to allow free flow of material into the chute at any angle of the chute, unlike the use of a hose which can choke as the chute angle varies. This chute intake hopper proved to be quite efficient and should be considered in the design of any hopper-chute configuration where the chute angle is allowed to vary. The chute was suspended by a pivot point on the bottom of the intake point of the chute and by a winch which was connected to the top of the outlet point of the chute and the ceiling of the lab. The winch allowed the chute to be varied from 16.5 to 40 degrees. A control gate was placed at the inlet of the test section of the chute to adjust flow conditions.

The conveyor was purchased from Omni-Lift Corporation which is located in Salt Lake City, Utah. The conveyor is 19'7" long from flange to flange and was designed to operate at a 75 degree incline. It is capable

of conveying course sand at a maximum flow rate of 70 tons per hour. In the experiments performed for this paper, a flow rate of approximately 40 tons per hour was produced using glass beads. The conveyor consists of a belt with integrally molded buckets. The belt is driven by a 10 HP three phase motor with a T.B. Woods adjustable speed control unit. The Omni-Lift conveyor proved to be durable and made performance of the experiments quite easy.

The conveyor discharges the material into an upper feed hopper. This hopper was constructed of sheet metal and is capable of holding approximately 250 lbs. of 100 $\frac{lb_m}{ft^3}$ material. A window was placed in the front wall of this hopper originally to visually track the level of the material in the hopper to make sure that the material did not overflow. Later this window was graduated to serve as a means of determining mass flow rates. A 6" pipe was connected to the top portion of a sidewall to prevent overflow. The conveyor outlet and hopper inlet were completely enclosed with a sheet metal enclosure and gaskets. Several holes were placed in the sheet metal enclosure and then covered with cloth to assure that a vacuum was not formed which could hamper the flow in the hopper. This hopper was supported by an 8-1/2 foot girder support which was constructed from 2"x2"x1/4" angle. This structure was bolted to the floor and also served as the support for the upper pivot point of the chute.

The exit of the chute discharged into a lower hopper which is capable of holding at least 1500 lbs. of 100 $\frac{lb_m}{ft^3}$ material. This lower hopper was

used to store the material and also was constructed from sheet metal. Great care was taken in the design of the hopper to assure a good fit with the conveyor. A slide gate was placed between this hopper and the inlet of the conveyor to serve as a flow control and to relieve back-pressure on the belt of the conveyor when the conveyor was started.

Because of the size of the experimental apparatus, a pit had to be excavated to accommodate the bottom of the conveyor and the lower hopper into. The pit measured 6 feet wide, 8 feet deep and 8 feet long. The walls of the pit were made from poured concrete with a 2 inch wide by 1 inch deep ridge around the top of the pit for wood planks to be placed. These planks made access to the chute during experimentation easier and also helped to avoid an accidental fall. Flanges were bolted into the sidewalls of the pit to support the lower hopper and a railing was placed around the entire pit for safety purposes.

The flow rate was measured by two means. First, as already described, the upper feed hopper was equipped with a graduated window and secondly, by a mass flow hopper (see figure 3.4). The mass flow hopper was capable of holding 100 lbs. of 100 $\frac{lb_m}{ft^3}$ material. This hopper was suspended from a beam and connected to the beam by a strain gauge. This beam was part of a structure which was placed on rails and was capable of moving in and out of the exit stream of the chute by means of a 3/4 horsepower three phase electric motor. Switches were placed in positions along the path of the structure so that a timer would

be activated as the device moved into the flow and deactivated as it exited the flow. A Hewlett Packard multimeter was used to measure the voltage output of the strain gauge. A trap door was placed in the bottom of the mass flow hopper so that after the weight of the material was measured, the door could be opened and the material would fall into the lower storage hopper. Both methods worked well but most measurements were taken using the first method described here.

Point probes were used to measure the depth flow of the material at 2 feet intervals down the chute (see figure 3.5). These point probes are exactly like those used by Campbell in his experimentation. The probes were mounted on aluminum supports which were tightened by thumb screws, thus allowing easy removal or repositioning during experimentation.

The final experimental apparatus was conceived and developed by the author of this work. This apparatus gave the first insight into the roll of the solid fraction in the characteristics of the flow and heat transfer of a granular material. Two parallel plates 14 inches apart were connected by a beam and the width of the were designed to fit snugly into the chute. By suddenly placing this into the flow, a mass of material is trapped and by measuring the mass of the trapped material, together with the knowledge of the flowing height, an average solid fraction at a given cross-section in the chute could be determined. This device is the sole most important contribution to the field of granular material flows

and heat transfer. A schematic of this device is shown in figure 3.6.

3.3 **Experimental Procedure for Shear Data**

The original procedure for obtaining data points was developed by Campbell in his open channel experiments. The use of a conveyor, however, made it possible to observe the flows for as long as necessary. There was no rush to obtain the measurements and simple observations of the flow could be performed without time constraints. This improvement made the experimentation much easier than in Campbell's case and the reliability and repeatability of the data was improved.

The experiments for this thesis are the first to give an insight into how changes in solid fraction influence the flow parameters. This was accomplished by placing the parallel plates into the flow as previously mentioned. The original assumption was that the solid fraction was constant for all flow conditions. A value of the solid fraction was chosen to be some critical state-ν_c. The use of the 3mm glass beads, however, made clear that this was far from true. The idea of placing the parallel plates into the flow was first used to test the constant solid fraction assumption. The results were conclusive. A variation of the solid fraction from the critical value, in some cases, was an order of magnitude or more. The consequences of these dramatic changes in solid fraction made it apparent that the equations used by Campbell and others needed to be modified to account for these variations.

The procedure for obtaining results for the shear flows was as follows:

i. Set a chute angle;

ii. Set a gate height;

iii. Allow a "steady flow" to develop;

iv. Measure the depth of the flow at the desired stations in the chute;

v. Measure the mass flow rate by either or both of the two methods available; and,

vi. Measure the average density at the desired stations in the chute.

The chute angle could be set from $16\frac{1}{2}$ to 40 degrees from the horizontal. The usual angles that were examined were $16\frac{1}{2}$, $17\frac{1}{2}$, 20, 25, 30, 35, and 40 degrees. The chute angle remained constant until the entire range of gate openings could be performed. The gate opening ranges were determined by the mass flow rate capability of the conveyor. The usual gate openings ranged from 1/2" to 3" for the large 3mm glass beads and 3/8" to 4" for the small .3mm glass beads. The gate generally was moved in 1/4" increments when the gate height was less than an inch and by 1/2" increments when the gate height was over an inch.

The measurement of the depths of the flow at the different stations in the chute were performed in the same manner as used by Campbell.

Four point probes were placed 2 feet apart with the upstream probe being 2.5 feet from the control gate. The depth of flow measurements for the small .3mm glass beads were attained quite easily and accurately. The point probes were lowered until a wake was observed in the flow. The probes were then adjusted until it was determined that the wake had just disappeared.

The height measurements for both sizes of glass beads were quite accurate when the solid fraction was high and the bulk velocity low. For the low solid fraction flows, however, these measurements were more difficult. Generally, a high value and a low value would be recorded and both would be used in reduction of the data.

The mass flow rate could be determined by two methods. The original design of the facility included a mass flow hopper. When a mass flow rate measurement was to be taken, this hopper was activated and moved into the flow by an electric motor. As this hopper moved into the flow, a timer was started. Once the hopper became full, the motor was reversed and the timer stopped. The hopper was suspended by a strain gauge and the amount of material in the hopper could be measured by a direct readout from the strain gauge. Thus, by knowing the amount of material in the mass flow hopper and the amount of time that the hopper was in the flow, the mass flow rate could be determined since it was assumed that the flow was steady. This method proved to be an accurate means for the measurement of the mass flow rate when the mass flow rates

were low. As the mass flow rate increased, the time that the hopper was in the flow became very short. To assure of the accuracy of the mass flow rate, another means for determining the mass flow rate was needed. The upper feed hopper was designed with a window so that the level of the material in the hopper could be monitored. This made it convenient to modify this hopper to develop another means of measuring the mass flow rate. The window was graduated so that once the conveyor filled the hopper to a desired amount, the conveyor was stopped and the time it took to discharge the material between two graduated marks on the window could be used to determine the mass flow rate, even at very high flow rates. Using both of these methods, an accurate measurement of the mass flow rate could be determined.

The solid fraction measurements were performed in a crude but simple way. Once the flow had been stabilized and the depth of flow measurements recorded, two parallel plates were jammed into the flow. The material which was trapped between the two plates was then weighed by raising the downstream plate while keeping the upstream plate firmly in place to hold back the upstream material. This allowed the trapped material to flow down the chute into a bucket that was placed at the outlet of the chute. The bucket was then weighed and the mass recorded. This procedure was then repeated at three different locations in the chute which were between the four point probes.

Granular jumps were generated to measure a wider range of flows. A

plate was placed into the flow near the exit of the chute causing a jump to propagate upstream until it reached the control gate. Once this condition was reached, the entire chute was sub-critical (Froude Number less than unity). This procedure allowed the study of very slow flows which are not usually characteristic of chute flows.

3.4 **Calculation of Flow Parameters**

The procedure that was just described allows the average quantities of the flow field to be determined at any cross-section. These techniques, however, do not allow the determination of local values, so local velocities and densities are not quantities which can be measured. It was believed that measurement of the average quantities would represent a first logical step in determining the characteristics of granular material flow and heat transfer.

The velocity at a given position in the chute was determined from the measurements of the mass flow rate, the depth of flow and the average density at a cross-section. Once a steady flow had been reached, the mass flow rate was obtained by weighing the mass that flowed through the chute in a given amount of time:

$$\dot{m} = \frac{measured\ mass}{measured\ time} \tag{3.1}$$

For steady flow, this mass flux may be related to other variables of the flow by the following equation;

$$\dot{m} = \rho\, U h b \tag{3.2}$$

where:

ρ is the bulk density;

U is the bulk velocity;

h is the depth of flow;

b is the chute width; and,

$\dot{m}$ is the mass flow rate.

The density of the flow is not easily determined. Since granular materials are made of individual particles, a volume sample of material contains both solid and air. The volume fraction of solid that occupies a given volume of material is known as the solid fraction and is generally denoted by ν. In practice, the mass rather than the volume of a given sample of material is measured. The density of a given sample may be written as;

$$\rho = \rho_p \nu + \rho_g (\nu - 1) \tag{3.3}$$

where:

ρ is the bulk density;

ρ_p is the solid density;

ρ_g is the density of the interstitial fluid; and,

ν is the solid fraction.

In almost all cases;

$$\rho_p \gg \rho_g$$

So that,

$$\rho \cong \rho_p \nu \tag{3.4}$$

By measuring the mass of material, the solid fraction can be determined;

$$\nu = \rho / \rho_p \tag{3.5}$$

or,

$$\nu = \frac{mass\ of\ material\ per\ unit\ volume}{density\ of\ the\ solid\ particles}$$

The determination of the solid fraction proved to be necessary for acceptable analysis of the flow. Figure 3.7, which is a graph of solid fraction as a function of depth of flow, shows the drastic changes that can occur in the solid fraction. The use of the density gauge as described earlier, made determination of the solid fraction possible. The solid fraction is then determined by the following equation;

$$\bar{\nu} = \frac{M}{\rho_p (bLh)} \tag{3.6}$$

where:

$\bar{\nu}$ is the average solid fraction;

M is the mass of material captured between the plates;

ρ_p is the solid density;

b is the width of the chute;

L is the distance between the plates; and,

h is the depth of flow.

Now that the average density at a given cross-section has been determined, the average velocity at that cross-section may be determined from;

$$\dot{m} = \rho_p \nu \, U h b$$

and (3.7)

$$U = \frac{\dot{m}}{\rho_p \nu \, h b}$$

or by using (3.4) one finds,

$$U = \frac{\dot{m} L}{M} \tag{3.8}$$

where:

U is the average velocity;

$\dot{m}$ is the mass flow rate;

L is the distance between the plates; and,

M is the mass of material captured between the plates

This relationship shows that the accuracy with which the velocity can be determined depends on the proper measurement of the mass flow rate

and the mass captured between the plates. The variation of velocity with mass flow rate, depth of flow and density are shown in figures 3.7, 3.8 and 3.9. The fact that these graphs are double valued is significant. These graphs emphasize the fact that these variables are interdependent. When the mass flow rate is held constant, the velocity, solid fraction and depth of flow vary in a manner that is not simply separable. As shown in figure 3.7, for example, for a given mass-flow rate the depth of flow changes a great deal without much change in the solid fraction. Once a certain depth of flow is reached, the solid fraction changes drastically without much change in the depth of flow. A minimum depth of flow is reached at some solid fraction and further reduction in the solid fraction causes the depth of flow to increase once again.

Similar results are seen in figures 3.8 and 3.9. By examining these graphs, three distinct zones may be defined. First, for a given mass flow rate when the velocity is low and the solid fraction is approximately equal to the value of the material in its resting state ν_c, the velocity varies linearly with the depth of flow. Next, when the solid fraction is low ($\nu \ll \nu_c$), the velocity decreases approximately linearly with the depth of flow. Finally, at the intermediate solid fractions, the velocity varies linearly with the solid fraction. These three zones must be connected in some way that includes the variations in all three parameters.

The fact that the solid fraction varies so dramatically shows that the assumption of a constant solid fraction used by Campbell and others was

not justified for certain flow conditions. The variations in solid fraction are equally as important as the variations in depth of flow or velocity. This means that the flow in a chute used to transport a granular material actually corresponds to a compressible fluid flow in an open channel. This concept may seem a bit unusual in the classical sense of fluid mechanics, but not when one considers that a granular material flow consists of discrete particles. When the solid fraction decreases, the fluctuation velocity, which causes this decrease, increases in a manner not unlike that in a gas. The fluctuation velocity is often referred to as the granular "temperature" (see Lun, et al. (1984)) but it must be remembered that no equation of state has been shown to exist for a granular material.

3.5 **Basic Flow Equations**

In the previous sections, it was shown that the basic quantities in the flow of a granular material may be measured or calculated. It was also shown that a variable solid fraction must be included in the flow equations. With this in mind, an equation for a compressible fluid flow in an open channel may be written. First, the integral form of the steady-state conservation of mass equation;

$$\frac{d}{dx}\{\int_0^h \rho u dy\} = 0 \tag{3.9}$$

where:

ρ is the bulk density;

u is the bulk velocity; and,

h is the depth of flow.

Now assume that ρ and u are independent of the depth of flow (no gradients in the y-direction),

$$u = u(x)$$

$$\rho = \rho(x)$$

and, therefore,

$$\frac{d}{dx}\{\rho u \int_0^h dy\} = 0$$

or, (3.10)

$$\frac{d}{dx}(\rho u h) = 0.$$

Now the integral form of the momentum equation may be written with the following assumptions:

i. Steady-state flow;

ii. Hydrostatic pressure;

iii. No variations in the flow parameters with depth of flow; and,

iv. No assumption of the form of the wall shear.

On this basis, one may write:

$$\rho u \frac{d}{dx}\{\int_o^h u dy\} = -\frac{d}{dx}\{\int_o^h P\, dy\} - \tau_w IP + \int_o^h (\rho g \cos\theta) dy \qquad (3.11)$$

where:

ρ = $\rho(x)$, the bulk density;

u = u(x), the bulk velocity;

P = $\rho v gh \cos(\theta)$, hydrostatic pressure;

τ_w = shear acting on the chute walls;

IP = wetted perimeter;

g = gravity;

θ = chute angle; and,

h = depth of flow.

Upon simplification one finds;

$$\frac{\tau_w IP}{\rho_p v g h \cos\theta} = \tan\theta + \frac{dh}{dx}(Fr^{*2} - 1) + \frac{h}{v}\frac{dv}{dx}(Fr^{*2} - 1/2) \qquad (3.12)$$

where:

$$Fr^{*2} = \frac{U^2}{gh\cos\theta} ,$$

which is the square of the Froude Number. (A complete derivation is given in Appendix A).

The term on the left hand side of the equation 3.12 is a friction coefficient. For sliding motion of a solid block on a solid surface, this friction coefficient is usually taken to be a constant and is called the Coulomb friction coefficient or Coulomb friction angle. The Coulomb friction angle corresponds to the inclination at which a block will begin to slide. The shear relations for granular material flows are so far not fully understood and this is a quantity will be investigated in detail as part of the present study.

The first term on the right hand side of equation 3.12 is the body force term. The remaining two terms are the correction terms due to the changes in the depth of flow, bulk velocity and solid fraction.

An interesting point that should be made is that without the third term on the right hand side of equation 3.12, this equation is identical to the flow of water, or some other incompressible fluid, in an open channel. When,

$$Fr^{*2} = 1,$$

the existence of an infinitesimal wave may be predicted. This kind of equation also indicates that a hydraulic jump can occur in an open channel and infact these jumps have been observed in granular material flows. If the solid fraction does not change through the discontinuity, a granular jump and a hydraulic jump are identical.

If the third term of equation 3.12 is included, the compressibility of

the flow is taken into account. This expression predicts that a discontinuity due to density changes may also exist in a granular material. This discontinuity is analogous to an infinitesimal wave in a gas. When the depth of flow in a chute is held constant and

$$Fr^{*2} = 1/2,$$

an infinitesimal density wave can exist in the flow.

In reality, the density does not stay constant in a granular jump and the depth of flow also will vary across a disturbance. What is generally seen is a high velocity, low density and shallow depth flow on the upstream side of the disturbance, and a low velocity, high density and deep flow on the downstream side of the disturbance. In other words, a combination of a granular jump and a granular shock wave occurs. Brennen, et al. (1982) studied these granular jumps to try and determine which parameters are the most important in granular material flows. Their combination of parameters did not show that any one variable was significantly more important than the others.

The momentum equation (eq. 3.12) was used to determine the shear, τ_w, instead of measuring this quantity by means of a shear cell. It was believed that this approach would yield more accurate results. The detailed measurements of the wall shear by the use of a shear cell was not pursued to any extent in this study; however, an attempt to measure the wall shear with a small shear cell was performed and a comparison

between the two sets of data were made. The results of these test will be discussed in Appendix A.

3.6 **Experimental Results**

3.6.1 **Practical Presentation of the Wall Shear**

This section will deal with presentation of the data in a way that might be helpful to a designer who is interested in building a granular flow device. The data are presented in such a way that direct estimates can be made for optimizing the design of a chute. The effects that the sidewalls play in the total shear at a cross section are also examined in detail.

In figure 3.10 the results obtained as part of the present investigation are shown. The graph shows the relationship between the friction coefficient and the Froude Number. If the friction coefficient were to remain constant throughout the entire range of Froude Numbers, then one may conclude that the simple Coulomb friction concept applies. Figure 3.10 shows that for a wide range of Froude Numbers the friction coefficient does remain fairly constant but when the Froude Number approaches higher values, this relationship is no longer valid. A drastic increase in the friction coefficient is observed and the Coulomb friction law no longer appears to be valid. Both sizes of glass beads show this increase.

It should be mentioned here that in computing the shear stress, τ_w, attention had to be given to assure that the sidewall contribution to the

overall wall shear was adequately accounted for. The effective wetted perimeter in the present work is given by;

$$I\!P = (b + \beta h)$$

where:

$I\!P$ is the effective wetted perimeter;

h is the depth of flow;

b is the width of the chute; and,

β is some constant to be determined.

The value of β was determined experimentally but the choices were based on some knowledge of the flows. There were four basic choices that were used to predict the value of β:

i. $\beta = 0$ or no contribution to the shear from the sidewalls;

ii. $\beta = 1/2$ or a flow rule contribution to the shear from the sidewalls;

iii. $\beta = 1$ or a Coulomb friction contribution from the sidewalls; and

iv. $\beta = 2$ or the shear acts equally over all surfaces.

The first choice for the value of β is obvious. If the shear acts only on the bottom of the chute, the contribution to the shear by the sidewalls is zero and so $\beta = 0$. There are cases where this may be applicable, for example the case of rough bottom chute with highly polished sides, but

in general the value of β will be different from zero.

The second value of β is derived from the constitutive relationship which is based on the Mohr-Coulomb yield criterion. Depending on the assumptions used to derive this relationship and the material properties of the granular material, the ratio between the normal stress against the sidewall and the normal stress against the bottom of the chute can range from approximately 1/4 to 3/4. On this basis, a value of $\beta = 1/2$ was selected as the second possible value for the sidewall contribution to the total wall shear.

The third value for β is based on two assumptions. The first is that the pressure is distributed hydrostatically and the second is that the shear acts Coulombically on all surfaces. Since the pressure distribution is assumed to be hydrostatic, the normal force acting on one wall is;

$$1/2\rho_p \nu g h^2 \cos\theta$$

so that the value of the normal force acting on both walls is twice that value or;

$$\rho_p \nu g h^2 \cos\theta.$$

But this is equal to the pressure acting on the bottom of the chute multiplied by the wetted area of one side. Therefore, as a consequence of these assumptions the ratio of the contribution to the wall shear by the sidewall to the contribution of the wall shear by the bottom of the chute

is unity, or $\beta = 1$.

The final possible choice for the value of β is based on the assumption that all surfaces contribute equally to the overall shear. This is the case for all Newtonian Fluids and if a Newtonian Fluid were used in the experimentation, an appropriate value of β.

The graphs shown in figure 3.11 give the plots for the various values of β. It appears from figure 3.11a, which has been prepared assuming no sidewall contribution, that the sidewalls must play some role in the overall wall shear for the following reasons. As the depth of the flow increases and the Froude number decreases, the value of the friction coefficient computed in this way also increases. Such an increase is not believed to be realistic and is simply attributed to the effect of the sidewalls. From inspection of the graphs, it appears that the value that best fits the data is $\beta = 1$. In this graph the friction coefficient approaches the Coulomb coefficient at low velocities as should be expected and it remains fairly constant in the low Froude number range. The graph also gives some indication that the hydrostatic pressure assumption used in the derivation of equation 3.12 is acceptable in this case. All further computations were based on a value of $\beta = 1$. One might add that the selection of β, fortunately, is not critical as the experiments were designed to minimize the sidewall effects.

In figure 3.10 the friction coefficient is plotted against Froude Number where the wall shear has been computed with $\beta = 1$. Figure 3.10

confirms the view that at low velocities and high densities the flow is governed by Coulomb friction. For the rapid flows, figure 3.10 indicates that a drastic change from Coulombic friction occurs. This fact was certainly not expected. Figure 3.12 presents more clearly the variation in the friction coefficient with the higher values of the Froude Number. The friction factor appears to become velocity (or Froude Number) dependent since an increase in the friction coefficient is observed. The data seem to follow a distinct curve for both the 3mm glass beads and the .3mm glass beads. More scatter is observed for the large glass beads but this scatter is probably due to measurement error rather than any unique flow conditions. The problem with the measurement of the large glass beads has been previously mentioned and an analysis of the problems in determining the flow parameters is given in Appendix A.

From the practical standpoint, figure 3.10 can be quite useful for the design of a chute. In the region where the Froude Number is low and the friction coefficient appears to be constant, a designer can determine the flow characteristics of a chute quite easily. A desirable design criterion is to operate a chute just below $Fr^{*2} = 1$, which will predict a low friction coefficient and a high mass flow rate.

3.6.2 Comparison of the Present Study with Other Experimental and Computational Works

In this section the experimental data of the present investigation will be presented in a way that is suitable for comparison with the experimental as well as the computational works of others. The direct comparison of the present work with other experimental work is somewhat difficult since most other works were performed using Couette Flow devices. Savage and Sayed (1980) and Hanes and Inmann (1984) both used Couette Flow devices to examine the shear relationships for granular materials. Even though these devices produce flows which are quite different from chute flows, the basic characteristics of these flows should be similar. With this cautionary statement in mind, an attempt will be made to compare the present work to other experimental works.

Savage and Sayed (1980), and Hanes and Inmann (1984) both performed their works in similar manners with the exception that Hanes and Inmann actually measured the shear zone in his Couette Flow device. Savage simply assumed that the material was shearing through the entire depth of flow. The comparison of these works with the present work will be done in terms of the friction coefficient versus Froude Number and is shown in figure 3.13. For easier comparison between the works, a slightly different Froude Number is being used, where $Fr^{*2'} = Fr^{*2}(d/h)$. The general trends should not be altered by this variation.

The comparison of the results of Savage and Sayed work to the data for glass beads used here are quite good considering the different means by which the data were obtained. The general trends seem to be be similar for both experiments. To compare the results obtained here to those of Savage for plastics, some exploratory data were obtained using 3mm polyethylene pellets. Although the density variations were not as carefully taken into account in obtaining these data, the results are believed to be applicable for this comparison. Figure 3.14 then shows the comparison of Savage's results with the data obtained in the chute using polyethylene pellets. Once again, the general trends are similar and reaffirm that granular materials do not behave Coulombically throughout the flow regimes.

The flows which are achieved in a chute cover a wider range than those that can be created in the Couette Flow devices described above. It is possible, however, to compare the present results to data covering the entire range of flows produced in the chute by referring to computational results. Campbell's computational Couette Flow and Chute Flow results allow the comparison of the present results through the complete ranges of flows that were produced in the chute. Even though the boundary conditions used by Campbell were somewhat different than for the actual chute flow, a qualitative comparison between the two works is meaningful.

The chute flow results from Campbell's computer simulation are

shown in figure 3.15 again in terms of the friction coefficient versus Froude Number. In addition, the experimental data of the present work for the two sizes of glass beads are shown. The general trends are again qualitatively similar but the computer results appear to predict high values of the Froude Number for a given friction coefficient. The fact that the flow parameters are somewhat different should not be unexpected since the boundary conditions used for his analysis are different than those for the actual chute flows. It is encouraging, however, that the general trends are very similar and once again show that the material will not conform to the Coulomb Friction Law.

3.6.3 **Comparison of the Present Study to Analytical Studies**

The previous comparisons are based on actual experimentation and computer simulations and do not require the assumption of any particular form for the shear relationship for granular flows. There have been several attempts to model granular material flows through analytical considerations. Several models have been produced by Savage and Jeffrey (1981), Lun, et al., (1984) to mention several. These models rely on the knowledge of the density variations in the flows rather than the velocity. Comparison of these theories with actual experimental flows has been hampered in the past because of lack of experimental information about the density. The development of the density gauge discussed in section 3.2, now makes it possible to make comparisons between the results of the analytical models and actual experimental flows for the

entire ranges of solid fractions.

The pertinent analytical results have been presented in terms of the friction coefficient versus the solid fraction. Figure 3.16 is a graph of friction coefficient versus solid fraction for both sizes of glass beads tested in this investigation. These figures show that the correlation between the friction coefficient and the solid fraction is not good. It is possible that the friction coefficient in the experimental work is not only dependent on ν but also on a length scale. The analytical works assumed a simple shear flow with little variation in any length scales but the present study clearly has a wide variety of depth of flow in the chute.

The comparison of the experimental results with several theories is shown in figure 3.17. Once again the assumptions used to develop these theories are somewhat different from the actual chute flows, but the general trends should be evident even with these discrepancies. Savage's early works show that the friction coefficient should be independent of the solid fraction for a given coefficient of restitution. Lun, et al. showed that the friction coefficient does vary somewhat with the solid fraction and that a unique curve corresponding to each value of the coefficient of restitution. The present work also shows that the friction coefficient depends on the solid fraction, but this dependency does not seem to be unique for a given material. It should be added that the above theories only show a unique curve for a given coefficient of restitution which is not the same as a unique curve for a given material. The information in

figure 3.18 may give an indication of the reasons for the difference between the analytical and experimental works. Figure 3.18 gives a plot of the variations in the coefficient of restitution with impact velocity. It becomes apparent that if the fluctuation velocities in the chute flows lie within the region where the coefficient of restitution is dependent on the impact velocity, a given material may not conform to a single curve but rather cross several of the predicted curves as the coefficient of restitution changes.

The incorporation of a length scale into the solid fraction for the comparison of this parameter to the friction factor may be done as follows;

$$\mu = \nu(\frac{h}{d})$$

A comparison of the friction factor to this solid fraction is shown in figure 3.19 for both the large and small glass beads. The data appear to correlate much better with the addition of the length scale and both sizes of glass beads seem to follow a unique curve.

Let us consider now the form of a possible constitutive relationship for the stresses. The most common form for the stresses for granular materials that appears in the literature was originally proposed by Bagnold. This form is similar to that which was used in the early mixing theories for turbulent flows. The basic form of such a relationship is as follows;

$$\sigma_{ij} = \rho_p f_{ij}(\nu) d^2 (du/dy)^2 \qquad (3.13)$$

where:

σ_{ij} is the stress tensor;

ρ_p is the partical density;

d is the partical diameter;

du/dy is the shear rate; and,

$f_{ij}(\nu)$ is an unknown function of the solid fraction.

In the above equation there is an unknown function of ν in the expression of the shear stress--$f_{xy}(\nu)$, and an unknown function of the normal stress-- $f_{yy}(\nu)$. These two functions are calculated from the knowledge of the other variables in equation 3.13. Thus, $f_{ij}(\nu)$ is not a measured quantity but is determined from the flow field.

The value for $f_{ij}(\nu)$ from the present experimental study was calculated with some approximations. The shear that is calculated is the wall shear so the values that appear in the above equation should be evaluated at the wall. This is not possible with the present techniques for evaluating the flow parameters so the average values of the flow are used. The shear rate at the wall will be approximated by the bulk velocity--U divided by the depth of flow--H. The bulk solid fraction at the wall is taken to be the average value of the solid fraction. It is also assumed that the shear relation will hold throughout the material and to the wall of the chute. The function, $f_{yy}(\nu)$ was determined with the

same assumptions but in addition, the normal stress was assumed to be hydrostatic. With these approximations in mind, an attempt will be made to compare the present work with other works.

The relationship between the solid fraction and $f_{xy}(\nu)$ is plotted for the large and small glass beads in figure 3.20. The two curves are very similar and both are of the same order of magnitude. A comparison between $f_{xy}(\nu)$ as derived from the present work and the results of othe experimental works are shown in figure 3.21. The results are qualitatively similar, but once again the relationships do not coincide. This should not be surprising when one considers the diverse means and assumptions that were used to arrive at the different results.

Figure 3.22 shows the relationship between the $f_{yy}(\nu)$ and the solid fraction for both sizes glass beads. A comparison between the present work and other works is shown in figure 3.23. The comparison between the present investigation and the analytical models shows that the results are similar.

It is interesting to note that for the large glass beads, an increase in the value of $f_{yy}(\nu)$ is observed at the very low solid fractions. This phenomenon was actually mentioned by Lun, et al. (1984) and they showed that this trend is an indication of an instability. This instability is somewhat unexpected, but one can imagine it to occur in the following way. By writing the conservation of mass and conservation of momentum in the direction normal to the flow:

$$\frac{\partial \rho}{\partial t} + u\frac{\partial \rho}{\partial x} + \rho\frac{\partial u}{\partial x} + v\frac{\partial \rho}{\partial y} + \rho\frac{\partial v}{\partial y} = 0$$

$$\frac{\partial v}{\partial t} + u\frac{\partial v}{\partial x} + v\frac{\partial v}{\partial y} = -\frac{1}{\rho}\frac{\partial P}{\partial y}$$

and now allowing for a small disturbance in the flow of the form;

$$\rho = \rho_o + \rho'(y,t)$$

$$u = u(y) + u'(y,t)$$

$$v = v'(y,t)$$

Placing these expressions into above equations gives:

$$\frac{\partial \rho'}{\partial t} + \rho_o\frac{\partial v'}{\partial y} = 0$$

$$\frac{\partial v'}{\partial t} = -\frac{1}{\rho_o}\frac{\partial P}{\partial \rho}\frac{\partial \rho}{\partial y} = -\frac{1}{\rho_o}\left(\frac{\partial P}{\partial \rho}\right)_o\frac{\partial \rho'}{\partial y}$$

so that;

$$\frac{\partial^2 \rho'}{\partial t^2} = -\rho_o\frac{\partial^2 v'}{\partial y\,\partial t}$$

and

$$\frac{\partial^2 v'}{\partial y\,\partial t} = -\left(\frac{1}{\rho_o}\frac{\partial P}{\partial \rho}\right)\frac{\partial^2 \rho'}{\partial y^2}$$

Thus, the momentum equation becomes;

$$\frac{\partial^2 \rho'}{\partial t^2} = \left(\frac{\partial P}{\partial \rho}\right) \frac{\partial^2 \rho'}{\partial y^2}$$

If $\frac{dP}{d\rho}$ is positive, the flow is stable; however, if $\frac{dP}{d\rho}$ is negative, as is indicated by figure 3.22 for the present investigation at low solid fractions, the flow will become unstable and continue to remain unstable. This could be one explanation for the difficulty in obtaining accurate and repeatable results for the large glass beads.

The ratio between $f_{xy}(\nu)$ and $f_{yy}(\nu)$ is the friction coefficient that has already been examined in the previous sections. By using these functions as the form of the stresses developed in a granular flow, a new combination of parameters may be developed. First note;

$$\frac{f_{xy}(\nu)}{f_{yy}(\nu)} = \frac{\tau_w}{\rho_p \nu g h \cos(\theta)} = \mu$$

Substituting equation 3.13 for $\sigma_{xy} = \tau_w$,

$$\mu = \frac{f_{xy}(\nu) d^2 (du/dy)^2}{\nu g h \cos(\theta)}.$$

By simple examination of this equation, the following parameters may be produced;

$$\frac{f_{xy}(\nu)}{\nu},$$

and,

$$Fr^{*2}(d/h)^2,$$

which gives a diameter dependency to the Froude Number.

Considering the possibility that $\frac{f_{xy}(\nu)}{\nu}$ depends exclusively on this new Froude Number, a graphical representation of the friction coefficient and the Froude Number with the incorporation of a diameter effect is shown in figure 3.24 for both the large and small glass beads. The addition of the diameter seems to bring the two different sizes of materials to a single curve. The study of other sizes of glass beads is needed to further test this correlation.

3.6.4 **Presentation of the Present Investigation in Terms of Fluid Flow Parameters**

Up to this point in the analysis of the shear, the approach has been to represent the data in terms of the friction coefficient which was defined as the ratio of the shear stress to the normal stress. This coefficient is not generally used in classical fluid mechanics. In this section we will approach the problem from a fluid mechanics standpoint to see if this will lead to additional insight.

The first step in examining the shear in a fluid is to analyze the shear relationship to the shear rate. For a Newtonian fluid the ratio would be constant. The results of such a relationship for the granular materials obtained here are shown in figure 3.25 for the large glass beads. The figure shows that no simple relationship exists between the shear and

the shear rate. Next, an attempt is made to examine the relationship between the shear and the solid fraction. Figure 3.26 shows the shear as a function of the solid fraction for the the large glass beads. These graphs, although not defining a clear relationship, do suggest that the solid fraction is more directly related to the shear than to the shear rate. Probably, however, there is an interdependency between all the flow parameters, as suggested by equation 3.12..

Perhaps the most interesting representation of the data is shown in figure 3.27, in which the friction factor, C_f, is plotted versus the Froude Number for the large glass beads and in figure 3.28 for the small glass beads. The friction factor is defined by;

$$C_f = \frac{\tau_w}{1/2\rho_p \nu U^2} \tag{3.14}$$

where:

C_f is the friction factor;

τ_w is the wall shear

ρ_p is the particle density;

ν is the solid fraction; and,

U is the bulk velocity.

The friction factor decreases linearly with the Froude Number for a wide range of Froude Numbers up to a point when this linearity deviates to a somewhat higher value than the linear relationship would predict. This

trend is seen in the results for both the large and small glass beads.

This correlation is similar to the results that are seen in a pipe flow for a Newtonian fluid as the Reynolds Number increases. In the lower Reynolds Number region of the C_f vs. Re curves, the friction factor is linearly related to the Reynolds Number up to a point where the flow becomes turbulent and the linear relationship breaks down. For a Newtonian fluid, in the linear portion of the curve the relationship between the friction factor and the Reynold's Number is given by;

$$C_f = \frac{64}{\mathrm{Re}}$$

where:

C_f is the friction factor; and,

Re is the Reynolds Number.

There are some analogies between the friction factor, C_f, and the Reynold's Number, Re, relation for a Newtonian fluid and the friction factor, C_f, and the Froude Number for a granular material in the following sense. First assume that the flow is Coulombic. This means that the shear at the wall is given by;

$$\tau_w = \mu \rho_p \nu g h \cos(\theta) \tag{3.15}$$

where:

τ_w is the shear at the wall;

ρ_p is the density of the solid particles;

ν is the solid fraction;

h is the depth of flow;

θ is the chute angle;

μ is the Coulomb friction angle; and,

g is the gravitational acceleration.

If this form of the wall shear is placed into the equation of the friction factor, the following is found;

$$C_f = \frac{\mu \rho_p \nu g h \cos\theta}{\frac{1}{2}\rho_p \nu U^2}$$

By rearranging this equation;

$$C_f = \frac{\mu g h \cos(\theta)}{\frac{1}{2}U^2}$$

or,

$$C_f = \frac{2\mu}{Fr^{*2}}. \qquad (3.16)$$

This relationship shows that there should be a linear relationship between the friction factor and the square of the Froude Number wherever the flow acts Coulombically. This fact was shown in figure 3.27 and figure 3.28. The same relationship was shown in figure 3.10, where the friction coefficient, μ, is plotted against the Froude Number. In that

plot, the linear region of figures 3.27 and 3.28 appears as a region of constant friction coefficient. This fact is also easily seen from equation 3.16, since $\frac{C_f Fr^{*2}}{2} = \mu$.

The similarities between the linear relationship between the friction factor, and the Reynolds Number for a Newtonian Fluid in the laminar region, and the friction factor and the Froude Number for a granular material in the Coulomb friction region represents a certain analogy. What is also interesting is that when a deviation from the linear relations do occur, the cause for both a Newtonian Fluid and a granular material is the change to a turbulent shear flow. This could lead one to believe that the similarities of a Newtonian fluid and a granular material are greater than might first be thought. This analogy can lead one to refer to the Coulomb Friction region of a granular material flow as a "laminar" flow and as the material deviates from this relationship as a "turbulent" flow.

CHAPTER 4

EXPERIMENTAL STUDY OF CONVECTIVE HEAT TRANSFER TO A FLOWING GRANULAR MATERIAL

4.1 General Comments

The applications of heat transfer to a flowing granular material are quite broad in scope. Detergents, such as those used for household applications, are processed at fairly high temperatures. The desire of the manufacturer is to move the material quickly from processing to packaging. The problem with this process is that if the detergent is not allowed to cool completely before packaging, the detergent changes from the desired powder to a coagulated brick. With a good understanding of the basic principles involved in the heat transfer from a granular material, new devices for transporting and cooling or heating these materials can be developed. This would provide a shorter time between processing and packaging in the production of these powdered detergents saving both time and energy to the manufacturer.

Granular materials also are being considered as the "fluid" for transporting heat in heat exchange processes. In a cycle proposed by engineers at Sandia, certain silicas are to transport heat from the solar collectors in a solar energy plant to the steam cycle. The thermal properties of some granular materials could make a more efficient means of transferring solar energy to steam. The use of granular materials in this process is not without problems. Transporting granular materials is not

easy, especially with the volume needed in this process. The abrasive nature of granular materials would also cause difficult problems. Even with these problems, granular materials are an attractive alternative to conventional heat exchanger fluids.

The use of a flat plate for the heating of the granular material in this paper proved to be prudent. Sullivan's (1973) work was performed with a flat plate in a hopper. In his work, the material essentially moved like a solid block past a rectangular heater. The hopper confined the flow so that velocity gradients and density gradients were negligible. Sullivan's assumption of a uniform plug flow past a flat heating plate was quite accurate; however, he was unable to examine flows with large density and/or velocity gradients. Spelt (1982) used a flat heating surface placed in a chute to examine the heat transfer properties of a flowing granular material at much higher flow rates than were possible by Sullivan. Spelt found a close agreement with Sullivan at low flow rates but as the flow rate increased, a maximum in the heat transfer coefficient was reached. With further increase in the bulk velocity, the heat transfer coefficient decreased. This phenomenon prompted further examination into the heat transfer to a flowing granular material using the facility already described and the use of the method for determining average density. The intention of this work was to shed further insight into the flow region where the heat transfer coefficient decreases with increased velocity.

4.2 **Description of Apparatus**

The basic flow of the material was produced in exactly the same manner as with the shear flows. The experimental setup was also exactly the same except for the addition of a heating plate approximately 8' from the chute control gate and placed in the base of the chute. The basic design of the heating plate and the placement of the heating plate in the chute was taken from Spelt's work with only minor changes.

The heating plate was 12" long and 4" wide. The thickness of the plate was approximately 1". The top portion of the plate which was exposed to the flow was made of 1/8" copper to assure good conductivity. A section 4" long and 1" wide was cut out of the center of the leading edge of the copper plate. This served as the actual test section of the heating plate. (See figure 4.1).

Six 4"x4" ribbon heaters were used as the heating source. Each heater was capable of delivering 50W of power. Three of the heaters were used to heat the flow. They were placed under the copper plate and on top of a 1/2" phenolic plate. The other three heaters were placed on the bottom of the phenolic plate with one side of the heater exposed to the atmosphere. The purpose of the phenolic plate and the bottom heaters was to provide insulation. It was necessary to make sure that the measured heat flux in the top heaters was actually the heat flux that was reaching the flowing material. By using the phenolic and adjusting the bottom heaters, the actual heat flux reaching the material was very

close to the measured heat flux of the top heaters.

The control of the heaters was performed by the use of 2 amp variacs. Four variacs were used for this purpose. Each of the three top heaters (the heaters which heated the flow), were separately controlled by a variac. This allowed the independent adjustment of these heaters so that either constant heat flux or constant plate temperature could be maintained during experimentation. The three bottom guard heaters (the heaters which minimized the loss of heat through the bottom of the heating plate) were connected in series and controlled by a single variac.

The temperatures were measured using 0.005in chromel-alumel wire which were coated with a 0.003in thick Teflon insulation. The thermocouples which measured the temperature of the copper plate were located at three positions on the test section and in the position corresponding to the center of the middle and downstream top heaters. These thermocouples were tack welded to the copper plate with approximately 1/8" between the junctions. The tack welding assured that the plate temperature was measured by making the plate part of the junction. Three thermocouples were placed between the top heaters and the phenolic plate and three were placed between the phenolic plate and the bottom guard heaters. The thermocouples were in the center of each heater. All the thermocouple wires were exited from their measurement points in the perpendicular direction to the flow to minimize any thermal gradients from the point of measurement to the ambient. The ther-

mocouple wires were connected to a thermally insulated box from which a Hewlett Packard multimeter was attached. The temperature of the flowing material was measured using a simply twisted thermocouple wire and was also attached to the thermally insulated box.

The plate was epoxied together, clamped and cured for 24 hours. The plate was then placed into the chute and clamped into place. Once the plate was adjusted properly, a bonding resin (trade name "Bond-O") was used to fill the gap between the plate and the chute bottom and to also fill the space caused by thermally isolating the test section from the rest of the copper plate. The "Bond-O" allowed a smooth transition from the aluminum bottom of the chute to the copper heating plate and thus eliminated the disturbance which would have influenced the flow due to the air gap between the test section and the rest of the copper plate. "Bond-O" is also a good insulator so that the insulation that was lost by using the "Bond-O" instead of leaving the air gap was far outweighed by the benefit of an undisturbed flow over the plate. (See figure 4.2).

4.3 **Experimental Procedure for Heat Transfer**

The basic design and experimental procedure was taken from Spelt. His experimentation was performed in a relatively small chute and his heating plate was much smaller than the one used in the present work. Spelt continually replenished the feed hopper for his chute by physically carrying the material from the outlet hopper to the feed hopper in a bucket. This proved to be quite exhausting since some of his

experimental runs took 30 minutes. The use of the new facility eliminated this problem. The conveyor made it possible to allow a steady state between the heating plate and the material to be reached without considering how long it would take to arrive at this steady state. This was fortunate since some of the experimental runs for the present work took over an hour to reach steady state. On the average, however, each run took about 45 minutes.

The technique which was developed to find the density changes in the chute proved to be a valuable tool in more accurately measuring the parameters which controlled the heat transfer process. As with the shear experimentation, the assumptions used by Spelt and others for evaluating the heat transfer to a flowing granular material was that the solid fraction remained constant at some critical value. The present work showed that this assumption was far from correct and the addition of the average solid fraction allowed a more accurate analysis of the heat transfer process.

The procedure used to acquire the heat transfer data was as follows:

i. Set the chute angle;

ii. Set the flow gate height and start the conveyor;

iii. Set variacs to assure a reasonable temperature difference between the flowing material and the copper heating plate;

iv. Measure the mass flow rate;

v. Measure the depth of flow at the midpoint of the heating test section;

vi. Allow the plate temperature to stabilize and make sure that the temperature difference across the phenolic is sufficiently small;

vii. Record the temperatures of the test section and the other temperatures from the plate;

viii. Measure the freestream temperature; and finally,

ix. Measure the average density at the test section.

The procedure followed in the heat transfer portion of the experimentation is not unlike that used for the shear investigation. The flow conditions are accomplished in exactly the same manner. The flow is initiated by setting the chute angle and control gate. The mass flow rate is measured in the same two manners as described in chapter 3. A single point probe, located in the center of the heating plate test section, was used to measure the depth of flow over the test section. There was no need for more than one point probe since it was assumed that the variations in the depth of flow over the test section were negligible. The average density at the test section was measured by inserting the two parallel plates into the flow and measuring the amount of mass captured in the process. Since the flowing depth of flow, chute width and the distance between the two plates were all known, the average density could be calculated. These procedures are identical to the method used for

gathering data for the shear portion of the experimentation with the exception that it was not necessary to account for the changes in the flow parameters over the test section.

The variacs, which controlled the top heaters of the heating plate, were adjusted to give a reasonable temperature difference between the plate and the flowing material. These variacs generally were set between 75V to 105V. This potential allowed at least a 10 degree F. temperature difference between the plate and the material. The guard heaters were adjusted to give a small temperature difference across the phenolic as possible. Once the temperature difference across the phenolic was small, then the heat flux being supplied to the top heaters became very close to the amount of heat flux reaching the material. Obtaining a small temperature difference across the phenolic was by far the most time consuming part of the heat transfer experimentation. The measurement of the freestream material temperature was done by two means. First, a simply twisted thermocouple wire was placed into the flow upstream of the heating plate. The depth that the probe was placed into the flow had minimal effects on the reading; however, there was some problem with the repeatability when using this method. The second method for measuring the freestream temperature was to collect about a gallon of the material and statically measure its temperature by placing the thermocouple into this collected material. The second method proved to give more repeatable results and became the basic method for measuring the freestream temperature.

4.4 **Background Information**

The measurements involved in the study of convective heat transfer to a flowing granular material are more reliable than those involved in the investigation of the shear. The results are based on direct measurements of the heat transfer with only a few generalized assumptions for the flow. The heat transfer data in general conformed well with the intuitive concept of the flow and the general trends in the convective behavior of the granular flow are plausible.

The global parameters of the flow, that is the bulk velocity, bulk density and average depth of flow over the test section, are measured in the same way as for the shear results. These parameters are assumed to be constant over the heating test section of the chute. This is a very good approximation as it was already shown in connection with the momentum equation that the correction terms that account for these changes in the direction of the flow are small. Moreover, if these terms were not properly accounted for, the variations in these parameters would still be small over the test section since the test section is not large in comparison with the other physical dimensions of the flow.

The convective heat transfer coefficient of a single phase fluid is found as follows. First, consider the expression for the Nusselt Number for a single phase fluid with the following assumptions:

i. The flow is one dimensional;

ii. The plate temperature is constant; and,

iii. Radiative heat transfer and viscous dissipation will be neglected.

Using these assumptions, it can be shown that;

$$Nu_L = hL/k = \frac{2}{\sqrt{\pi}}\sqrt{Pe_L} \qquad (4.1)$$

where:

Nu_L is the Nusselt Number;

Pe_L is the Peclet Number; UL/α;

α is the bulk diffusivity;

L is the length of the heating plate; and,

h is the film coefficient.

(A more complete derivation may be found in Sullivan (1973)).

Sullivan and Sabersky compared the results obtained using equation 4.1 to the results for convective heat transfer of granular materials. Their results showed little correlation between the measured film coefficient and the single phase continuum prediction. This proves that the flows are more complicated than a simple single phase continuum flow. Figure 4.3 shows the comparison of Sullivans and Sabersky's experimental results with this continuum prediction.

Sullivan and Sabersky (1975) next developed a new model for the heat transfer to flowing granular materials. This model includes an added

resistance to the flow of heat due to the interstitial fluid effects. Their model is basically equivalent to a solid block moving past a rectangular heater with a contact resistance. The corresponding Nusselt Number from their model may be expressed as:

$$\overline{Nu_d^*} = \frac{1}{\chi + \frac{\sqrt{\pi}}{2}\sqrt{\frac{1}{Pe_L^*}}} \tag{4.2}$$

where:

χ is an experimental constant accounting for the added resistance at the wall due to the interstitial fluid;

Pe_L^* is special Peclet Number; $(\frac{k}{k_g})^2(\frac{d}{L})^2 Pe_L$;

$\overline{Nu_d^*}$ is the special Nusselt Number; $\frac{hd}{k_g}$;

k is the bulk conductivity;

k_g is the conductivity of the interstitial fluid;

d is the particle diameter;

L is the length of the heating plate; and,

h is the film coefficient.

In a further development, Spelt, Brennen and Sabersky (1982) used an open channel to test the validity of the above equation for the wider flow regimes which can be produced in these channels. Their results show

that the simple model (used by Sullivan and Sabersky) can not adequately represent the entire flow regimes of granular materials. The results of Spelt, Brennen and Sabersky are shown in figure 4.4 along with the predicted value of the Nusselt Number from equation 4.2. The unusual phenomenon of a decrease in heat transfer with increased convective velocity is seen at the higher velocities in their flows. They found a correlation between the depth of flow over the test section and the heat transfer coefficient. This representation of the data is somewhat surprising since one would think that the heat transfer transfer should be dependent on more general flow parameters and not on a dimensional quantity such as the depth of the flow. The depth of flow, therefore, is probably an indirect indication of a more general factor, such as the density of the flow. Thus, an attempt will be made to develop an expression between heat transfer and the solid fraction.

4.5 **Experimental Results**

The results of the present work are shown in figure 4.5 in terms of the special Nusselt Number, $\overline{Nu}_d^*$, and Peclet Number, Pe_L^*, used by Sullivan and Sabersky. The data were reduced in this way so that a direct comparison could be made to the works done by Sullivan and Sabersky (1975) and Spelt, Brennen and Sabersky (1982). A comparison of the present investigation to these works, using these parameters, is shown in figure 4.6. It is important to point out, however, that the velocity which appears in the Peclet Number has been computed taking into account

the actual measured density of the flow. In Spelt's work, the density was assumed to be constant. As a significant consequence of properly accounting for the density in the computation of the velocity, the effect of different depths of flow no longer appears significant and the family of curves for each depth of flow that was presented by Spelt collapse onto one curve. Even after correctly accounting for the density changes in computing the velocity, the data for the two sizes of glass beads still define two separate curves, indicating that the presentation of the data in terms of Pe^* is not yet universal, and that other parameters may be involved.

The results of the present work conform well with the predicted values from equation 4.2 for the special Nusselt Number, $\overline{Nu_d^*}$, and the special Peclet Number, Pe_L^*, when the flows are relatively slow and well packed. When the flow begins to reach the point where the solid fraction may no longer be assumed constant, however, equation 4.2 fails to represent the proper trends.

To better represent the transition between the slow packed flows that can be modeled well by equation 4.2, and the flows where the heat transfer decreases with increased velocity, a plot of Nusselt Number, $\overline{Nu_d^*}$, versus solid fraction is shown in figure 4.7 for the large glass beads and figure 4.8 for the small glass beads. The data show that the Nusselt Number initially increases as the velocity increases. In this case, the density does not vary much from its critical value and the bulk proper-

ties used in equation 4.2 are still valid and this relationship models the flow quite well. The sudden change in the solid fraction coincides with the rapid decrease in the film coefficient and thus a decrease of the Nusselt Number. It appears that the Nusselt Number decreases exponentially with the solid fraction but the data show too much scatter to predict the actual form of the curve other than showing the general trends between these two parameters. It is reassuring that both the small glass beads and the large glass beads show the same trends between the Nusselt Number and the solid fraction and the maximum Nusselt Number occurs at almost the exact same solid fraction for both materials.

In a further attempt to derive the pertinent parameters for this investigation, it seems apparent that the correlation of the convective heat transfer should also involve parameters which describe the flow. The flow of granular material in a chute seemed to best be correlated by the densinometric Froude Number, Fr^{*2}_{v/v_c}. In order to investigate the effects of this Froude Number on the heat transfer, the Nusselt Number is plotted versus this densinometric Froude Number in figures 4.9 and 4.10. The correlation is surprisingly good for both the large and small glass beads. Not only is the increase in the Nusselt Number with this Froude Number observed, but also the region where the Nusselt Number decreases with the increased velocity correlates quite well. This seems to indicate that the Peclet Number used by Sullivan and Sabersky in equa-

tion 4.2 should be replaced by, or complemented with, this Froude Number.

A further step in investigating the relationship between the convective heat transfer and the flow parameters is to examine the results in terms of the Stanton Number and the friction coefficient. The definition of the Stanton Number, St, is as follows:

$$St = \frac{Nu}{\mathrm{Re}\ Pr}$$

where:

St is the Stanton Number;

Nu is the Nusselt Number;

Re is the Reynolds Number; and,

Pr is the Prandtl.

For a granular material, the Reynolds Number and the Prandtl Number have no significance. However, using the following definition of the Peclet Number:

$$Pe = \mathrm{Re}\ Pr,$$

the Stanton Number may be written as:

$$St = \frac{Nu}{Pe}$$

where:

St is the granular Stanton Number;

Nu is the granular Nusselt Number; and,

Pe is the granular Peclet Number.

The Stanton Number is the heat transfer parameter which has a direct relationship to the friction factor, C_f, in many fluid mechanics problems. For this reason, the Stanton Number was selected for the comparison between the heat transfer and the flow parameters.

Figure 4.11 shows the Stanton Number in terms of the friction factor for both sizes of glass beads. The correlation is not the same as for a Newtonian Fluid but it is encouraging that the data follow a general curve. The portion of the curve where the relationship is fairly linear is the portion of the flow which corresponds to Coulomb Friction and, as mentioned in the previous chapter, can be thought of as a "laminar" type flow. The region where the flow varies from this linear relationship is where the flow no longer conforms to the Coulomb Friction Law and acts more as a "turbulent" flow. A Newtonian Fluid also deviates from a linear relationship when the flow becomes turbulent. The fact that figure 4.11 follows a general curve gives some confidence to the idea that there is a relationship between the shear and the heat transfer.

With these ideas in mind, the following relationship for the Nusselt Number has been developed:

$$\overline{Nu_d^*} = \frac{1}{\chi + \frac{\sqrt{\pi}}{2}\sqrt{\frac{1}{Pe_L^*}}\left(1 + \frac{\beta}{\mu}\frac{\varepsilon}{\varepsilon_t}\frac{(Fr^{*2}_{\nu/\nu_c})^*}{\sqrt{Pe_L^*}}\right)} \qquad (4.3)$$

where:

$\overline{Nu_d^*}$ is the granular Nusselt Number from Equation 4.2;

Pe_L^* is the Peclet Number from Equation 4.2;

$(Fr^{*2}_{\nu/\nu_c})^*$ is the densinometric Froude Number multiplied by $(\frac{d}{L})(\frac{k}{k_g})$;

β is assumed to be a constant;

μ is the Coulomb Friction angle; and,

$\frac{\varepsilon}{\varepsilon_h}$ is the ratio of "turbulent" viscosity to "turbulent" diffusivity = "turbulent" Prandtl Number, Pr_t.

The development is given in Appendix B. The development is based on concepts which are analogous to those used to determine relationships between heat transfer and friction for a fluid flow. The Prandtl-Taylor relationship would be an example. Accordingly, the flow of a granular material is divided into three regions. The first region is dominant by the interstitial fluid, so that a thin film of air can be imagined to be between the heating surface and the first layer of particles. This concept assumes that the contact point between the heating plate and the

solid particles are infinitesimal so that no heat can be transferred directly into the solid particles at these contact points. Next a small distance from the wall, the interstitial fluid can transfer heat directly to the particles and thus the particles become the dominate mode of heat transfer. These two regions are identical to those defined in the derivation given by Sullivan and Sabersky (1975). The third region, at some distance δ from the heating plate to the bulk of the material, the heat transport mechanism is the same as the momentum transport mechanism. This is the equivalent of the Reynolds Analogy. From these concepts and a few additional simplifications, equation 4.3 may be derived.

It is interesting to note that if the densinometric Froude Number is small, this equation reduces to the form of equation 4.2 for the heat transfer to a flowing packed bed of granular material. This means that the additional term in the above equation is an added resistance due to the chaotic behavior of the particles. It seems apparent that as the shear between the particles increases, the random motion of the particles also increases and as noted in the last chapter, this motion is the cause for the decrease in the solid fraction. The above equation reflects this decrease in the density and this density in turn is probably directly related to the densinometric Froude Number.

A graphical representation of equation 4.3 is shown in figure 4.12. The plot is in terms of the special Nusselt Number versus the special Peclet Number as defined in equation 4.2. In addition, lines of constant densi-

nometric Froude Number are shown. The top curve where $(Fr^{*2}_{v}/_{v_c})^* = 0$, is identical to Sullivan and Sabersky's equation 4.2. As the densinometric Froude Number increases, the curves are shifted to represent a decrease in the Nusselt Number or an increase in the thermal resistance due to a decrease in the bulk density. A comparison of the experimental result obtained in this investigation to the predicted values from equation 4.3 are shown in figure 4.13. The equation can predict the general trends of the flow for both the low velocity - high density flows and the high velocity - low density flows.

CHAPTER 5

CONCLUSIONS

5.1 Conclusions and Possible Extensions of the Present Shear Results

The results from the shear flow experimentation showed several interesting trends. The development of the density gauge proved that the changes in the solid fraction are equally as important as the other flow quantities. The derivation of a compressible open channel momentum equation was necessary to properly account for these changes in the solid fraction. The wall shear was calculated with the aid of this equation and it was shown that uniform flow is possible for all of the chute angles tested. This differs from the conclusion drawn by Savage (1979) based on his analytical results for chute flow.

The ratio between the shear stress and normal stress, μ, showed a distinct variation from the Coulomb Friction value for both sizes of glass beads and the polyethylene pellets for large Froude Numbers. For well packed, low velocity flow, the friction coefficient, μ, appears to be approximately equal to the Coulomb Friction value, but as the velocity increases and the solid fraction decreases, this simple relationship is no longer applicable.

A great deal of attention was given to the sidewall shear contributions to the total wall shear. The results showed that for the small Froude Number flows, the sidewall effect were best represented by including half of the "wetted" sidewalls in the total wall shear. This means that the flow

under these conditions can be modeled as Coulombic shear with a hydrostatic pressure distribution acting on the "wetted" perimeter. No simple correlation for the sidewall contribution to the total wall shear could be found for the high Froude Numbers, thus, the sidewalls were assumed to contribute in the manner previously described for all flow conditions.

The development of the density gauge during the course of this investigation allow the study of the Bagnold/Savage constitutive equation for the stress tensor;

$$\sigma_{ij} = \rho_p f_{ij}(\nu) d^2 (\frac{du}{dy})^2.$$

The calculated value of the function $f_{ij}(\nu)$ gave qualitative agreement to other experimental, computational and analytical results. An examination of the friction coefficient's dependency on the solid fraction did not lead to a unique curve for the glass beads, as predicted by the analytical and computational results. However, by adding a length scale to the solid fraction, the data for both sizes of glass beads collapsed to a unique curve for the friction coefficient, μ, as a function of $\nu\frac{h}{d}$. The data for both sizes of glass beads also collapsed to a unique curve when the friction coefficient was presented in terms of a special Froude Number, $Fr^{*2}(\frac{d}{h})^2$. Other experimental investigations show similar trends when the friction coefficient is presented in terms of this Froude

Number. The present investigation also indicates the Savage/Bagnold stress tensor is a valid form for the stresses developed in a flowing granular material.

The results of the present investigation were also represented in terms of the friction factor, C_f, as a function of the Froude Number, $\overline{Fr}^{*2}$. Over a wide range of Froude Numbers, a linear dependency was observed between the friction factor and the Froude Number. By assuming a Coulombic wall shear; the relationship between the friction factor and Froude Number was shown to be;

$$C_f = \frac{2\mu}{\overline{Fr}^{*2}}.$$

This relationship gave good agreement to the experimental results in the region where the friction coefficient remains constant with the Froude Number.

The calculation of the wall shear by means of the momentum equation proved to give new insight into the shear flows of granular materials. The general trends of these shear flows have been established during this investigation. A more systematic evaluation of many different materials could be performed to further investigate the trends seen in this work. The chute surface could also be roughened to examine the effects of surface roughness to the wall shear. These ideas could be performed with only minor alterations in the facility designed for this investigation.

An alternate method for examining the wall shear could be to build a shear cell similar to the one used to test the polyethylene pellets in Appendix A. This shear cell could give direct measurements of the shear caused by flowing granular material. A pressure transducer could also be placed in the shear cell so that the friction coefficient, μ, could be directly measured. This method for examining the wall shear is a project that could easily be adapted to the facility designed and built for the present research.

5.2 Conclusions and Possible Extensions of the Present Convective Heat Transfer Results

The convective heat transfer results obtained during this investigation were revealing for the following reasons. The density gauge allowed a more accurate calculation of the convective velocity. Using this convective velocity, the results conformed to a single curve for each size of glass beads when presented in terms of the special Nusselt Number, $\overline{Nu_d^*}$ and Peclet Number, Pe_L^*. This fact proves the correlation proposed by Spelt (1982), that the data should be reduced by depth of flow, was only a surrogate for proper analysis of the density.

The present investigation also showed that the flow quantities are important in the analysis of convective heat transfer to a flowing granular material. The data conformed to a unique curve for each size of glass beads when plotted as $\overline{Nu_d^*}$ versus the densinometric Froude Number, Fr^{*2}_{ν/ν_c}. Good agreement was also seen when the $\overline{Nu_d^*}$ was

plotted as a function of solid fraction.

A relationship between the friction factor, C_f, and the Stanton Number, St, was presented. The data conformed to a unique curve for each size of glass beads when presented in this manner. As the friction factor decreased, the Stanton Number also decreased until a point, which corresponds to the deviation from Coulombic type wall shear, where an increase was once again observed in the friction factor with further decrease in Stanton Number.

A form of an equation for convective heat transfer to a flowing granular material was presented using the concept of a relationship between wall shear and heat transfer. The equation may be expressed in terms of the densinometric Froude Number or the friction coefficient along with the other parameters that were presented by Sullivan and Sabersky (1975). The equation shows qualitative agreement with the present results.

To continue the heat transfer experimentation, many different materials should be tested that have a wide variety of thermal properties and sizes. The heating plate could also be roughened to examine surface roughness effects on convective heat transfer. Both of these extensions of the research could benefit the industrial community and further test the equation for convective heat transfer derived in the present investigation.

APPENDIX A

A.1 Preliminary Comments

Equations for a compressible flow is an open channel (with the inclusion of the time averaged behavior of the flow variables) will be developed in Appendix A. The methods used for developing these equations are not new, but the concept of a compressible flow in an open channel is unusual.

To develop any flow with time averaged behavior takes some preliminary knowledge of steady turbulent motion. The general procedure for developing time averaged behavior in a flow field is as follows. The flow variable is divided into two parts. First, the variable has a time mean value which is denoted as $\overline{f}$. Secondly, the variable has a fluctuational component which is denoted as f'. Thus, the flow variable may be represented as follows:

$$f = \overline{f} + f' \tag{A.1}$$

and,

$$\overline{f} = \frac{1}{T}\int_{t_o}^{t_o+T} f \, dt \tag{A.2}$$

By definition $\overline{f}' = 0$, but the magnitude of f' can be different from zero. The usual means for determining the magnitude of f' is to take the

square of f', or;

$$\overline{f'^2} = \frac{1}{T}\int_{t_o}^{t_o+T} f'^2 dt \qquad (A.3)$$

$$\overline{|f'|} = \frac{1}{T}\int_{t_o}^{t_o+T} |f'| dt$$

From equation A.3, it is apparent that only the quadratic terms of f' need be retained in practice. If there are two variables in the flow, say f_1', and f_2', then the quadratics of f_1', and f_2', and also the cross products of f_1' and f_2' or $\overline{f_1' f_2'}$ must be retained. With these definitions in mind, the equation for a compressible flow in an open channel with time averaged behavior can be developed.

A.2 Development of the Compressible Flow Open Channel Equation with Time Averaged Behavior

In Chapter 3 the equation for the compressible flow in an open channel was given with little details of the derivation. At this point, the complete derivation of this equation including the time averaged terms will be developed with the following assumptions;

i) The bulk of the flow may be considered a continuum;

ii) The flow will be considered to be steady-state;

iii) There are no variations in the flow variables through the depth of flow;

iv) The pressure will be assumed isotropic;

v) No form of the shear will be assumed;

vi) The flow variables may be modeled as a time mean value and a fluctuational component, or;

$$f = \bar{f} + f'$$

vii) The flow equations will assume a unit width of flow.

The equations of motion may now be written with the above assumptions.

A.2.1 **Conservation of Mass**

The general integral form of the conservation of mass is as follows:

$$\int_V \{\frac{\partial \rho}{\partial t} + \frac{\partial}{\partial x_k}(\rho u_k)\} dV = 0 \qquad \text{(A.4)}$$

where:

ρ is the fluid density;

V is the fluid volume;

x_k is the spacial coordinates (x,y,z);

u_k is the velocity field (u,v,w); and,

t is the time.

Using assumption (ii), equation A.4 may be written as follows;

$$\int_V \{\frac{d}{dx_k}(\rho u_k)\} dV = 0 \qquad (A.5)$$

By using (iii);

$$\int_V \{\frac{d}{dx_k}(\rho u_k)\} dV = \int_o^h \{\frac{d}{dx}(\rho u)\} dy = 0$$

and (A.6)

$$\frac{d}{dx}(\rho u)\int_o^h dy = \frac{d}{dx}(\rho u h) = 0$$

Thus;

$$\frac{d}{dx}(\rho u h) = 0 \qquad (A.7)$$

where:

ρ is the density;

u is the convective velocity; and

h is the depth of flow:

From assumption (vii), equation A.8 may be written as;

$$\frac{d}{dx}\{(\bar{\rho} + \rho')(\bar{u} + u')(\bar{h} + h')\} = 0 \qquad (A.8)$$

Expanding A.8 and saving only the quadratic terms representing terms of the fluctuational variables;

$$\frac{d}{dx}\left[\bar{\rho}\,\bar{u}\,\bar{h}(1 + \frac{\overline{u'h'}}{\bar{u}\,\bar{h}} + \frac{\overline{\rho'h'}}{\bar{\rho}\,\bar{h}} + \frac{\overline{\rho'u'}}{\bar{\rho}\,\bar{u}})\right] = 0 \qquad (A.9)$$

A.2.2 **Conservation of Momentum**

The integral form of the momentum equation with no shear stress may be written as;

$$\int_V \{\frac{\partial}{\partial t}(\rho u_j) + \frac{\partial}{\partial x_k}(\rho u_j u_k)\} dV = \int_V (\frac{\partial \sigma_{ij}}{\partial x_i}) dV + \int_V (\rho f_j) dV \qquad (A.10)$$

where:

σ_{ij} is the stress acting on the volume; and,

f_j is the body force term acting over the volume.

By using (ii);

$$\int_V \{\frac{\partial}{\partial x_k}(\rho u_j u_k)\} dV = \int_V (\frac{\partial \sigma_{ij}}{\partial x_i}) dV + \int_V (\rho f_j) dV \qquad (A.11)$$

Assuming (iii) and using equation (A.7) gives;

$$\frac{d}{dx}\{\int_o^h (\rho u^2) dy\} = \frac{d}{dx}\{\int_o^h (\sigma_{ii}) dy\} + \int_o^h (\rho f) dy$$

or (A.12)

$$\rho u h \frac{du}{dx} = -\frac{d\sigma_{ii} h}{dx} + \rho f h$$

where:

σ_{ii} will be set equal to the hydrostatic pressure, P;

$P = -1/2 \rho g h \cos\theta$;

$f = g \sin\theta$.

Placing these parameters into equation (A.12) gives;

$$\rho u h \frac{du}{dx} = -\frac{d}{dx}(1/2\rho g h^2 \cos\theta) + \rho g h \sin\theta \qquad \text{(A.13)}$$

Examining the left hand side of equation (A.13);

$$\rho u h \frac{du}{dx} = (\bar{\rho} + \rho')(\bar{u} + u')(\bar{h} + h')\frac{d}{dx}(\bar{u} + u')$$

$$= \{\bar{\rho}\,\bar{h} + \overline{\rho' h'}\}\{\bar{u}\frac{d\bar{u}}{dx} + 1/2\frac{d\overline{u'^2}}{dx}\}$$

Thus, the net change of momentum flux through the control volume is;

$$\{\bar{\rho}\,\bar{h} + \overline{\rho' h'}\}\{\bar{u}\frac{d\bar{u}}{dx} + 1/2\frac{d\overline{u'^2}}{dx}\} \qquad \text{(A.13a)}$$

The pressure term may be evaluated as follows;

$$P = \bar{P} + P' = \frac{1}{2}(\bar{\rho} + \rho')(\bar{h} + h')g\cos\theta$$

and

$$PA = \frac{1}{2}(\bar{\rho} + \rho')(\bar{h} + h')^2 g\cos\theta$$

Thus,

$$(\bar{P} + P')(\bar{h} + h') = \frac{1}{2}g\cos\theta\{\bar{\rho}\,\bar{h}^2 + \bar{\rho}\,\overline{h'^2} + 2\bar{h}\,\overline{\rho' h'}\}$$

Now;

$$-\frac{dPh}{dx} = -\frac{g\cos\theta}{2}\frac{d}{dx}(\bar{\rho}\overline{h^2} + \bar{\rho}\overline{h'^2} + 2\bar{h}\,\overline{\rho'h'}) \qquad \text{(A.13b)}$$

which is the net pressure change across the control volume.

Finally, the body force term may be evaluated as follows;

$$\rho g h \sin\theta = (\bar{\rho} + \rho')(\bar{h} + h')g\sin\theta = (\bar{\rho}\,\bar{h} + \overline{\rho'h'})g\sin\theta.$$

Thus, the net body force acting over the control volume is;

$$(\bar{\rho}\,\bar{h} + \overline{\rho'h'})g\sin\theta \qquad \text{(A.13c)}$$

Combining (A.13a), (A.13b) and (A.13c), the conservation of momentum may be written as;

$$(\bar{\rho}\,\bar{h} + \overline{\rho'h'})\{\bar{u}\frac{d\bar{u}}{dx} + 1/2\frac{d\overline{u'^2}}{dx}\} = -\frac{g\cos\theta}{2}\frac{d}{dx}\{\bar{\rho}\overline{h^2} + \bar{\rho}\,\overline{h'^2} + 2\bar{h}\,\overline{\rho'h'}\}$$

$$+ (\bar{\rho}\,\bar{h} + \overline{\rho'h'})g\sin\theta \qquad \text{(A.13d)}$$

Dividing (A.13d) by $(\bar{\rho}\,\bar{h} + \overline{\rho'h'})$;

$$\bar{u}\frac{d\bar{u}}{dx} + 1/2\frac{d\overline{u'^2}}{dx} = -\frac{g\cos\theta}{2}\left[\frac{\frac{d}{dx}(\bar{\rho}\,\overline{h^2} + \overline{h'^2}\bar{\rho} + 2\bar{h}\overline{\rho'h'})}{(\bar{\rho}\,\bar{h} + \overline{\rho'h'})}\right] + g\sin\theta. \qquad \text{(A.14)}$$

The pressure term must once again be examined;

$$\frac{\frac{d}{dx}(\bar{\rho}\,\overline{h^2} + \bar{\rho}\overline{h'^2} + 2\bar{h}\,\overline{\rho'h'})}{\bar{\rho}\,\bar{h}(1 + \frac{\overline{\rho'h'}}{\bar{\rho}\,\bar{h}})}$$

Assuming that, $\frac{\overline{\rho' h'}}{\bar{\rho}\,\bar{h}} \ll 1$,

$$\frac{1}{\bar{\rho}\,\bar{h}(1 + \frac{\overline{\rho' h'}}{\bar{\rho}\,\bar{h}})} \simeq \frac{1}{\bar{\rho}\,\bar{h}}(1 - \frac{\overline{\rho' h'}}{\bar{\rho}\,\bar{h}})$$

Thus, the pressure term may be written as;

$$\frac{1}{\bar{\rho}\,\bar{h}}\frac{d}{dx}(\bar{\rho}\overline{h^2}) + \frac{1}{\bar{\rho}\,\bar{h}}\left[(1 - \frac{\overline{\rho' h'}}{\bar{\rho}\,\bar{h}})\frac{d}{dx}(\bar{\rho}\overline{h'^2} + 2\bar{h}\,\overline{\rho' h'})\right]$$

$$- \frac{\overline{\rho' h'}}{\bar{\rho}\,\bar{h}}\frac{d}{dx}(\bar{\rho}\overline{h^2}) \quad .$$

Placing this new form of the pressure into the momentum equation and re-arranging the terms;

$$\bar{u}\frac{d\bar{u}}{dx} = -1/2\frac{g\cos\theta}{\bar{\rho}\bar{h}}\frac{d}{dx}(\bar{\rho}\overline{h^2}) + g\sin\theta - \left[1/2\frac{d\overline{u'^2}}{dx}\right.$$

$$\left. + \frac{g\cos\theta}{2\bar{\rho}\,\bar{h}}\left[(1 - \frac{\overline{\rho' h'}}{\bar{\rho}\,\bar{h}})\frac{d}{dx}(\overline{h'^2}\,\bar{\rho} + 2\bar{h}\,\overline{\rho' h'}) - \frac{\overline{\rho' h'}}{\bar{\rho}\,\bar{h}}\frac{d}{dx}(\bar{\rho}\,\overline{h^2})\right]\right] \qquad \text{(A.15)}$$

The frictionless compressible open channel equation with time dependent behavior may be written as;

$$\bar{u}\frac{d\bar{u}}{dx} = -\frac{g\cos\theta}{2\bar{\rho}\,\bar{h}}\frac{d(\bar{\rho}\overline{h^2})}{dx} + g\sin\theta + \Phi \qquad \text{(A.16)}$$

where:

$$\Phi = -\left[1/2\frac{d\overline{u'^2}}{dx} + \frac{g\cos\theta}{2\bar{\rho}\,\bar{h}}\left[(1 - \frac{\overline{\rho'h'}}{\bar{\rho}\,\bar{h}})\frac{d}{dx}(\overline{h'^2}\,\bar{\rho} + 2\bar{h}\,\overline{\rho'h'}) - \frac{\overline{\rho'h'}}{\bar{\rho}\,\bar{h}}\frac{d}{dx}(\bar{\rho}\overline{h^2})\right]\right.$$

If it is assumed that Φ is small; (this will be discussed in detail in the next section), the compressible open channel equation may be written as;

$$\bar{\rho}\,\bar{h}\,\bar{u}\,\frac{d\bar{u}}{dx} = -1/2g\cos\theta\frac{d}{dx}(\bar{\rho}\overline{h^2}) + \bar{\rho}g\bar{h}\sin\theta \qquad \text{(A.17)}$$

Using A.9, the equation for a compressible substance in an open channel becomes;

$$-\rho_p U^2\frac{d\,\nu h}{dx} = -\rho_p\nu gh\cos\theta\frac{dh}{dx} - 1/2\,\rho_p gh^2\cos\theta\frac{d\nu}{dx}$$

$$+\rho_p\nu gh\sin\theta$$

Using assumption (v), and adding the shear term;

$$-\frac{U^2}{gh\cos\theta}\frac{d\,\nu h}{dx} = -\frac{dh}{dx} - 1/2\frac{h}{\nu}\frac{d\nu}{dx} - \frac{\tau_w I\!P}{\rho_p\nu gh\cos\theta} + \tan\theta$$

Excluding the fluctuating terms the open channel equation for a compressible substance may be written as;

$$\frac{\tau_w I\!P}{\rho_p\nu gh\cos\theta} = \tan\theta + \frac{dh}{dx}(Fr^{*2}-1) + \frac{h}{\nu}\frac{d\nu}{dx}(Fr^{*2} - 1/2) \qquad \text{(A.18)}$$

where:

τ_w is the wall shear;

IP is the wetted perimeter;

ρ_p is the particle density;

ν is the solid fraction;

g is gravity;

h is the depth of flow;

θ is the chute angle;

Fr^{*2} is the Froude Number = $\frac{U^2}{gh\cos\theta}$.

which is equation 3.12.

A.3. **Possible Explanations for the Trends in the Shear Results**

This section will present possible explanations for the reason that the friction coefficient, μ, varies from the Coulomb friction value. This Coulomb friction value is what might be expected for the motion of two solids in contact. First, the actual experimental results will be examined for possible errors in the calculation of the shear. Next, possible physical mechanisms for the variation of the friction coefficient from the Coulombic value will be presented.

First, the error associated with the determination of the friction factor will now be presented. The mass flow rate is a quantity which can be determined very accurately. The mass flow rate was measured by two methods and the values of these two methods fall consistently between 3% of one another. The measurement of the depth of flow is a quantity

which can be measured within 1/2 of a particle diameter for the low-velocity, high density flows. As the density decreases, however, the determination of the depth of flow becomes more difficult. Depending on what is taken to the actual free-surface, the value of the depth of flow may vary as much as 20%. If a consistent method is used for determining the depth of flow, as was done in the present investigation, this variation can be taken to be 5%. The mass of material captured between the plates to determine the solid fraction was a consistent measurement. The fluctuations in this measurement were at most 5%. These are the basic quantities measured in the flow. The chute angle is a quantity which had negligible error.

To summarize these errors, the preceding description is shown as follows;

i) The mass flow rate can be measured as,

$$\dot{m} = \overline{\dot{m}}(1 \pm .03);$$

ii) The depth of flow can be measured as,

$$h = \bar{h}(1 \pm .05); \textit{and},$$

iii) The mass captured between the plates can be measured as,

$$M = \overline{M}(1 \pm .05).$$

With these estimates of the basic quantities of the flow, estimates of the flow parameters may be made. Using the standard means of determining the total error associated with combinations of quantities with their own error, the flow parameters can be estimated with the following degree of confidence;

i) The bulk velocity can be calculated as,

$$U = \overline{U}(1 \pm .058);$$

ii) The bulk density can be calculated as,

$$\nu = \overline{\nu}(1 \pm .071);$$

iii) The Froude Number can be calculated as,

$$Fr^{*2} = \overline{Fr^{*2}}(1 \pm .096); \textit{and},$$

iv) The friction coefficient can be calculated as,

$$\frac{\tau_w}{\rho_p \nu g h \cos\theta} = \mu = \overline{\mu}(1 \pm .20).$$

The actual calculation of these parameters is probably better than these estimates show. Even with these high values for the error associated with the flow parameters, the friction coefficient still appears to increase.

Another aspect in the determination of the friction coefficient con-

cerns the possible existence of an inherent error in the equation used to calculate this coefficient. Considering first, the assumption of no variation in the flow variables through the depth of flow in equation A.18, one may conclude that this will have a minor effect only, as Coulomb Friction is velocity independent and the profiles are not expected to change drastically along the direction of flow. Next, equation A.15 shows that if the time dependent values of the flow variables are included in the analysis, an extra "Reynold Stress" term, Φ, should be included in the basic flow equation. During the derivation of equation A.18, this term was assumed to be small. At this point, estimates of Φ will be made. The measurement of the components of Φ are not possible; however, by using the computational results of Campbell and Gong (1985), an estimate of this term can be made. From Campbell and Gong a reasonable estimate for Φ to the total stresses in a granular flow can be at most 10%. This is not a large enough variation to account for the drastic increase seen in the friction coefficient. It may therefore be concluded that these effects would not change the observed trends of the friction coefficient and that the increase in the friction coefficient is not due to experimental or computational error.

To further prove that the increase in the friction coefficient is real, some results for the friction coefficient as measured with a shear cell is shown in figure A.1. The figure shows calculated values of the friction coefficient using a simplified form of equation A.15 and measured values of the friction from the shear cell as a function of the Froude Number.

Figure A.1 clearly shows that the measured and calculated value of the friction coefficient are well above the Coulomb Friction value and also that the calculated value of the friction coefficient closely correlates to the value measured by the shear cell for a given Froude Number. It seems apparent that the friction coefficient actually does increase with the Froude Number and the Coulomb Friction concept can not be used to predict the wall shear for the entire ranges of granular material flows.

It seems obvious that the ratio between the shear force and the normal force does increase with Froude Number. An attempt to show possible reasons for this increase will now be given. Deformation of the individual particles and deformation of the wall during a particle collision with the wall could be one explanation for the increase in the friction coefficient.

The general procedure for evaluating the collision of two spheres by using Hertz Impact Theory. (Some caution needs to be used when expanding this theory for a sphere in contact with a flat plate. The assumptions used in the derivation of the Hertz Impact Theory is that the duration of impact is large compared with the lowest mode of vibration of the sphere. This may not be true for the impact of a sphere with an infinite plate. Goodier, Jahsman and Ripperger (1959) studied this problem and found that the Hertz Impact Theory predicts this problem within a reasonable margin for the present consideration.) By using this theory, it can be shown for a glass sphere on an aluminum wall, the wall

can deform as much as 2% of the total diameter. This may be enough deformation to cause the observed increase in the friction coefficient as the fluctuational velocity increases.

Even though there is no clear explanation for the mechanism leading to the increase in the friction, the present study shows that an increase does occur. The actual mechanism controlling this phenomena will be left for later studies.

APPENDIX B

B.1 **General Comments**

The development of a convective heat transfer equation for granular materials is shown in this appendix. This equation is derived as a possible means for explaining the convective heat transfer characteristics of granular materials. The experimental procedures that were followed to obtain the flow variables and the film coefficient are not adequate to completely confirm this equation, but the general trends that are seen for the film coefficient are predicted by this equation.

The concept used to derive this equation are analogous to the Prandtl's modification of the Reynold's analogy. The idea for the development of this equation is that as a particle comes in contact with the heating plate, the heat from the plate is transferred to the particle through a gas film layer next to the heating plate. This process is the one that Sullivan and Sabersky (1975) used to describe the heat transfer to a packed granular material moving past a heating plate. Next, as the particle leaves the heating plate, it carries with it an elevated temperature that was acquired while in contact with the heating plate. As soon as the particle leaves the heating plate, the particle begins to transmit its acquired temperature to the gas or the particles which are not "close" to the heating plate. This process causes a diffusion of the energy/heat from the heating plate to its surrounding environment by using the particles as an exchange medium in addition to the gas layer

next to the heating plate. A graphical representation of this process is shown in Figure B.1.

The process which was just described is analogous to the transfer of momentum in a turbulent shear layer. As a particle comes in contact with the wall, shear reduces the tangential momentum of of the particle. As the particle moves a distance δ from the wall, it comes in contact with particles of higher velocity parallel to the wall if a shear layer is present in the flow. Since this particle is at a lower average velocity than the particles a distance δ from the wall, momentum is exchanged between these particles.

Bagnold used this concept to produce his form of the stresses developed in a simple granular shear flow:

$$\tau = \rho_p \, f\,(\nu) d^2 (du/dy)^2 \qquad \text{(B.1)}$$

as mentioned earlier. It was also mentioned that this is a similar form for the turbulent shear stress for a Newtonian Fluid. The concept used to develop the equation for the convective heat transfer to a granular material, makes use of the fact that there are similarities between the process described by Bagnold for the momentum exchange in a simple granular shear flow and the process described here for the transfer of heat in a flowing granular material.

B.2 **Convective Heat Transfer to a Granular Material**

Now by using the concepts that have been described, the shear stress for a granular material may be represented as;

$$\tau = \rho_p \, \varepsilon \, du/dy \tag{B.2}$$

where:

τ is the shear stress;

ρ_p is the solid fraction;

du/dy is the shear rate; and,

ε is the turbulent eddy viscosity.

The turbulent eddy viscosity, ε, is defined as:

$$\varepsilon = f(\nu) \, d^2 \, (du/dy),$$

which makes Equation B.1 correspond with Equation B.2.

The turbulent heat flux may also be represented in a similar form as B.2. Assuming that the mechanism for transporting momentum is similar to the mechanism for transporting heat, the turbulent heat flux equation may be represented as:

$$q'' = -\rho_p \, c_p \, \varepsilon_h \, (dT/dy) \tag{B.3}$$

where:

q'' is the heat flux;

ρ_p is the solid density;

c_p is the bulk specific heat;

dT/dy is the temperature gradient; and,

ε_h is the turbulent eddy diffusivity.

When a particle is within some distance δ from the heating plate, it is assumed that the Sullivan and Sabersky (1975) correlation will hold. Outside δ, the above forms for the shear and the heat flux will be assumed to be valid. Thus, using a Reynold's analogy at points beyond δ,

$$\frac{\tau_\delta c_p \varepsilon_h}{U - U_\delta} = \frac{q''_\delta \varepsilon}{T_\delta - T} \tag{B.4}$$

where:

τ_δ is the shear at $y = \delta$;

U_δ is the velocity at $y = \delta$;

U is the freestream velocity;

$\frac{\varepsilon}{\varepsilon_h}$ is the "turbulent Prandtl Number;

q''_δ is the heat flux at $y = \delta$;

T_δ is the temperature at $y = \delta$

T is the bulk temperature; and,

c_p is the bulk specific heat.

It is assumed that the shear and the heat flux do not vary from the heating plate to δ; thus,

$$\frac{\tau_o c_p \varepsilon_h}{U - U_\delta} = \frac{q_o'' \varepsilon}{T_\delta - T} \tag{B.5}$$

The heat flux from the heating plate to δ is defined as the film coefficient as defined by Sullivan and Sabersky (1975);

$$q_o'' = h_s(T_p - T_\delta). \tag{B.6}$$

where:

h_s is the film coefficient as defined by Sullivan and Sabersky (1975); and,

T_p is the plate temperature.

The definition of the film coefficient will now be used;

$$h = \frac{q''}{(T_p - T)} \tag{B.7}$$

Using Equation B.6, Equation B.7 becomes,

$$h = h_s\left(\frac{T_p - T_\delta}{T_p - T}\right) \tag{B.8}$$

and also using Equations B.5 and B.7,

$$h = \frac{\tau_o c_p}{U - U_\delta}\left[\frac{T_\delta - T}{T_p - T}\right]\left(\frac{\varepsilon_h}{\varepsilon}\right) = \frac{\tau_o c_p}{U - U_\delta}\left[1 - \frac{T_p - T_\delta}{T_p - T}\right]\left(\frac{\varepsilon_h}{\varepsilon}\right) \qquad \text{(B.9)}$$

Now solving these two equations for h gives:

$$h = \frac{\tau_o c_p}{U - U_\delta}\left[1 - \frac{h}{h_s}\right]\left(\frac{\varepsilon_h}{\varepsilon}\right) \qquad \text{(B.10)}$$

or;

$$h = \frac{1}{\frac{1}{h_s} + \frac{(U - U_\delta)\,\varepsilon}{\tau_o c_p \varepsilon_h}} \qquad \text{(B.11)}$$

Making the assumption;

$$\tau_o = \mu\, \rho_p \nu g h \cos\theta \qquad \text{(B.12)}$$

where:

μ is the Coulomb Friction coefficient;

ρ_p is the solid density;

ν is the solid fraction;

g is gravity;

h is the depth of flow; and,

θ is the chute angle.

Equation B.11 may be written as;

$$h = \frac{1}{\frac{1}{h_s} + \frac{(U - U_\delta)\varepsilon / \varepsilon_h}{\mu\, \rho_p \nu c_p g h \cos\theta}} \qquad \text{(B.13)}$$

Multiplying the second term in the denominator by;

$$\frac{\overline{U^2}}{\overline{U^2}} \frac{L}{L} \frac{k}{k} \frac{\nu_c}{\nu_c} = 1$$

gives;

$$h = \frac{1}{\frac{1}{h_s} + \frac{(U - U_\delta)}{\mu \overline{U}} \left(\frac{\varepsilon}{\varepsilon_h}\right)\left(\frac{\overline{U^2}}{ghcos\,\theta}\right)\left(\frac{k}{\rho_p \nu_c}\right)\left(\frac{\nu_c}{\nu}\right)\left(\frac{L}{k}\right)\frac{1}{\overline{U}L}} \qquad \text{(B.14)}$$

and by regrouping these terms;

$$h = \frac{1}{\frac{1}{h_s} + \frac{(U - U_\delta)}{\mu \overline{U}} \left(\frac{\varepsilon}{\varepsilon_h}\right)\left(Fr^{*2}_{\nu/\nu_c}\right)\left(\frac{\alpha}{\overline{U}L}\right)\left(\frac{L}{k}\right)} \qquad \text{(B.15)}$$

where:

$\overline{U}$ is the bulk velocity;

Fr^{*2}_{ν/ν_c} is the densinometric Froude Number = $\frac{\nu_c}{\nu} \frac{\overline{U^2}}{ghcos\,\theta}$; and,

α is the bulk diffusivity = $\frac{k}{\rho_p \nu_c}$

Now noting that $\frac{\alpha}{\overline{U}L}$ is the Peclet Number and multiplying by $\frac{d}{k_g}$;

$$\overline{Nu_d^*} = \frac{hd}{k_g} = \frac{1}{\frac{k_g}{h_s d} + \left\{\frac{U - U_\delta}{\mu \overline{U}} \left(\frac{\varepsilon}{\varepsilon_h}\right)\left(\frac{L}{d}\right)\left(\frac{k_g}{k}\right) \frac{Fr_{\nu/\nu_c}}{Pe}\right\}} \qquad \text{(B.16)}$$

and substituting for h_s;

$$\overline{Nu_d^*} = \frac{1}{\chi + \frac{\sqrt{\pi}}{2}\frac{1}{\sqrt{Pe^*}}\left(1 + \frac{\beta^*}{\mu}\left(\frac{\varepsilon}{\varepsilon_h}\right)\frac{(Fr^{*2}_{\nu/\nu_c})^*}{\sqrt{Pe^*}}\right)} \qquad \text{(B.17)}$$

where:

$\overline{Nu_d^*}$ is the granular Nusselt Number;

χ is an experimental parameter;

$\overline{Pe^*}$ is the granular Peclet Number = $(\frac{d}{L})^2(\frac{k}{k_g})^2(\frac{\overline{U}L}{\alpha})$;

β^* is taken to be a constant = $\frac{2}{\sqrt{\pi}}(\frac{U - U_\delta}{\overline{U}})$

μ is the Coulomb Friction coefficient;

$\frac{\varepsilon}{\varepsilon_h}$ is the "turbulent" Prandtl Number;

$(Fr^{*2}_{\nu/\nu_c})^*$ is the densinometric Froude Number multiplied by $(\frac{d}{L})(\frac{k}{k_g})$;

d is the particle diameter;

L is the length of the heating plate;

k is the bulk conductivity;

k_g is the conductivity of the interstitial fluid; and,

α is the bulk diffusivity.

This is equation (4.3) of Chapter 4. Further developments can be made by using the fact that the heat transfer is related to the wall shear by use of the friction factor C_f. Returning to Equation B.11

$$h = \frac{1}{\frac{1}{h_s} + \frac{U - U_\delta}{\tau_o c_p}\left(\frac{\varepsilon}{\varepsilon_h}\right)}$$

and noting that;

$$C_f = \frac{\tau_o}{1/2\rho_p \nu \overline{U^2}}, \tag{B.18}$$

The following may be written;

$$h = \frac{1}{\frac{1}{h_s} + \frac{U - U_\delta}{1/2\rho_p \nu c_p C_f \overline{U^2}}\left(\frac{\varepsilon}{\varepsilon_h}\right)} \tag{B.19}$$

and by multiplication of identities;

$$h = \frac{1}{\frac{1}{h_s} + \frac{U - U_\delta}{1/2\ \overline{U}\ C_f}\left[\frac{\frac{k}{\rho_p \nu_c c_p}}{\overline{U}L}\right]\left(\frac{\nu_c}{\nu}\right)\left(\frac{L}{k}\right)\left(\frac{\varepsilon}{\varepsilon_h}\right)} \tag{B.20}$$

which may be written as;

$$h = \frac{1}{\frac{1}{h_s} + \frac{2(U - U_\delta)}{\overline{U}}\ \frac{1}{Pe}\left(\frac{\nu_c}{\nu}\right)\frac{1}{C_f}\left(\frac{L}{k}\right)\frac{\varepsilon}{\varepsilon_h}}. \tag{B.21}$$

Using the same parameters as with Equation B.17;

$$\overline{Nu_d^*} = \frac{1}{\chi + \frac{\sqrt{\pi}}{2}\frac{1}{\sqrt{Pe^*}}\left[1 + \beta^*\left(\frac{\varepsilon}{\varepsilon_h}\right)\frac{1}{C_f^*}\frac{1}{\sqrt{Pe^*}}\right]}$$

where:

C_f^* is the friction factor multiplied by $\left(\frac{\nu}{\nu_c}\right)\left(\frac{L}{d}\right)\left(\frac{k_g}{k}\right)$

Pe_L^* is the Peclet Number; $\frac{UL}{\alpha}$.

This form of the convective heat transfer equation makes direct use of the wall shear. This might actually be more useful than equation B.17, but does not give the same insight into the flow parameters effect on the convective heat transfer as does equation B.17. This equation does not rely on any *form* for the wall shear and thus may be more practical in nature.

BIBLIOGRAPHY

Augenstein, D. A., and Hogg, R., "Friction Factors for Powder Flow," Powder Technology, 10, 43, 1974.

Augenstein, D. A., and Hogg, R., "An Experimental Study of the Flow of Dry Powders on Inclined Surfaces," Powder Technology, 19, 205, 1978.

Bagnold, R. A., "Experiments on a Gravity Free Dispersion of Large Solid Spheres in a Newtonian Fluid," Proc. Roy. Soc., 225, 49, 1954.

Bagnold, R. A., "The Flow of Cohesionless Grains in Fluids," Phil. Trans. R. Soc. London, Ser. A, 249, 235, 1956.

Bagnold, R. A., "The Shearing and Dilatation of Dry Sand and the "Singing Mechanism," Proc. Roy. Soc. A., 295, 219, 1966.

Bailard, J., "An Experimental Study of Granular - Fluid Flow," Ph.D. Thesis, University of California, San Diego, 1978.

Bauer, R., and Schlunder, E. U., "Effective Radial Thermal Conductivity of Packings in Gas Flow. Part I. Convective Transport Coefficient," Int. Chem. Eng., Vol. 18, No.2, 181, 1978a.

Bauer, R., and Schlunder, E. U., "Effective Radial Thermal Conductivity of Packing in Gas Flow. Part II. Thermal Conductivity of the Packing without Gas Flow," Int. Chem. Eng., Vol. 18, No.2, 189, 1978b.

Botterill, J. S. M., and Williams, J. R., "The Mechanism of Heat Transfer To Gas-Fluid Beds," Trans. Instn. Chem. Engrs., Vol. 41, 217, 1963.

Botterill, J. S. M., Butt, M. H. D., Cain, G. L., and Redish, K. A., "The Effect of Gas and Solids Thermal Properties on the Rate of Heat Transfer to Gas-Fluidized Beds," Int. Symp. on Fluidization, Netherlands Univ. Press, Amsterdam, 422, 1967.

Brennen, C. E., and Pearce, J. C., "Granular Material Flow in Two-Dimensional Hoppers," J. App. Mech., 100, 43, 1978.

Brennen, C. E., Sieck, K., and Paslaski, J., "Hydraulic Jumps in Granular Materials," Powder Technology, 35, 31, 1983.

Campbell, C. S., "Shear Flows of Granular Materials," Ph.D. Thesis, California Institute of Technology, Pasadena, Ca., 1982.

Campbell, C. S., and Brennen, C. E., "Computer Simulations of Granular Shear Flows," J. Fluid Mechanics, to appear, 1985a.

Campbell, C. S., and Brennen, C. E., "Chute Flows of Granular Materials: Some Computer Simulations," J. App. Mech., to appear, 1985b.

Campbell, C. S., Brennen, C. E. and Sabersky, R. H., "Flow Regimes in Inclined Open Channel Flows of Granular Materials," to be submitted.

Campbell, C. S., and Gong, A., "The Stress Tensor in a Two Dimensional Granular Flow," J. Fluid Mech., to appear, 1985.

Donskov, S. V., "Heat Loss from Round Cylinders and Transverse Flow of Loose Body," Teploenergetika, Moscow, USSR, Vol. 5, No. 10, 67, 1958a.

Donskov, S. V., "Heat Transfer from Bundles of Pipe in Transverse Flow of Grainy Material," Teploenergetika, Moscow, USSR, Vol. 5, No. 11, 1958b.

Gabor, J. D., "Wall-to-Bed Heat Transfer in Fluidized and Packed Beds," Chem. Eng. Progress Symp. Series, No. 105, Vol. 66, 76, 1970.

Goodier, J. N., Jahsmen, W. E., and Ripperger, E. A., "An Experimental Surface-Wave Method for Recording Force-Time Curves in Elastic Impacts," J. Appl. Mech., vol. 26, 3, 1959.

Hanes, D. M., and Inman, D. L., "Observations of Rapid Flowing Granular Materials" submitted to J. Fluid Mechanics, 1984.

Heyde, M., and Klocke, H., "Heat Transfer between Fluidized Beds and Heat Exchanger Installations," Int. Chem. Eng., Vol. 20, No. 4, 583, 1980.

Hill, H. M., "Bed Forms Due to a Fluid Stream," J. Hydr. Div. Proc. ASCE, 92, 127, 1966.

Hui, K., and Haff, P. K., "Rapid Grain Flow in Verticle Channels," submitted J. Fluid Mech., 1984.

Ishida, M., Hantano, H., and Shirai, T., "The Flow of Solid Particles in an Aerated Inclined Channel," Powder Technology, 27, 7, 1980.

Jenkins, J. T., and Savage, S. B., "A Theory for the Rapid Flow of Identical Smooth, Nearly Elastic Particles," J. Fluid Mech., 130, 187, 1983.

Jenike, A. W., and Shield, R. T., "On the Plastic Flow of Coulomb Solids beyond Original Failure," J. App. Mech., 26, 599,1959.

Kubie, J., and Broughton, J., "A Model of Heat Transfer in Gas Fluidized Beds," Int. J. Heat and Mass Transfer, Vol. 18, 289, 1975.

Lun, C.K.K., and Savage, S.B., "A Simple Kinetic Theory for Granular Flow of Rough, Inelastic, Sphericle Particles," J. App. Mech. to appear, 1985.

Lun, C.K.K., Savage, S.B., Jeffrey, D.J., and Chepurniy, N., "Kinetic Theories for Granular Flow: Inelastic Particles in a Couette Flow and Slightly Inelastic Particles in a General Flow Field," J. Fluid Mech., 140, 223, 1984.

Martin, H., "Fluidized Bed Heat Exchangers," *Seminar on Advances in* Heat Exchangers, Dubrovnik, Hemisphere Publ. Corp., Washington, 1981.

Mickley, H. S., and Trilling, C. A., "Heat Transfer Characteristics of Fluidized Beds," Industrial and Engineering Chemistry, Vol. 41, No. 6, 1949.

Muchowski, E., "Heat Transfer from the Bottom of Vibrated Vessels to Packing of Spheres at Atmospheric Pressure and under Vacuum," Int. Chem. Eng., Vol. 20, No. 4, 564, 1980.

Muchowski, E., and Mannchen, E., "Heat Transfer from the Bottom of Vibrated Vessels to Stirred Packing of Spheres at Atmospheric Pressure and under Vacuum," Int. Chem. Eng., Vol. 20, No. 4, 577, 1980.

Nguyen, T., "Studies of the of Granular Materials," Ph.D. Thesis, California Institute of Technology, 1979.

Nguyen, T., Brennen, C. E., and Sabersky, R. H., "Gravity Flow of Granular Material in Conical Hoppers," J. App. Mech., 46, 529, 1979.

Pearce, J. C., and Sabersky, R. H., "Thermal Wake and Separation Point for the Flow of a Granular Medium around a Heated Cylinder," Letters in Heat and Mass Transfer, 4, 1, 1977.

Ridgeway, K., and Rupp, R., "Flow of Granular Material down Chutes," Chem. Proc. Eng., 52, 82, 1970.

Savage, S. B., "Gravity Flow of Cohesionless Granular Material in Chutes and Channels," J. Fluid. Mech., Vol. 92, Part 1, 53, 1979.

Savage, S. B., "The Mechanics of Rapid Granular Flows," Adv. Appl. Mechanics, 24, 289, 1984.

Savage, S. B., and Jeffrey, D. J., "The Stress Tensor in a Granular Flow at High Shear Rates," J. Fluid Mech., 110, 255, 1981.

Savage, S. B., and Sayed, M., "Stresses Developed by Dry Cohesionless Granular Material Sheared in an Annular Shear Cell," submitted to J. Fluid Mech., 1982.

Sayed, M. and Savage, S. B., "Rapid Gravity Flow of Cohesionless Granular Materials down Inclined Chutes," submitted to J. App. Math. Phys., 1982.

Schlunder, E. U., "Particle Heat Transfer," Proc. Seventh Int. Heat Transfer Conf. Munich, 1, Hemisphere Pub. Co., 1982.

Scheiwiller, T., and Hutter, K., "On Granular Flow of Cohesionless Granular Materials Down an Inclined Chute," Laboratory of Hydraulics, Hydrology and Glaciology, ETH Zurich, 1984.

Spelt, J. K., Brennen, C. E.,and Sabersky, R. H., "Heat Transfer to Flowing Granular Material," Int. J. Heat and Mass Transfer, Vol. 25, No. 6, 791, 1982.

Sullivan, W. N., "Heat Transfer to Flowing Granular Materials," Ph.D. Thesis, California Institute of Technology, Pasadena, Ca., 1973.

Sullivan, W. N., and Sabersky, R. H., "Heat Transfer to a Flowing Granular Media," Int. J. Heat and Mass Transfer, Vol. 18, 97, 1975.

Syromyatnikov, N. I., "Conductive Component of Heat Transfer," Kirov Ural Polytechnic Institute, Sverdlovsk, Vol. 21, No. 6, 979, 1971.

Takahashi, K., "On Dynamic Properties of Granular Mass," Geophysical Mag., 11, 165, 1937.

Tolmachev, E. M., Korolev, V. N., and Syromyatnikov, "Structure of a Fixed and Fluidized Bed of Granular Material Near an Immersed Surface," Kirov Ural Polytechnical Institute, Sverdlovsk, Vol. 21, No. 6, 973, 1971.

Wunschmann, J., and Schlunder, E. U., "Heat Transfer from Heated Surfaces to Spherical Packings," Int. Chem. Eng., Vol. 20, No. 40, 555, 1980.

Yoshida, K., Kunii, D., and Levenspiel, O., "Heat Transfer Mechanisms between Surfaces and Fluidized Beds," Int. J. Heat and Mass Transfer, Vol. 12, 529, 1969.

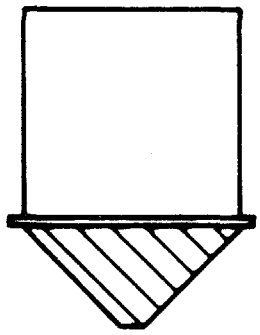

HOPPER-BIN CONFIGURATION

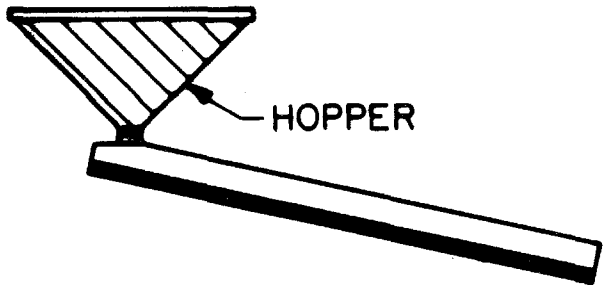

HOPPER-CHUTE CONFIGURATION

Figure 3.1 Schematic of hoppers and chutes.

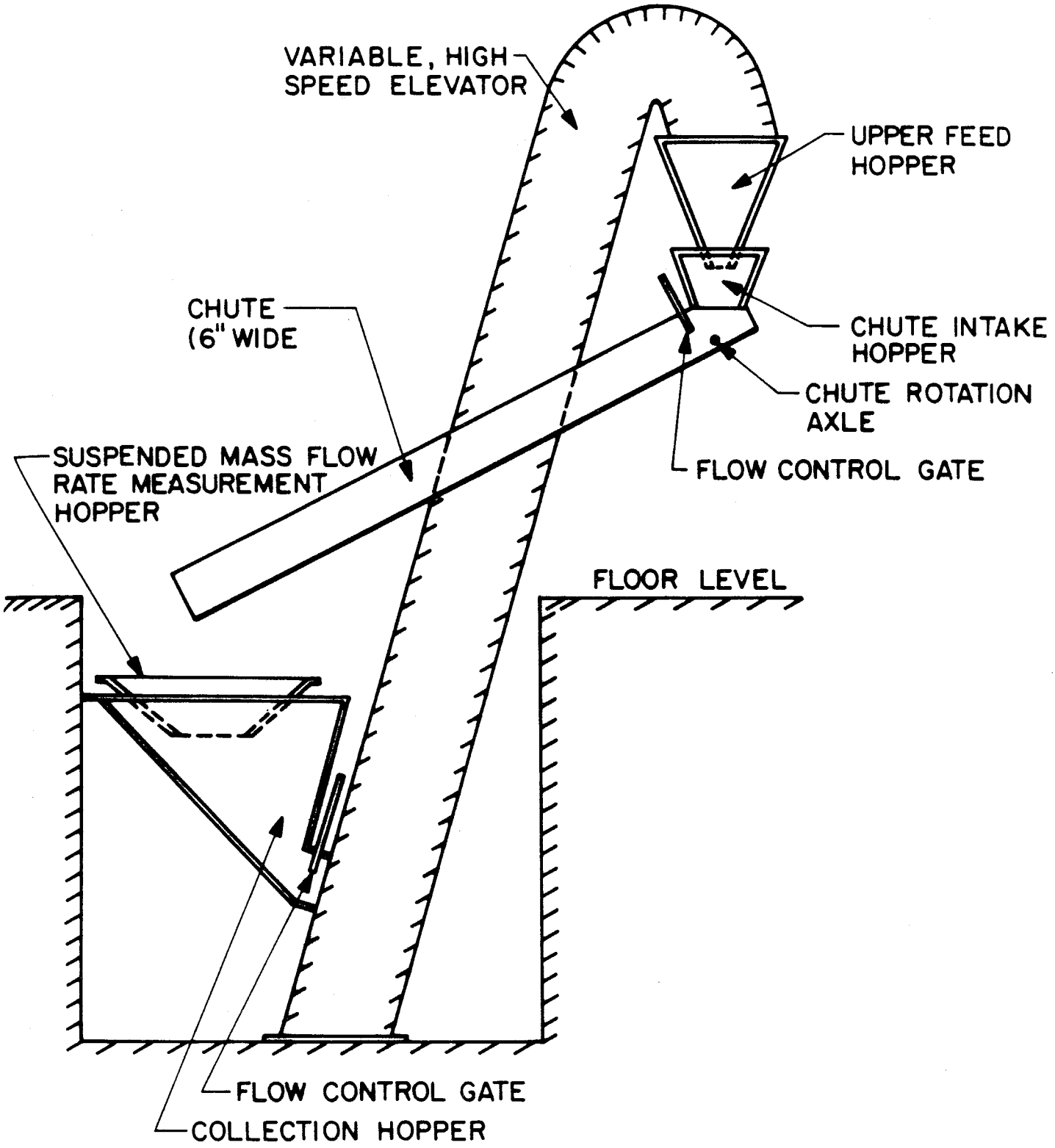

Figure 3.2 Schematic of the experimental facility.

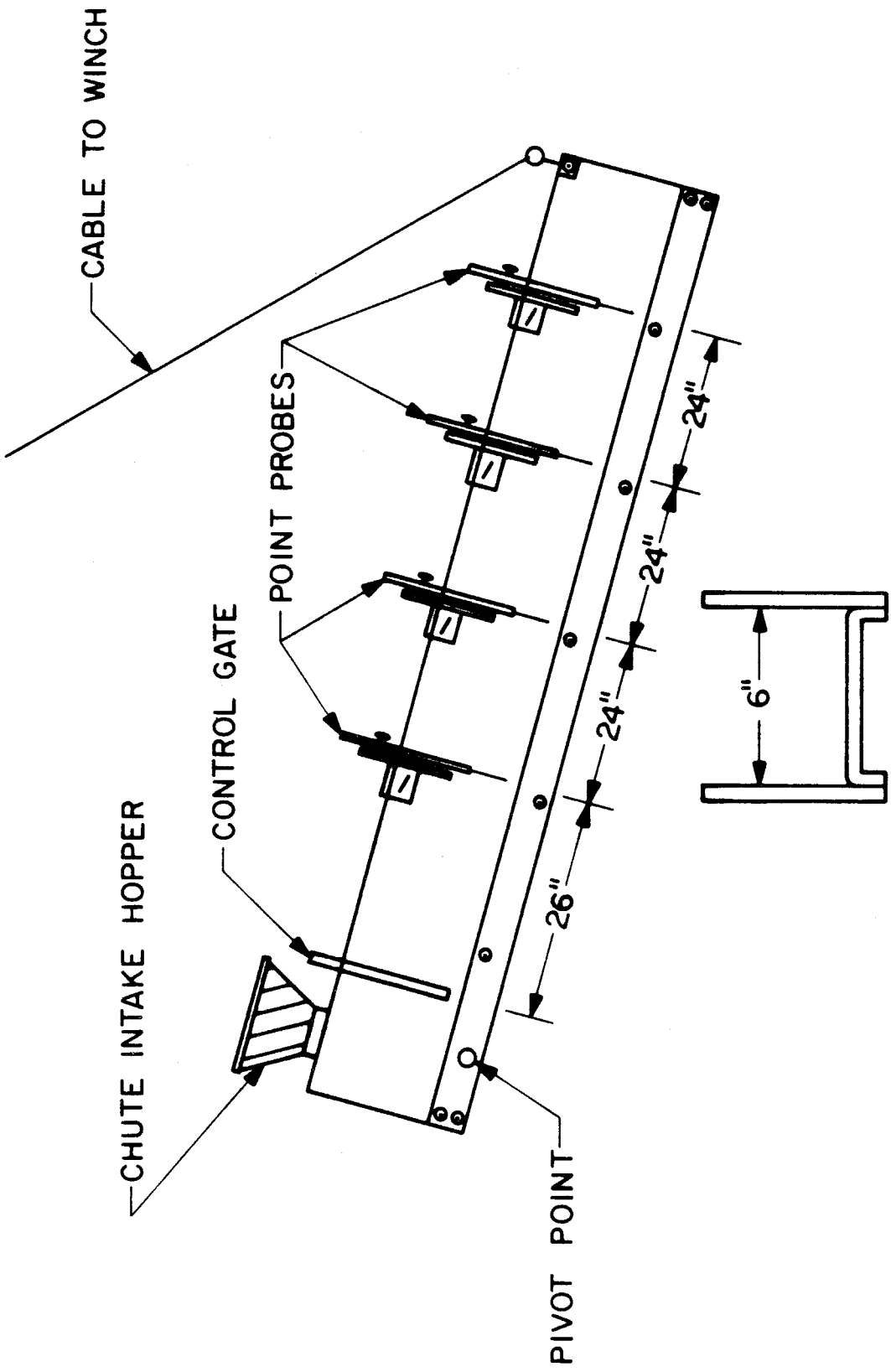

Figure 3.3 Schematic of the test chute.

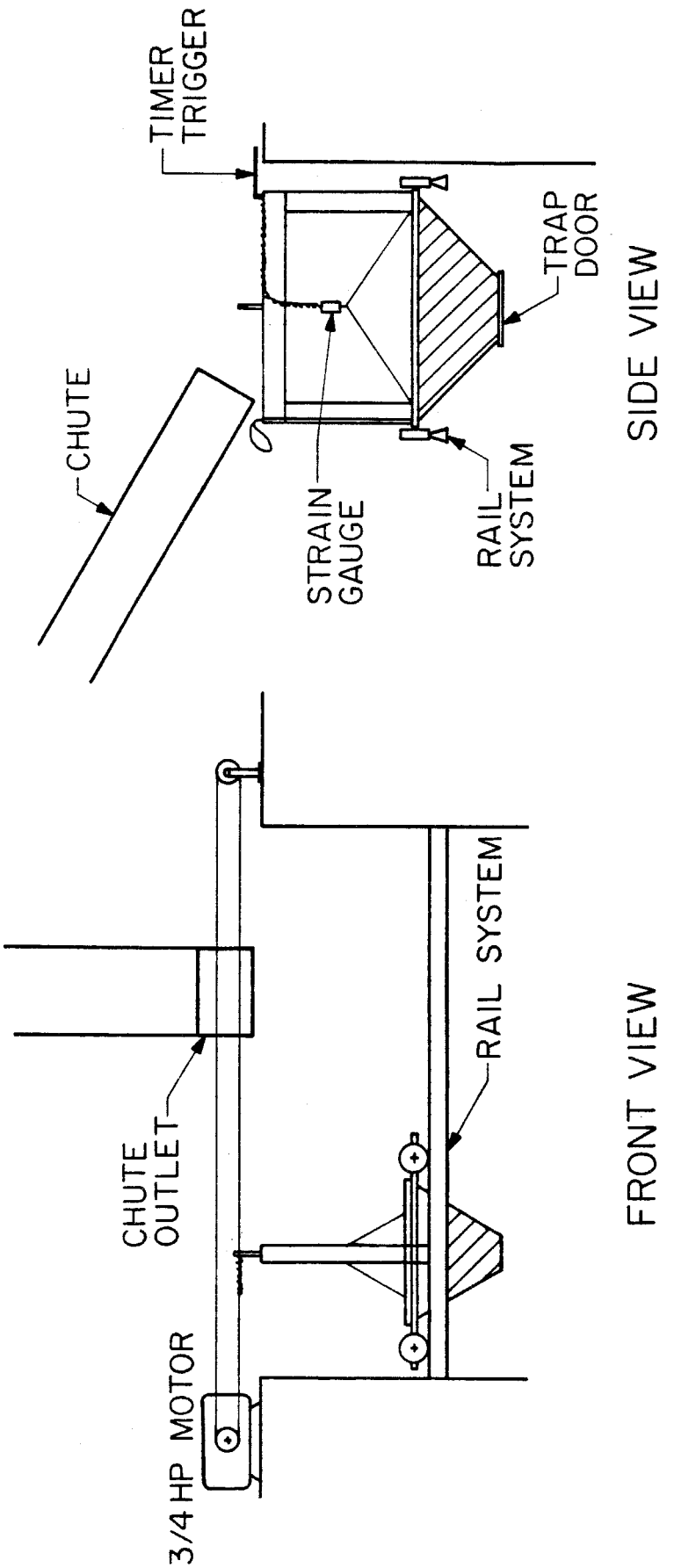

Figure 3.4 Schematic of the movable hopper for aquiring mass flow readings.

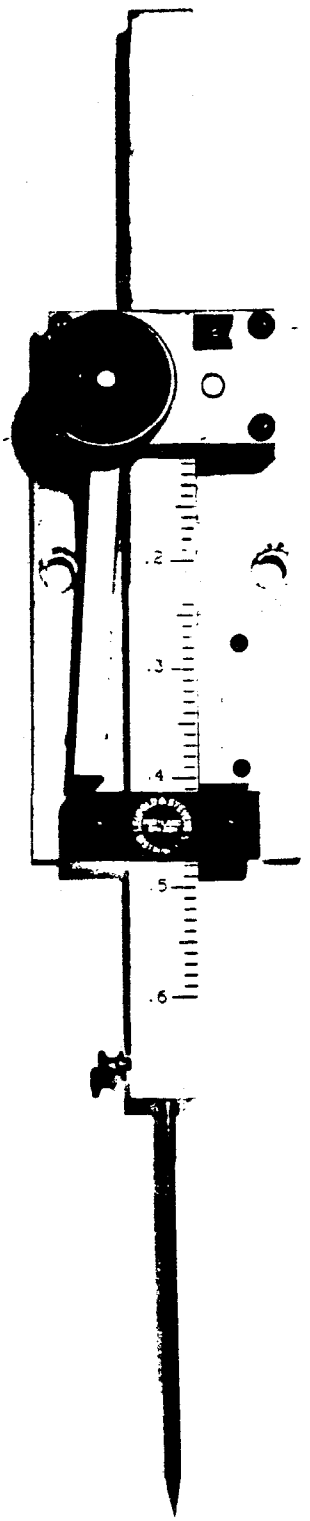

Figure 3.5 Photograph of point probes. (From Campbell (1982).)

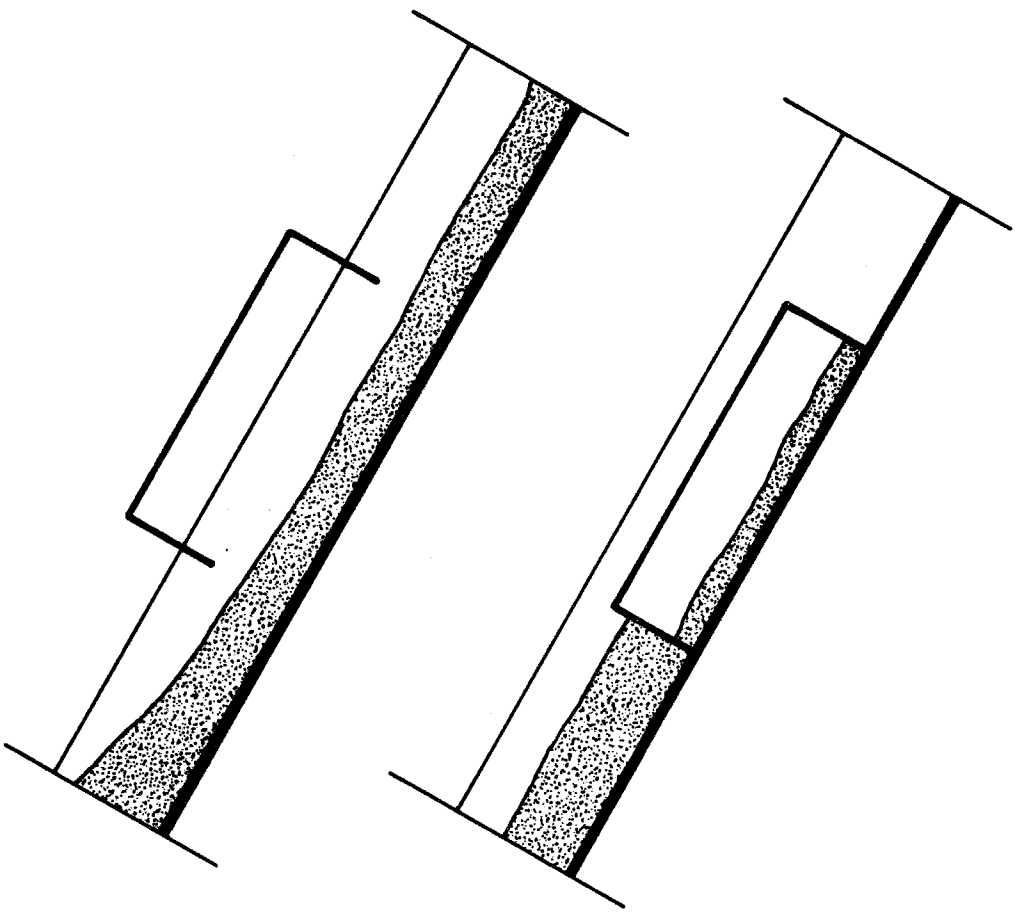

Figure 3.6 Schematic of density gauge.

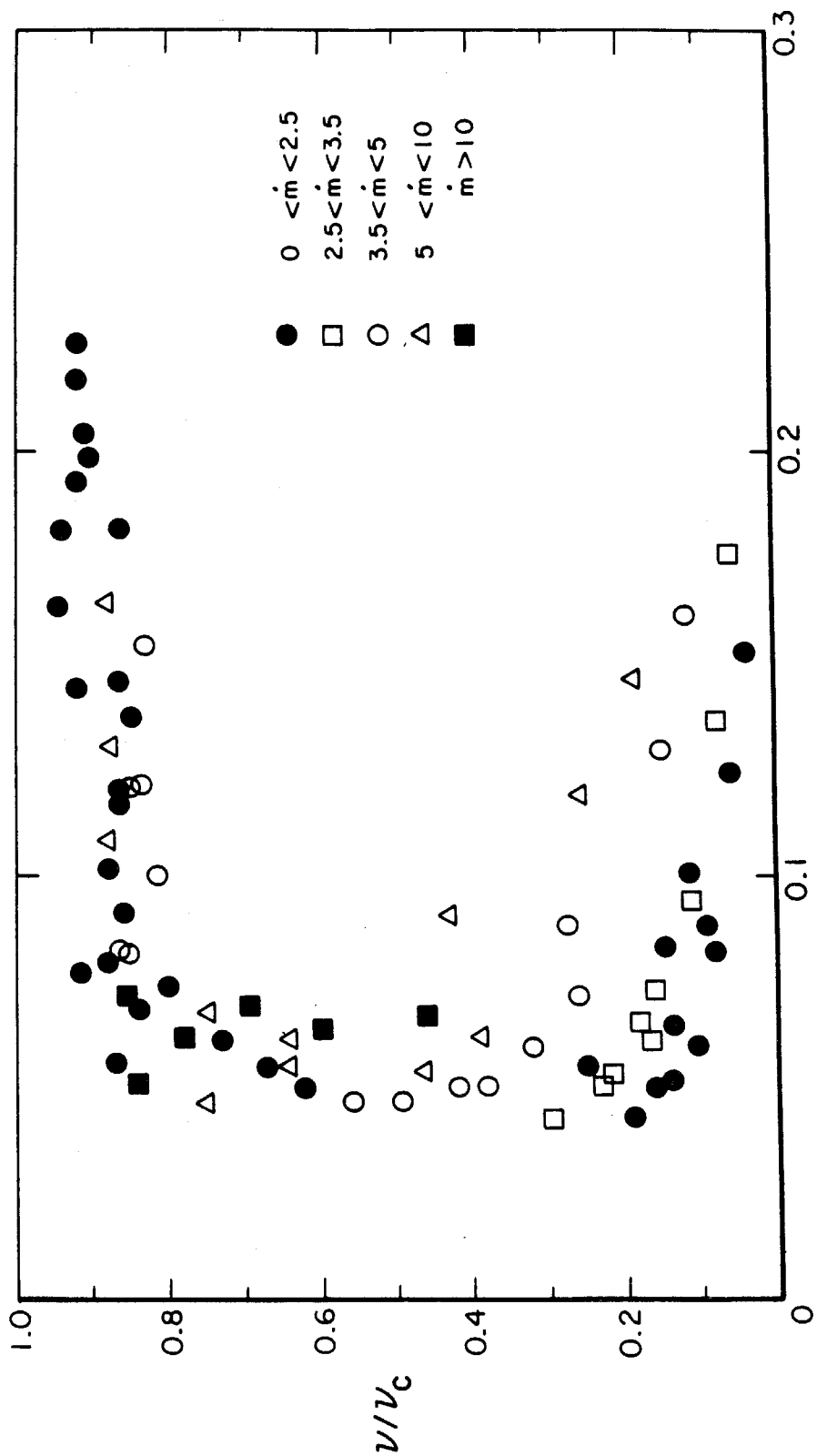

Figure 3.7 The variation in the depth of flow, h(ft), as a function of solid fraction, ν/ν_c for various mass flow rates, $\dot{m}(lb_m/sec)$. (All points shown are for the 3mm glass beads.)

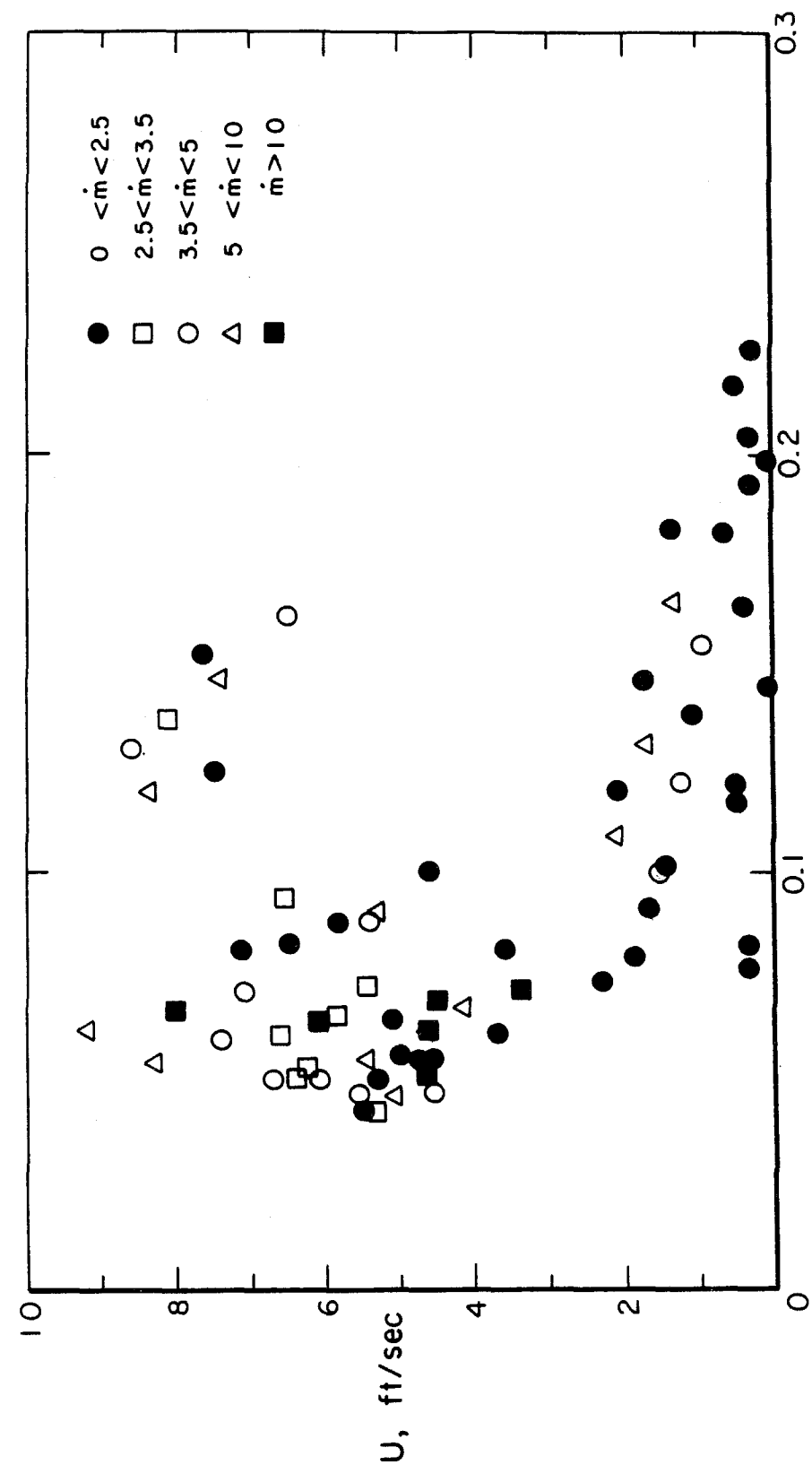

Figure 3.8 The variation of the velocity, U(ft/sec), as a function of the depth of flow, h(ft) for various mass flow rates, $\dot{m}(lb_m/sec)$. (All points shown are for the 3mm glass beads.)

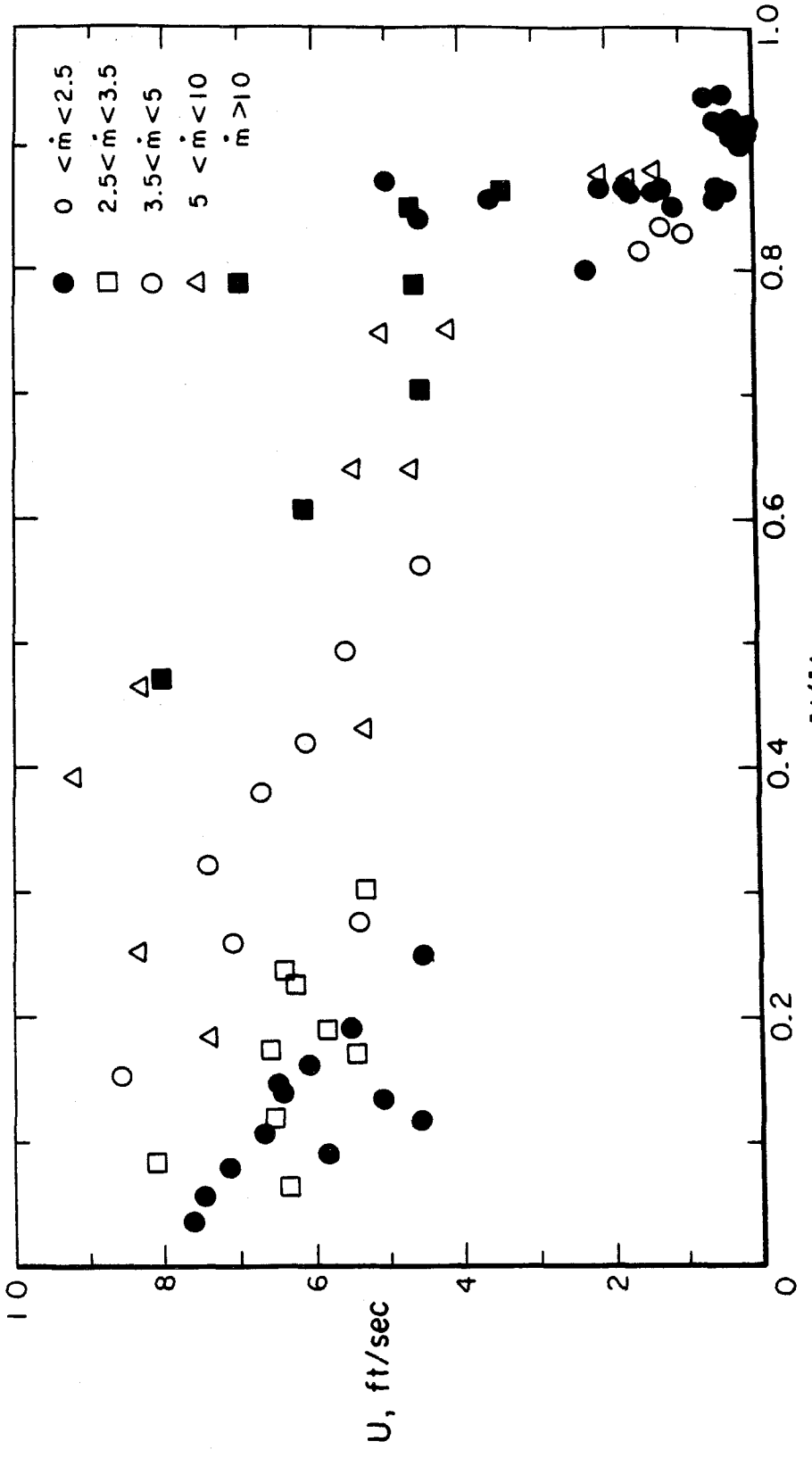

Figure 3.9 The variation of the solid fraction, ν/ν_c, as a function of velocity, U(ft/sec), for various mass flow rates $\dot{m}(lb_m/sec)$. (All points shown are for the 3mm glass beads.)

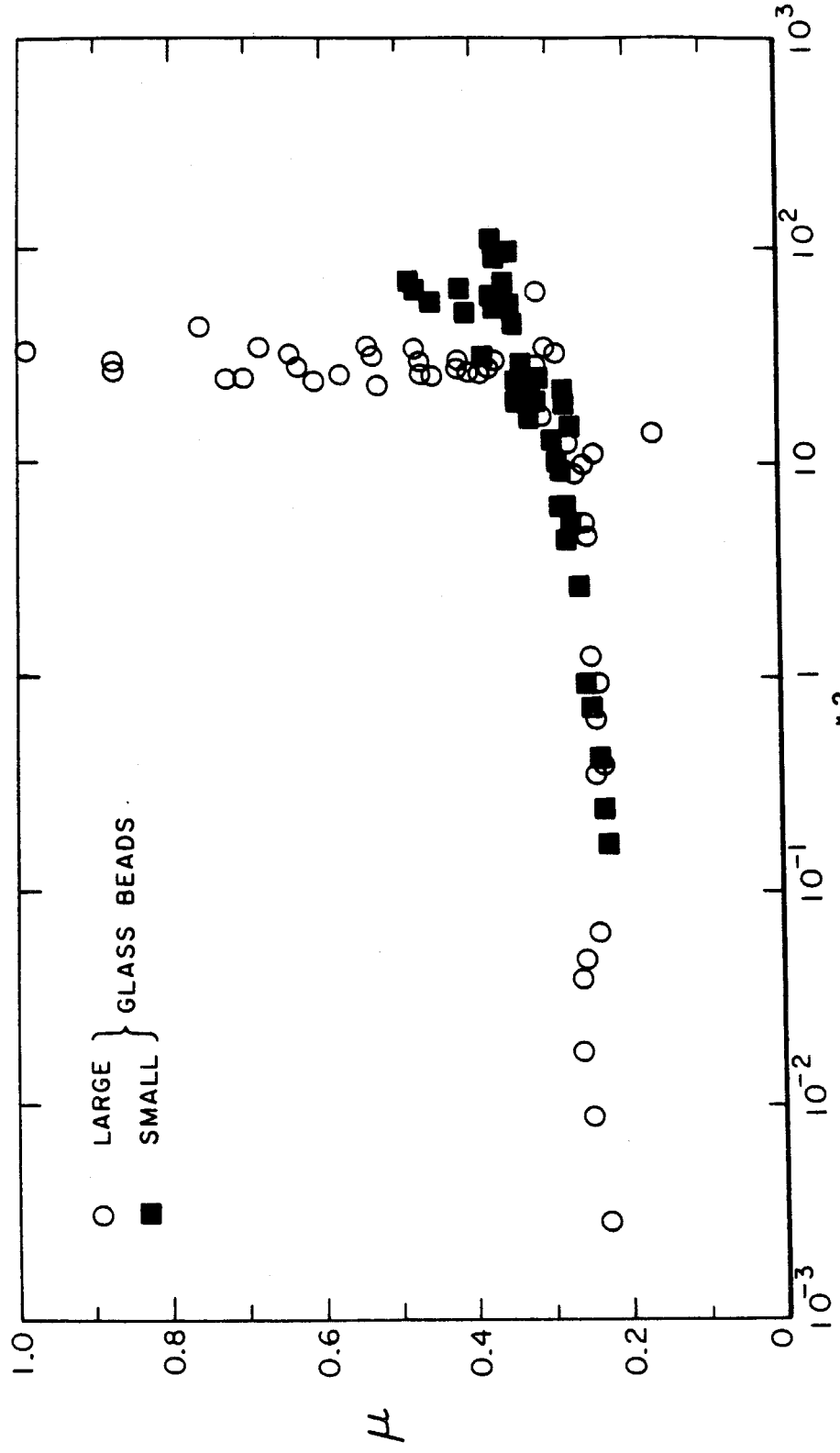

Figure 3.10 The variation of the friction coefficient, μ, as a function of Froude Number Fr^{*2}. (Both 3mm and .3mm glass beads are shown.)

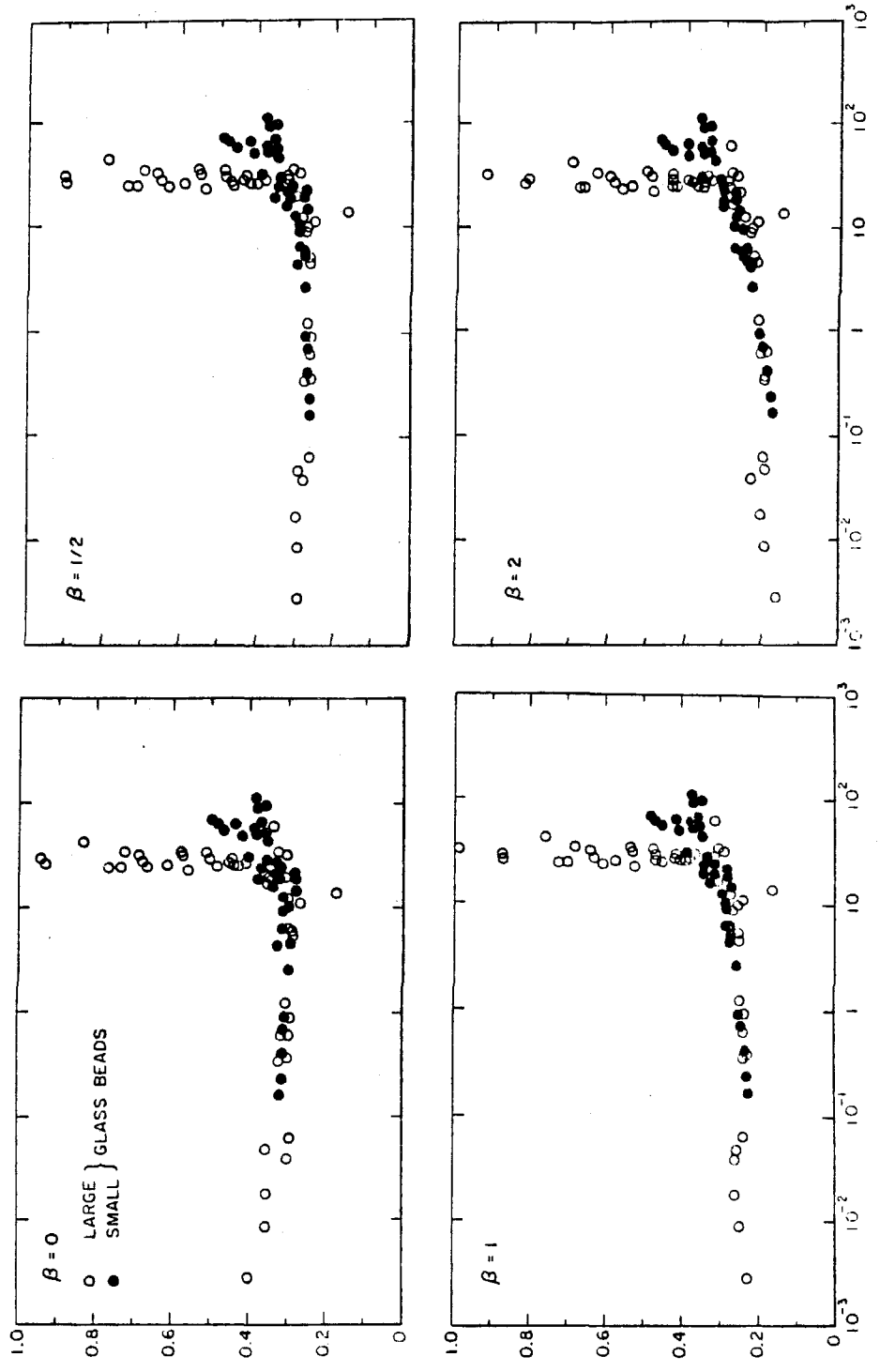

Figure 3.11 The variation of the friction coefficient, μ, as a function of Froude Number, Fr^{*2} for various values of the sidewall contribution to the total shear, β. (All points shown are 3mm glass beads.)

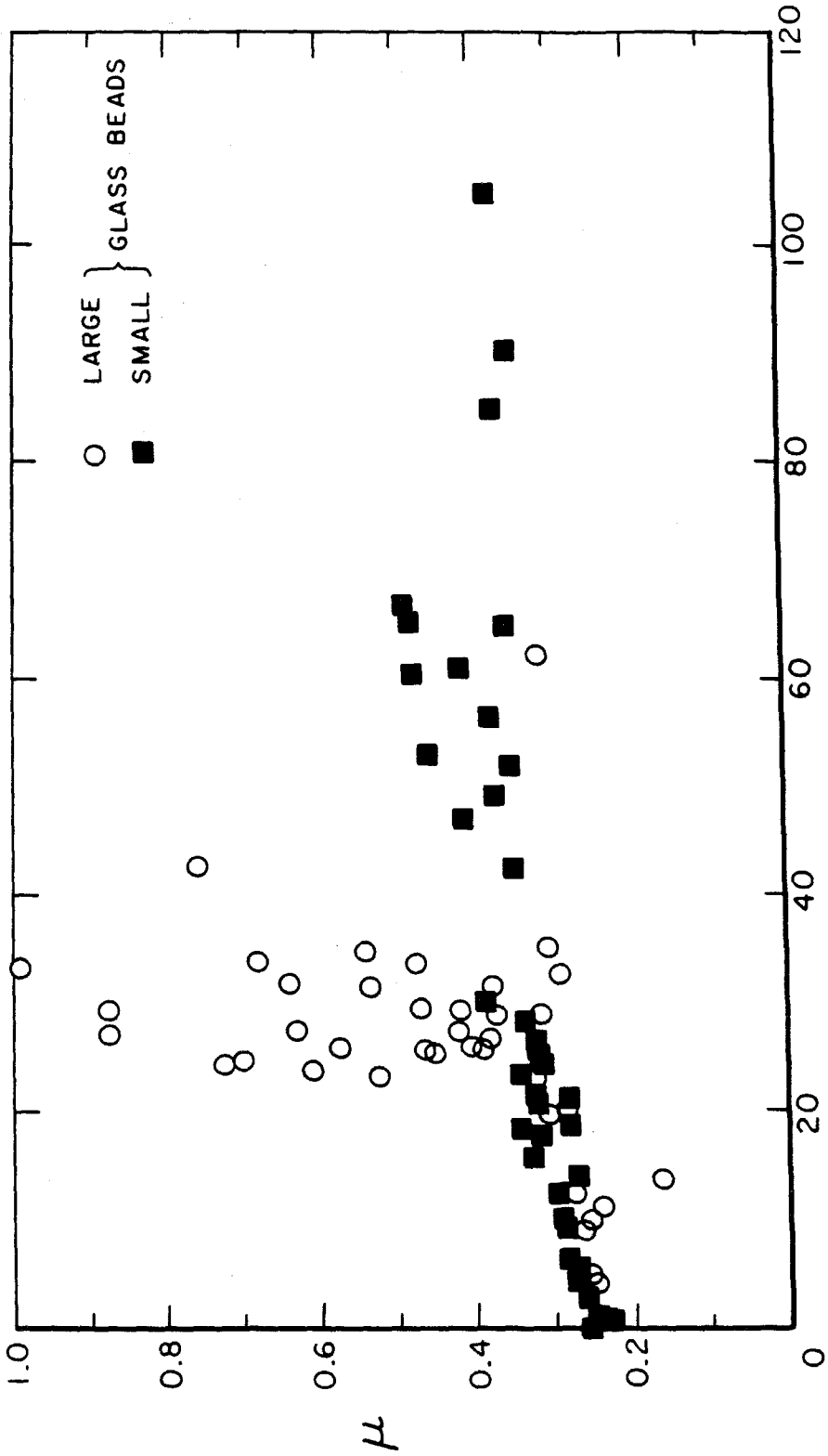

Figure 3.12 The variation of the friction coefficient, μ, as a function of Froude Number, Fr^{*2} on a linear scale. (Both sizes of glass beads are shown.)

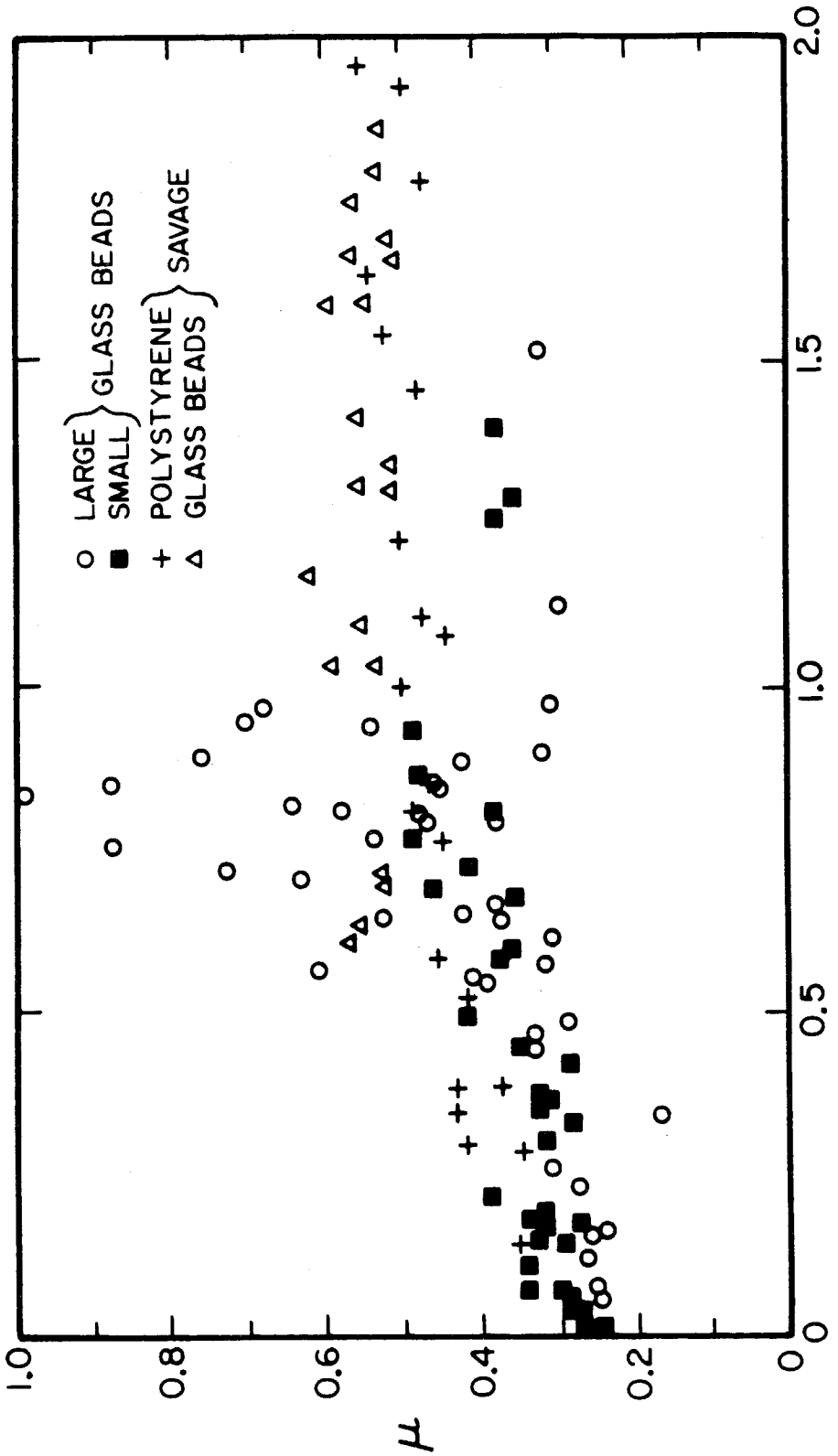

Figure 3.13 The variation of the friction coefficient, μ, as a function of Froude Number, $Fr^{*'} = Fr^{*}\sqrt{\frac{d}{h}}$

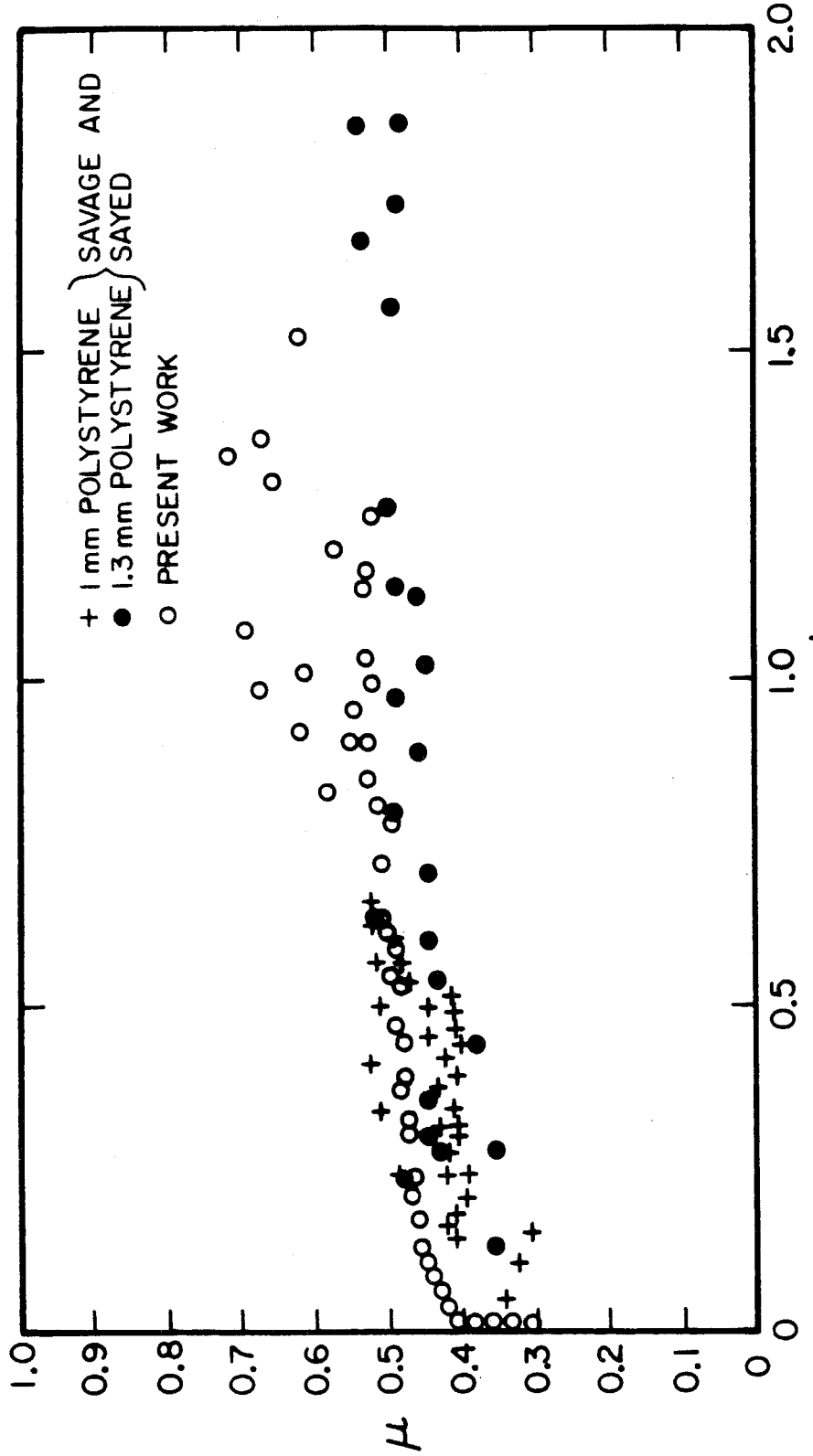

Figure 3.14 The variation of the friction coefficient, μ, as a function of Froude Number, $Fr^{*'} = Fr^{*}\sqrt{\frac{d}{h}}$

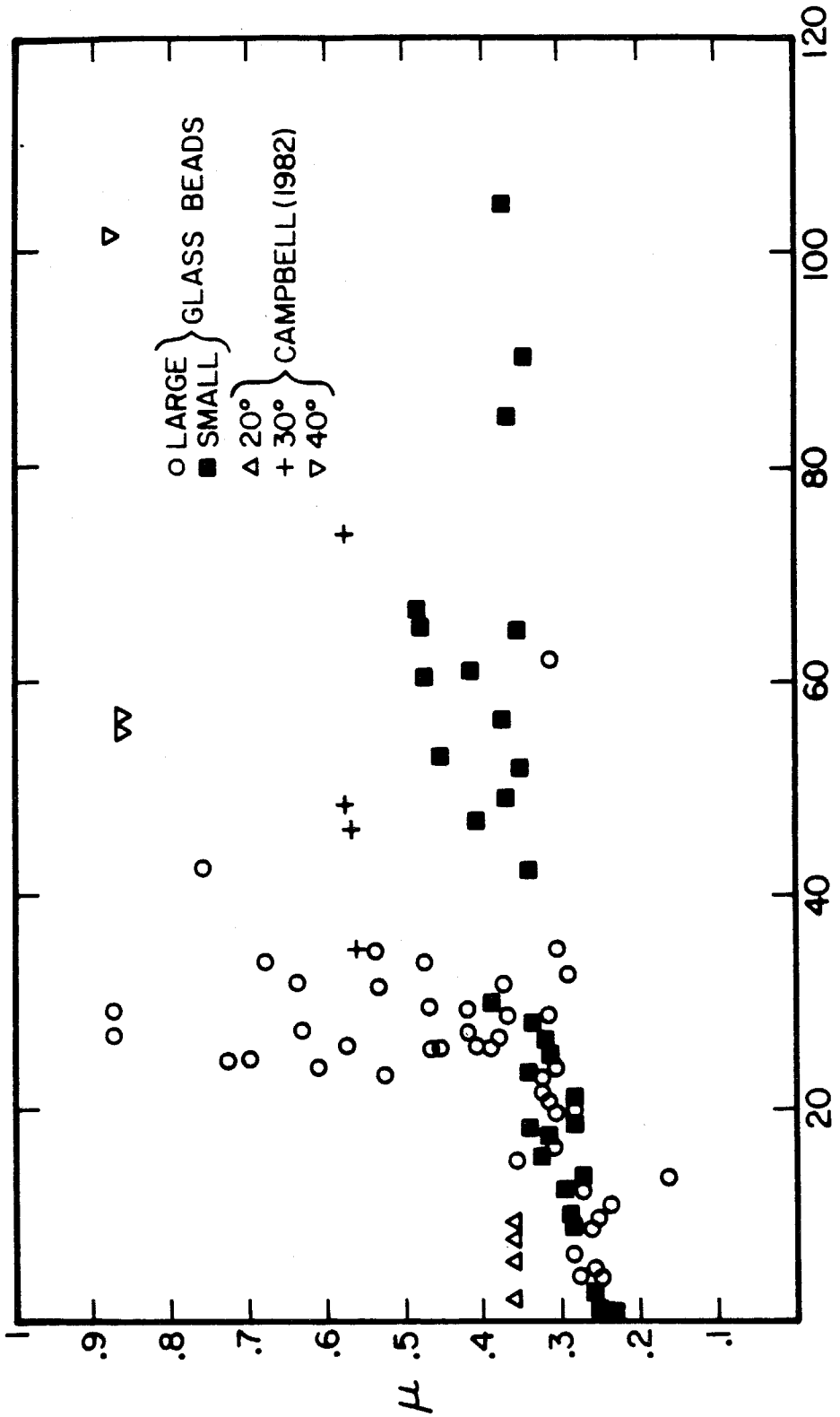

Figure 3.15 The variation of the friction coefficient, μ, as a function of Froude Number, Fr^{*2}.

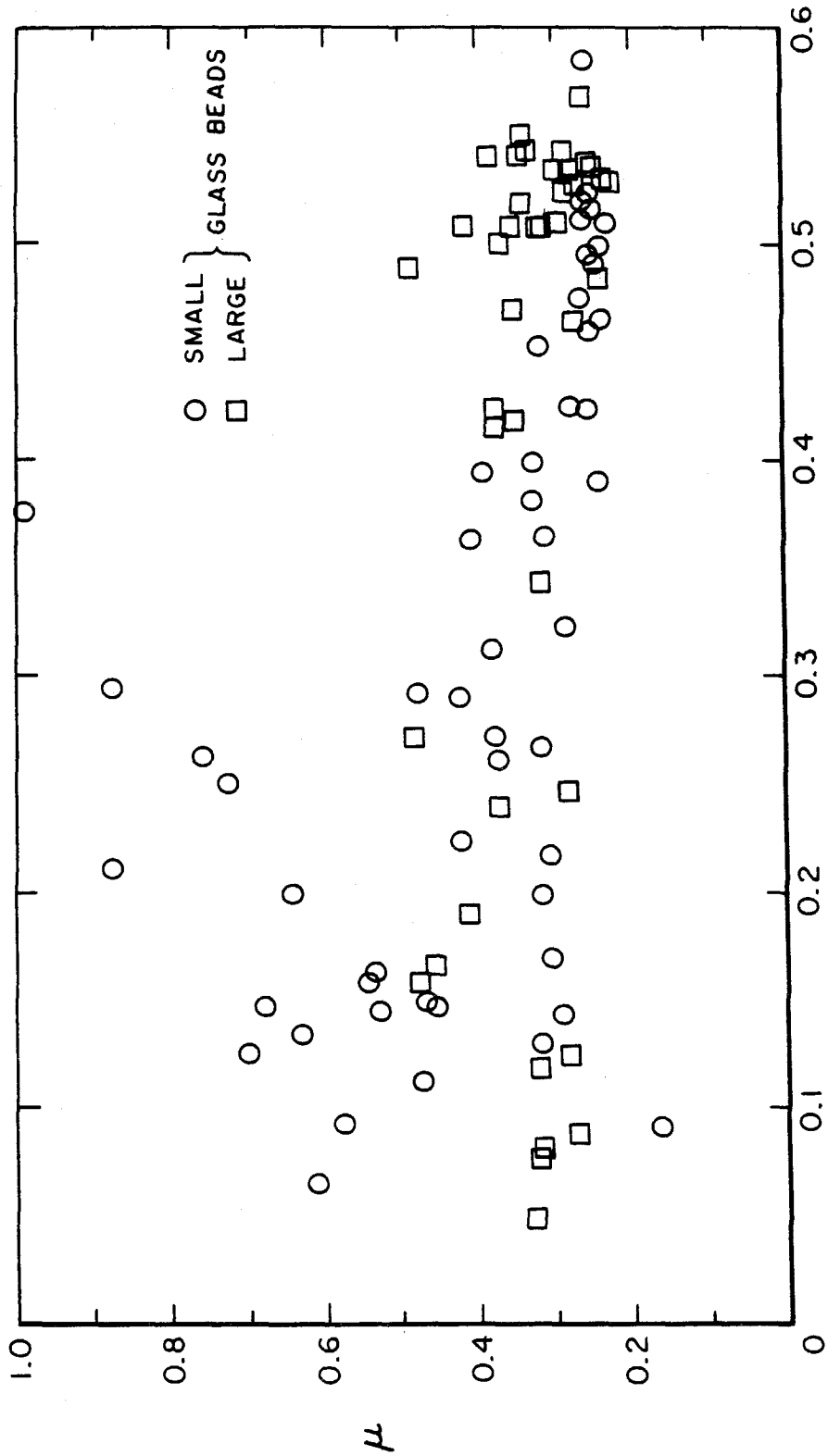

Figure 3.16 The variation of the friction coefficient, μ, as a function of the solid fraction, ν. (Both sizes of glass beads are shown.)

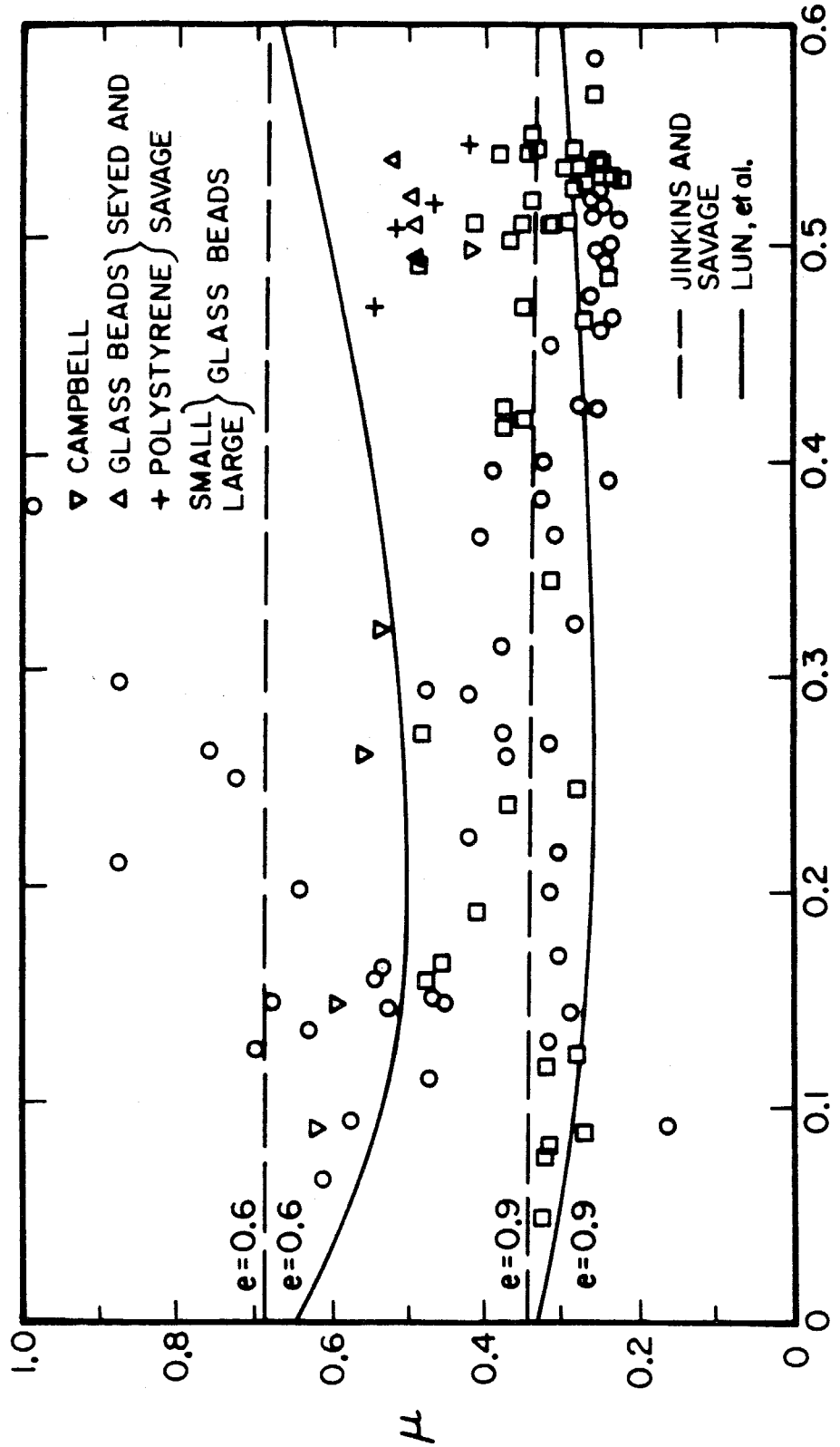

Figure 3.17 The variation of the friction coefficient, μ, as a function of the solid fraction, ν.

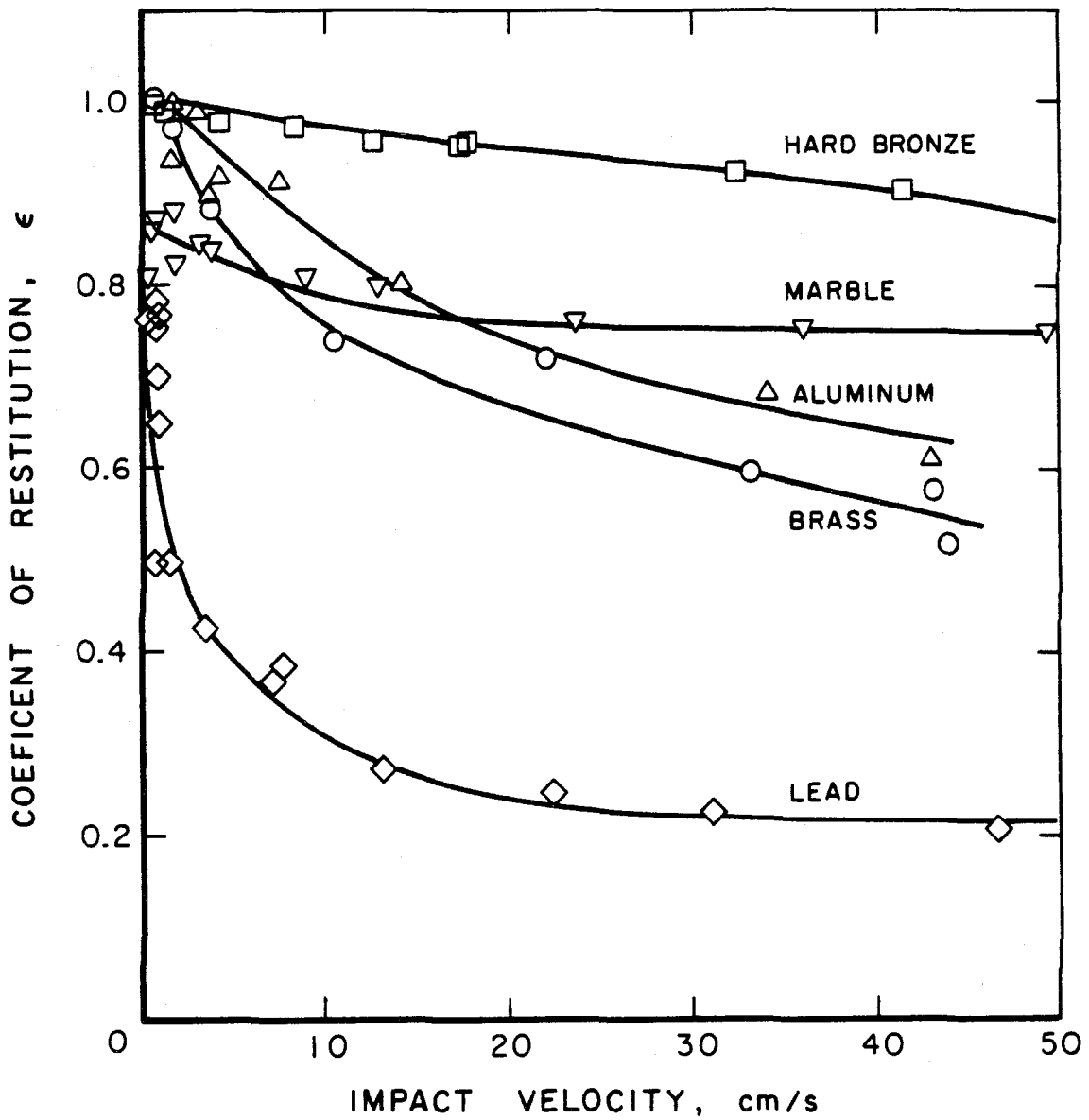

Figure 3.18 The variation of the coefficient of restitution as a function of impact velocity for various materials (Taken from Campbell, 1982.)

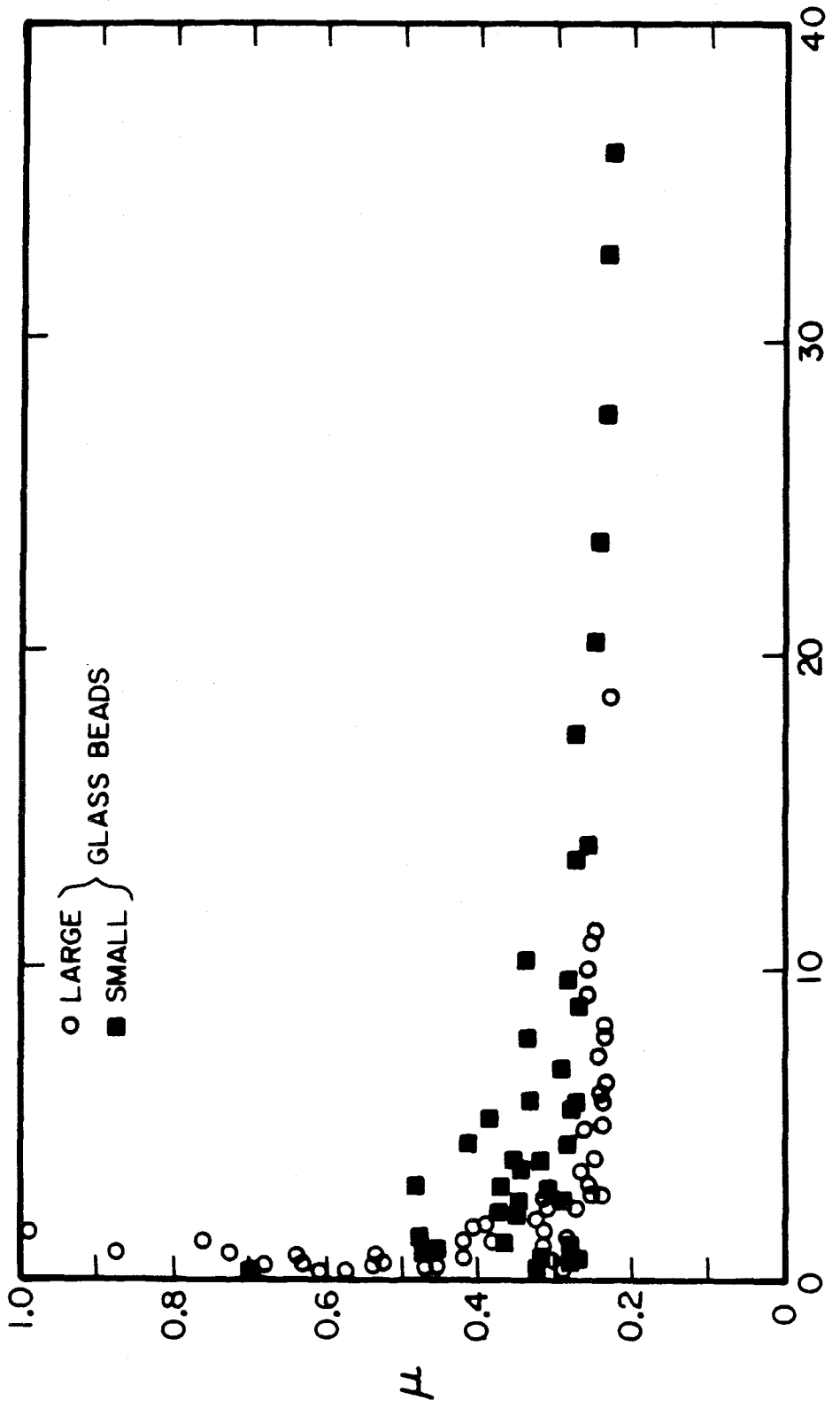

Figure 3.19 The variation of the friction coefficient, μ, as a function of $\nu(h/d)$. (Both sizes of glass beads are shown.)

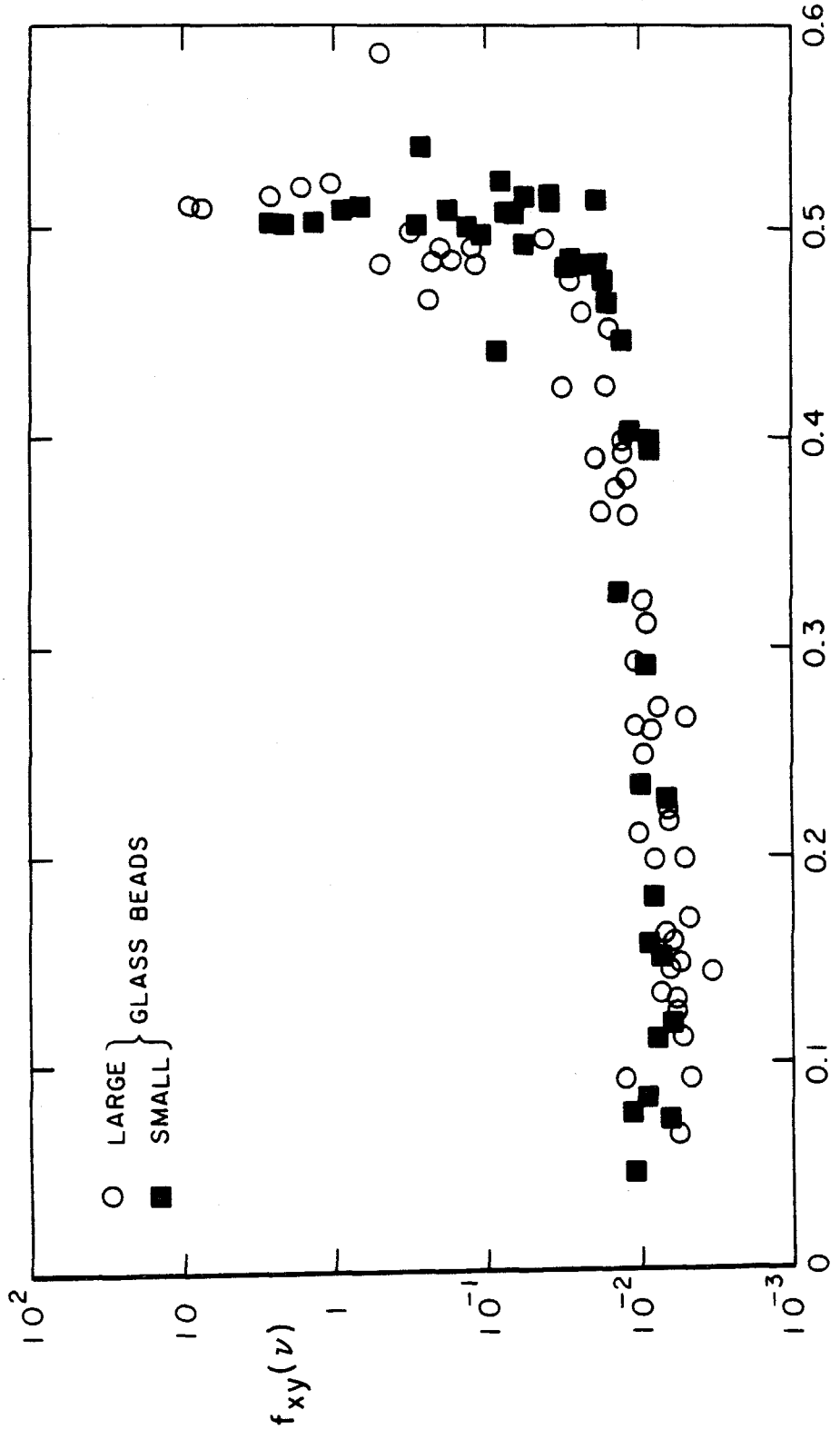

Figure 3.20 The variation of $f_{xy}(\nu)$ as a function of ν. (Both sizes of glass beads are shown.)

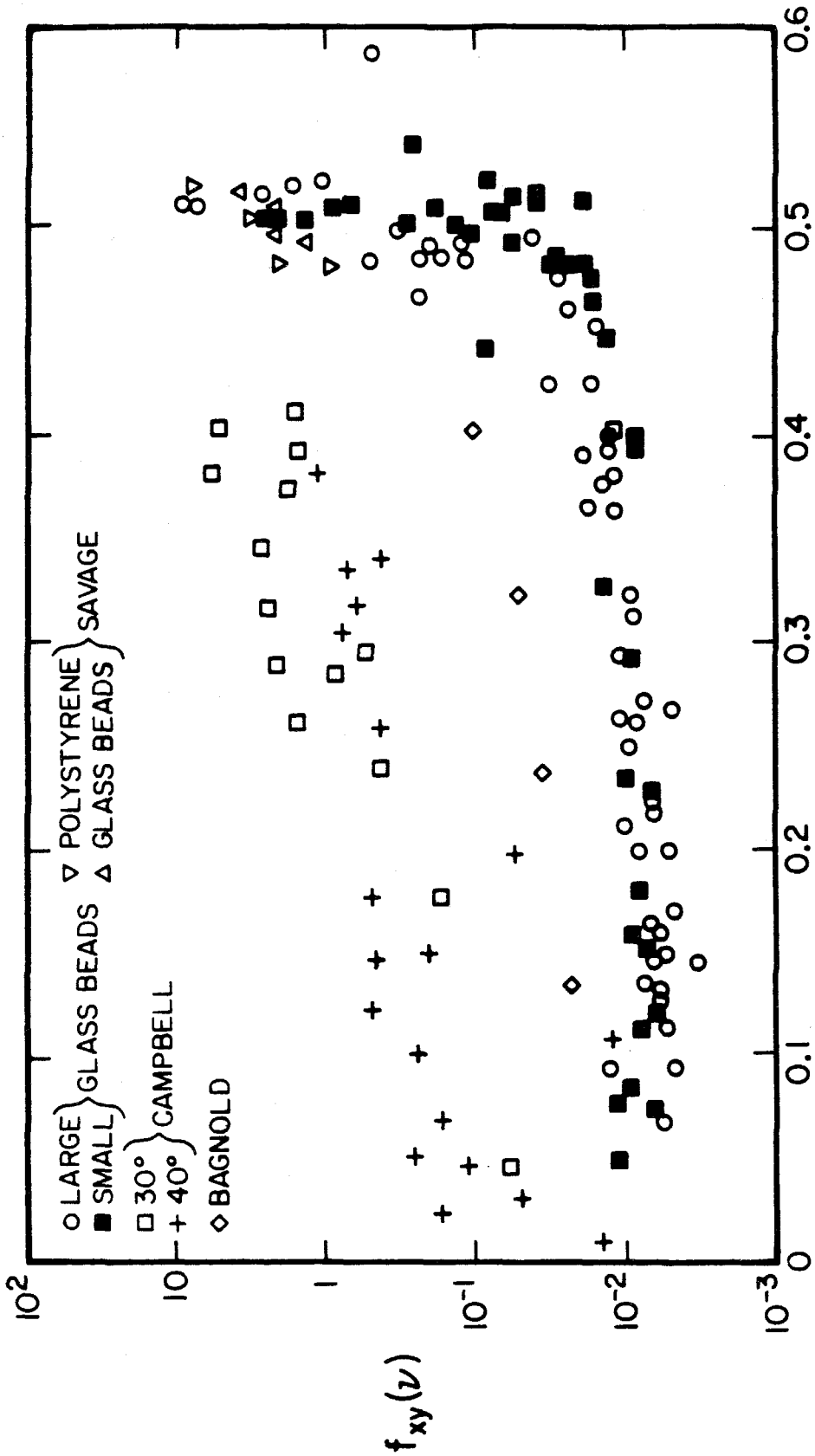

Figure 3.21 The variation of $f_{xy}(\nu)$ as a function of ν.

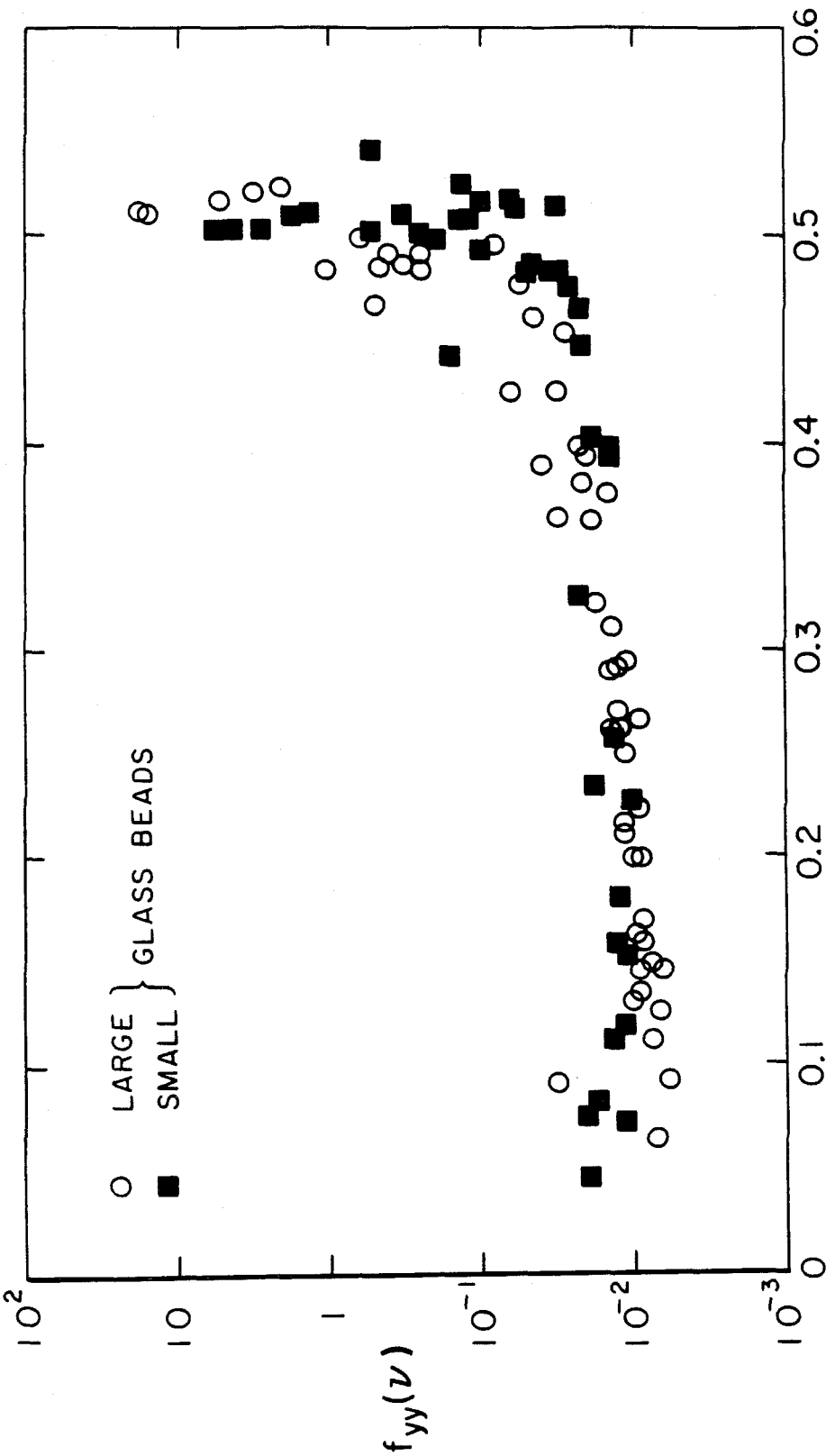

Figure 3.22 The variation of $f_{yy}(\nu)$ as a function of ν. (Both sizes of glass beads.)

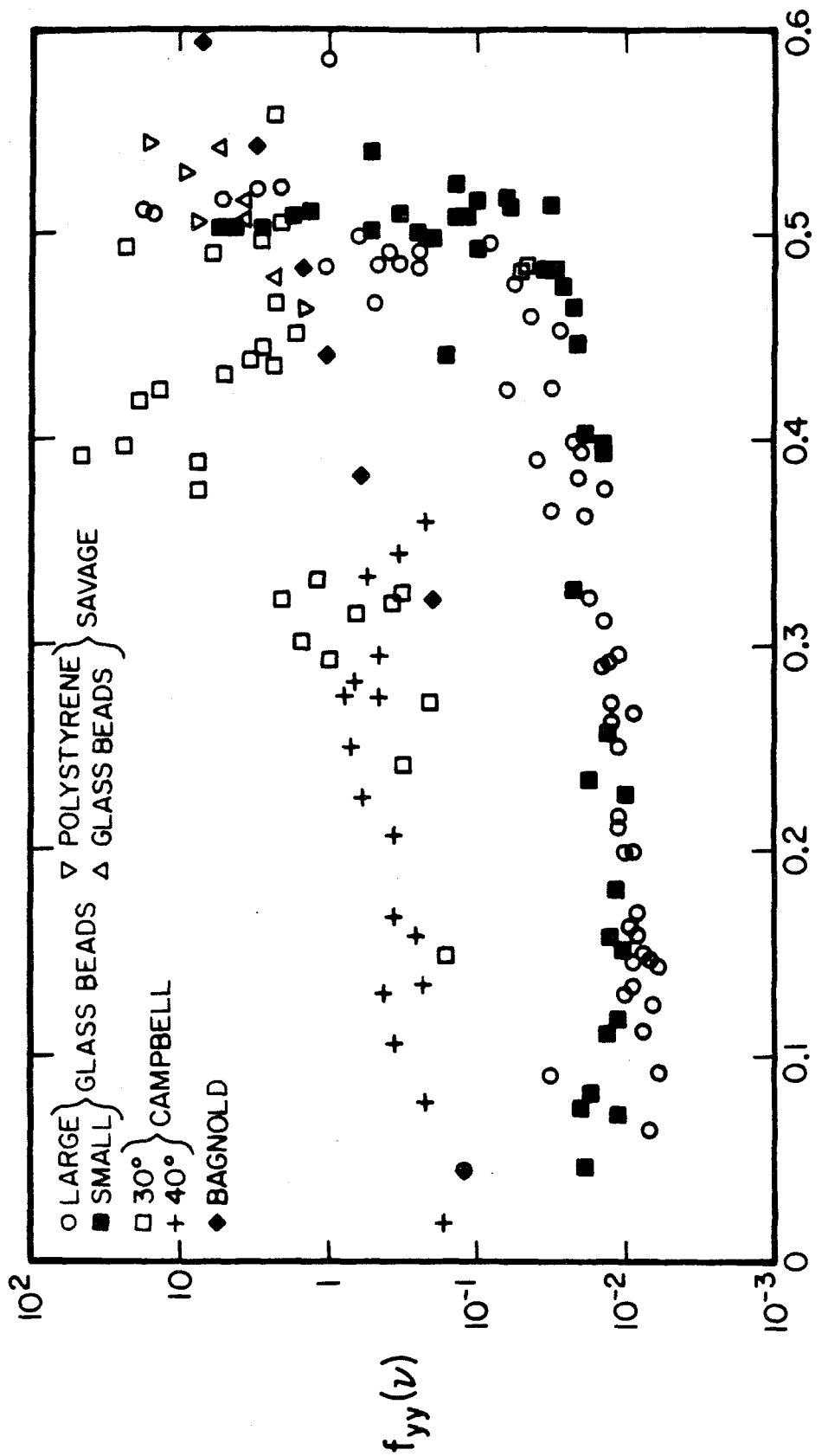

Figure 3.23 The variation of $f_{yy}(\nu)$ as a function of ν.

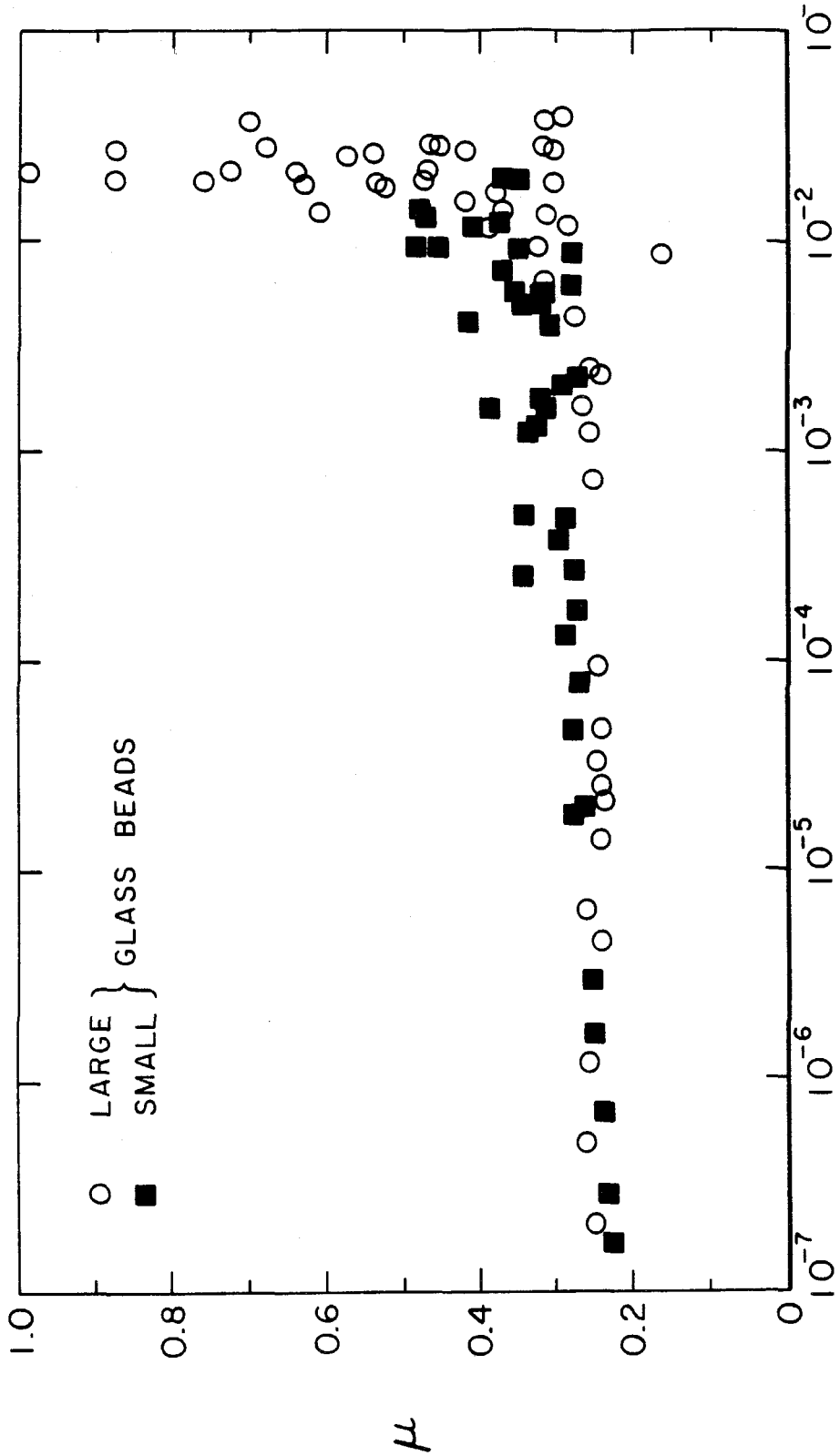

Figure 3.24 The variation of the friction coefficient, μ, as a function of Froude Number, $Fr^{*2'} = Fr^{*2}(\frac{d}{h})^2$. (Both sizes of glass beads are shown.)

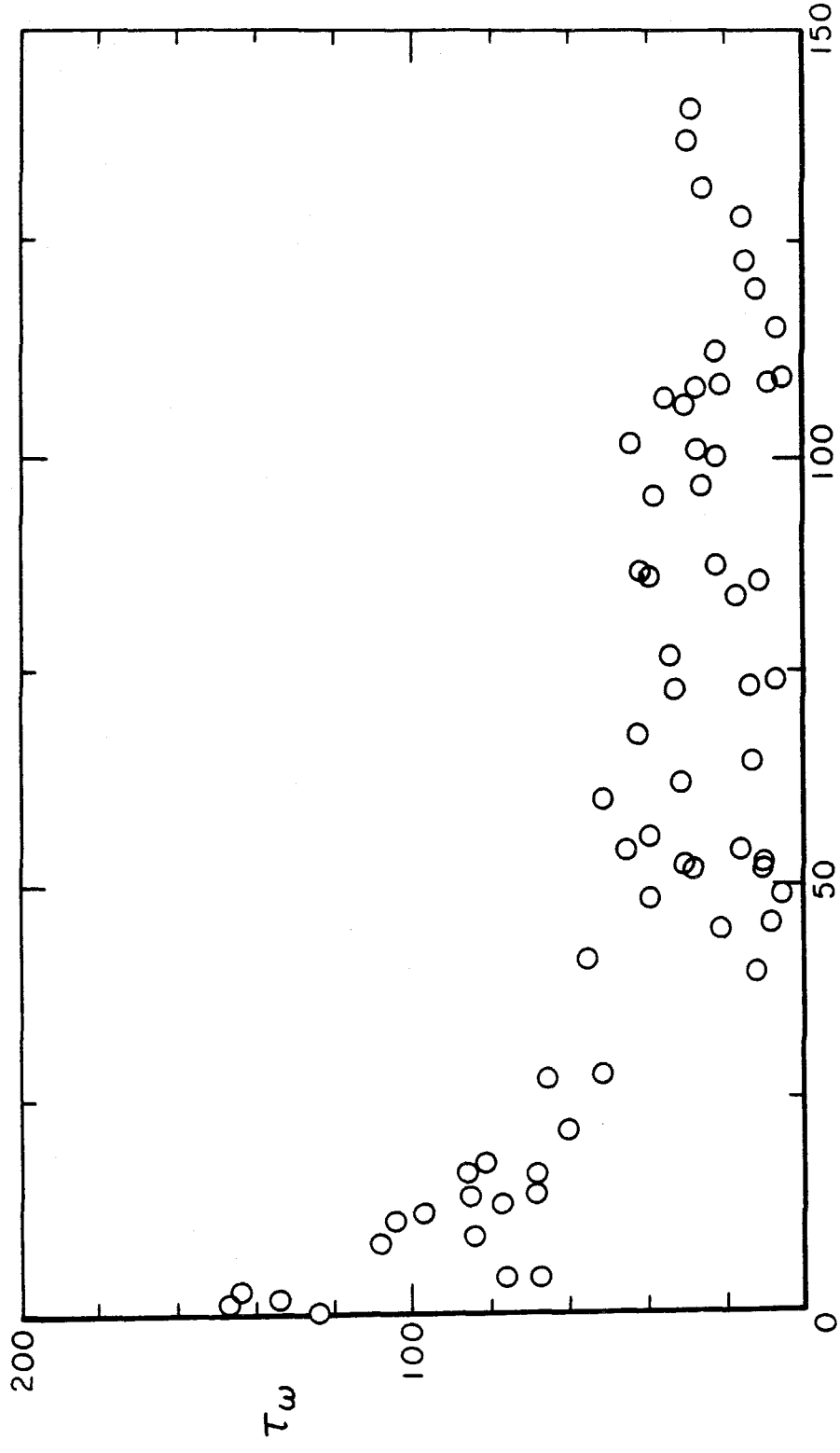

Figure 3.25 The variation of the wall shear, $\tau_w(lb_f/ft^2)$, as a function of the shear rate, U/H(1/sec), for the large 3mm glass beads.

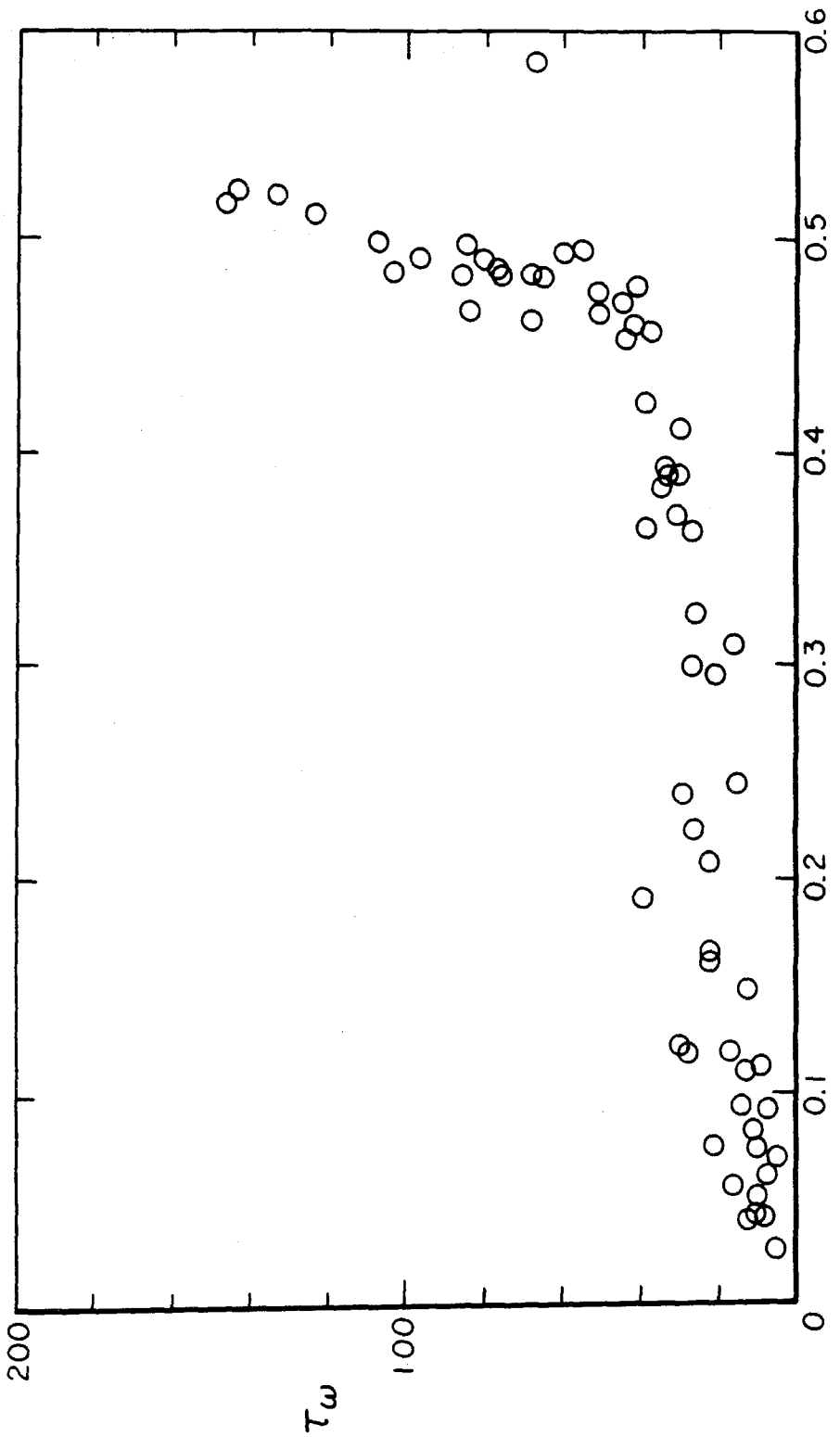

Figure 3.26 The variation of the wall shear, $\tau_\omega(lb_f/ft^2)$, as a function of the solid fraction, ν, for the large 3mm glass beads.

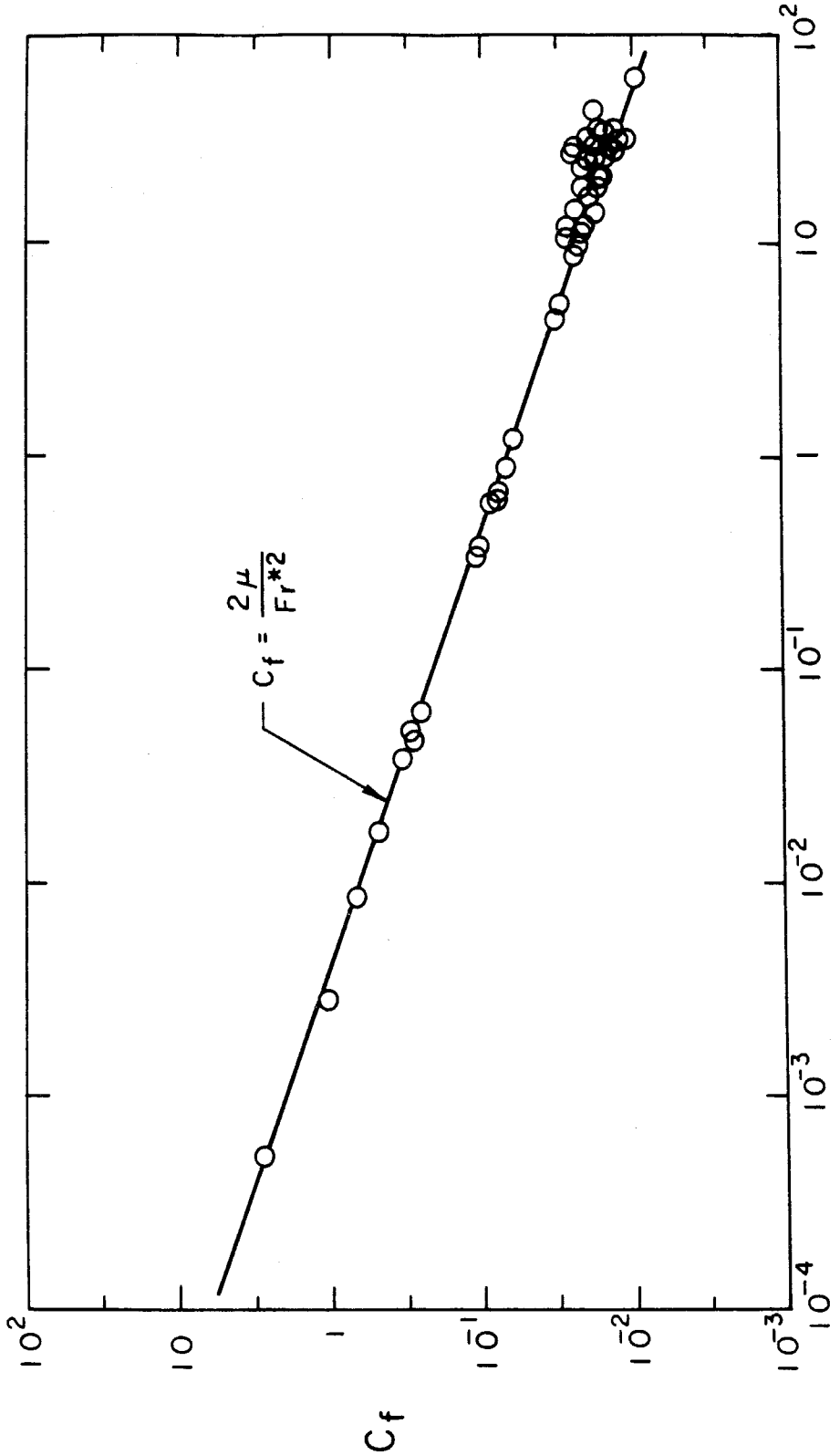

Figure 3.27 The variation of the friction factor, C_f, as a function of Froude Number, Fr^{*2} for the large 3mm glass beads.

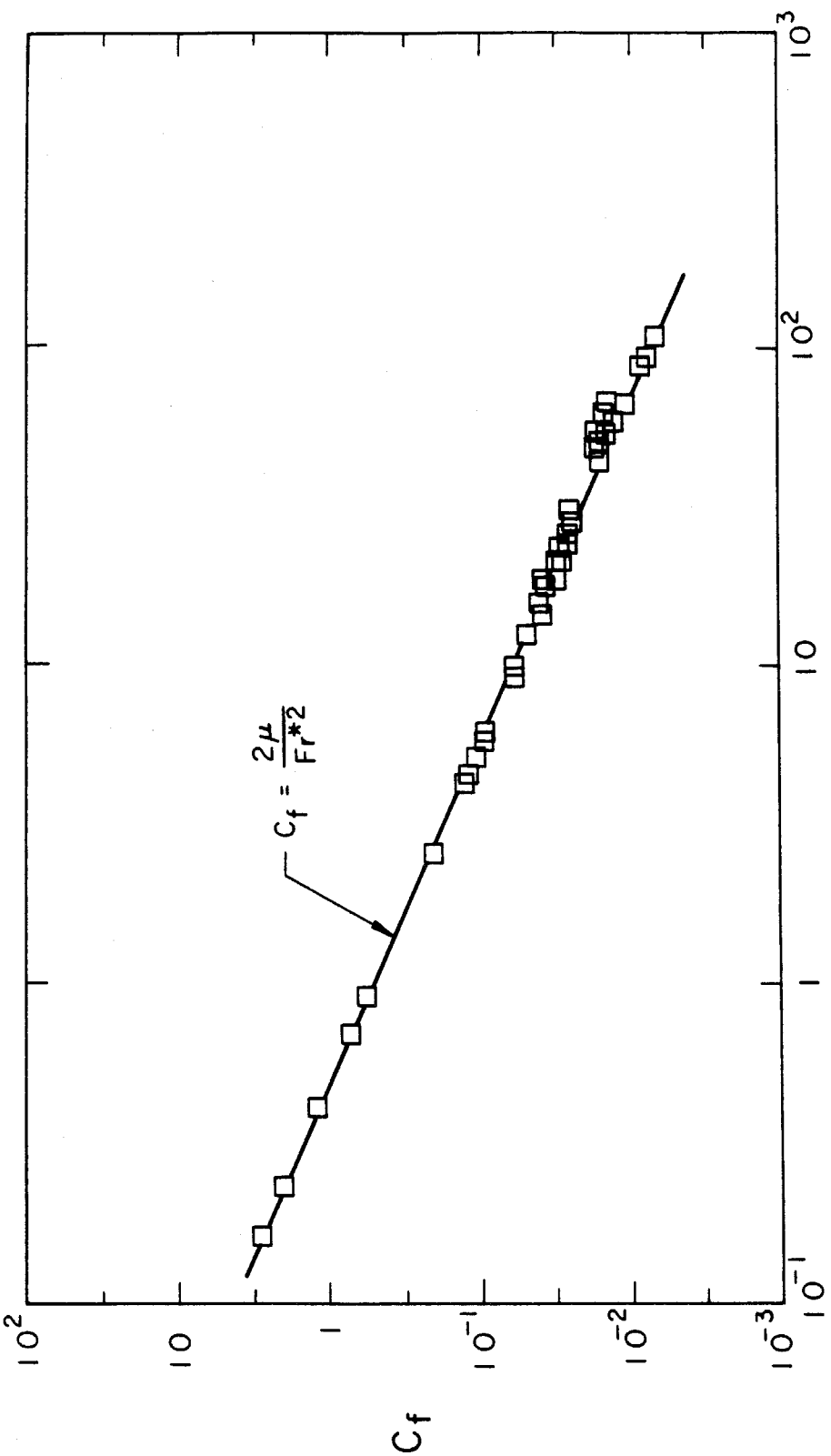

Figure 3.28 The variation of the friction factor, C_f, as a function of Froude Number, Fr^{*2} for the small .3mm glass beads.

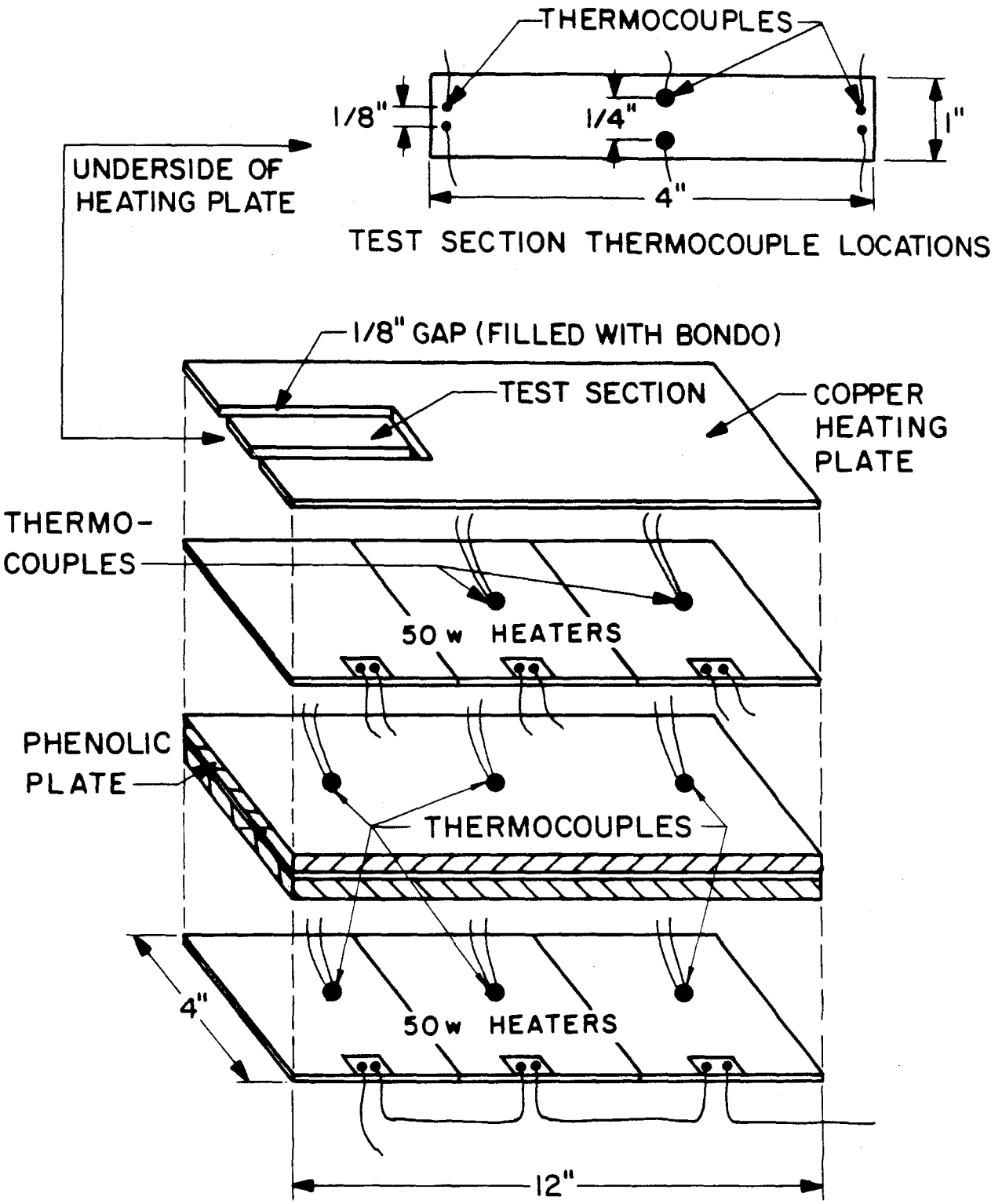

Figure 4.1 Schematic of the heating plate.

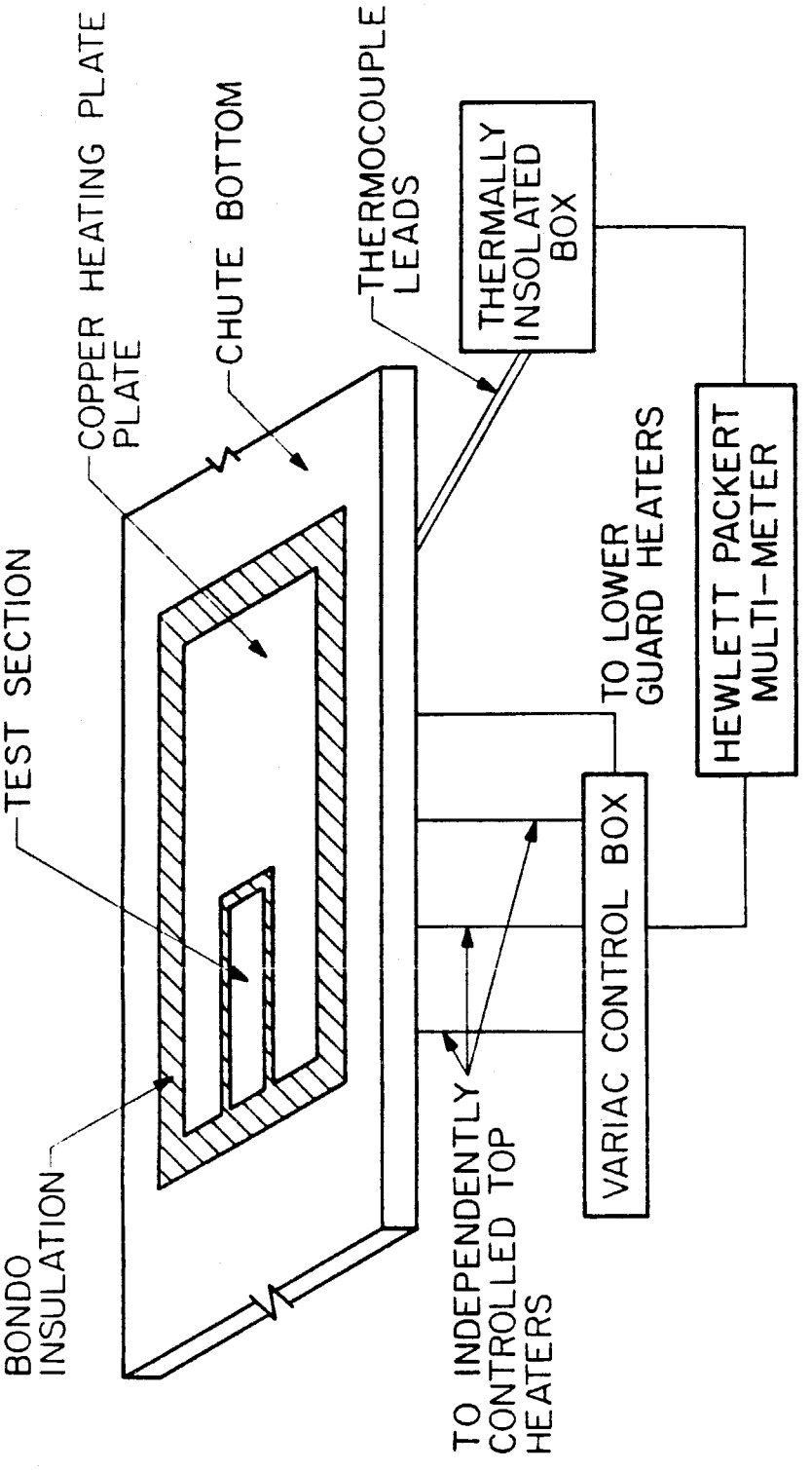

Figure 4.2 Schematic of heating system.

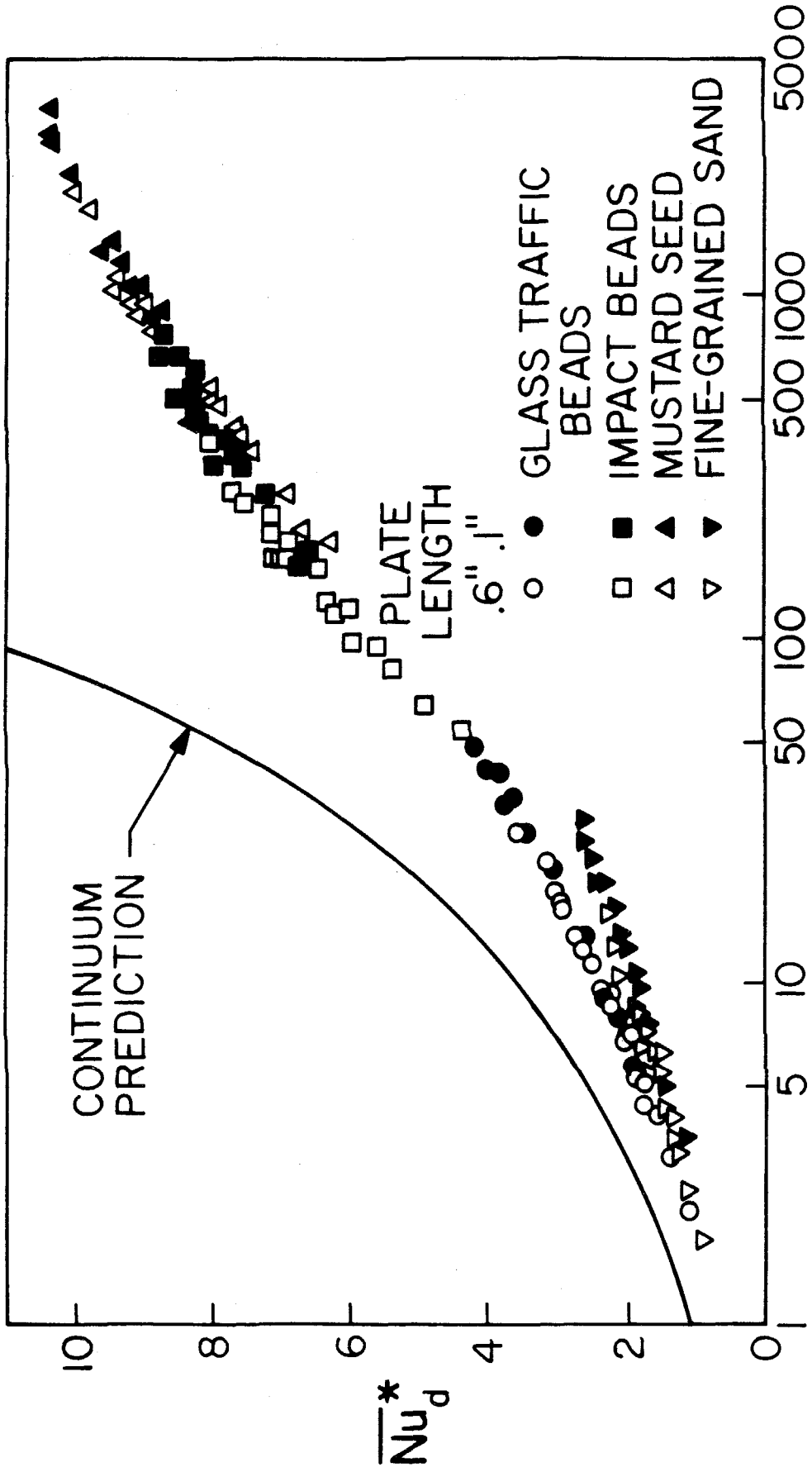

Figure 4.3 Comparison of the single phase Nusselt Number, $\overline{Nu}_d$, to the experimental values of the Nusselt Number, $\overline{Nu}_d^*$. (From Sullivan (1973).)

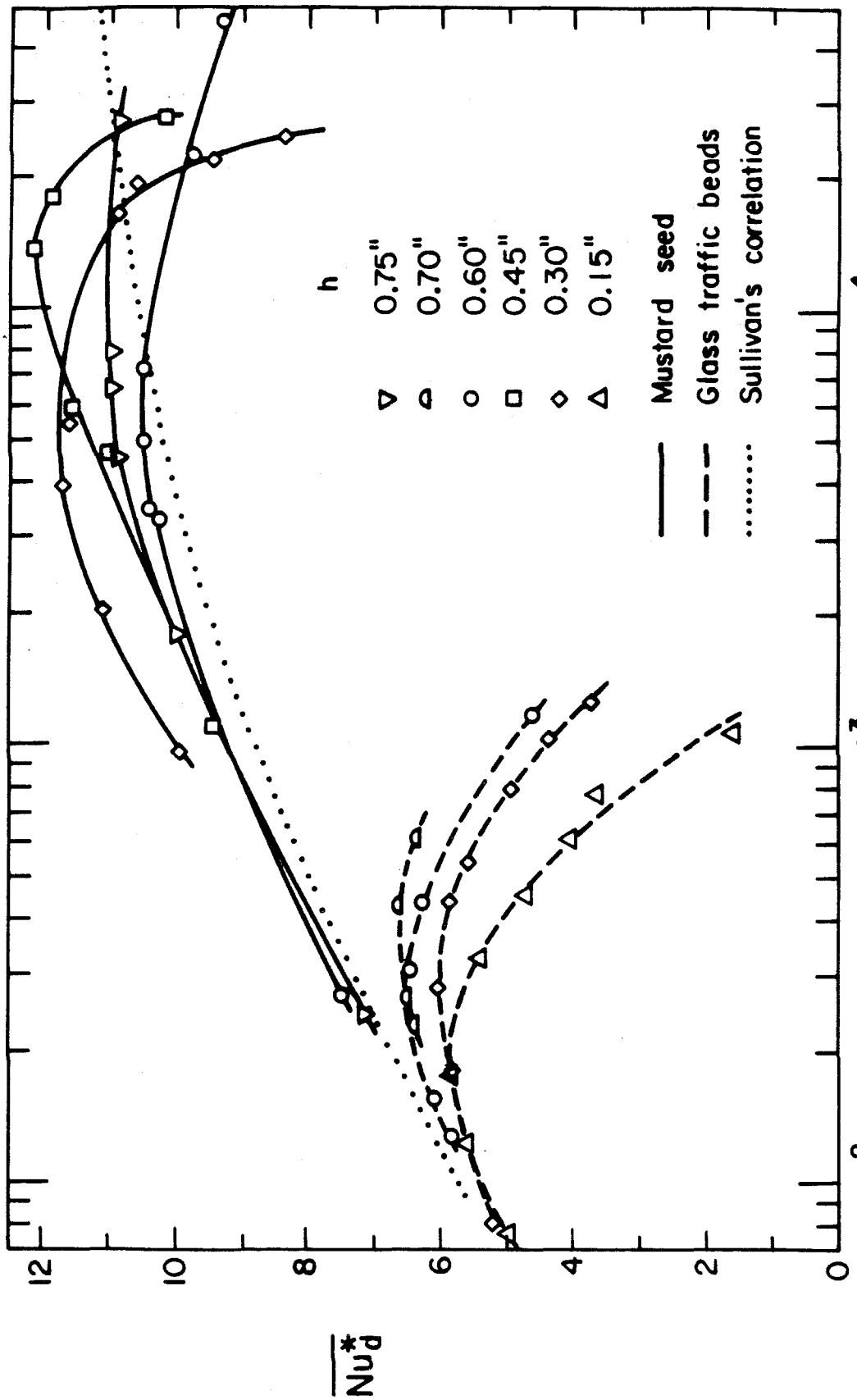

Figure 4.4 The variation of the Nusselt Number, $\overline{Nu}_d^*$, as a function of Peclet Number, Pe_L^* as presented by Spelt, et al. (1982).

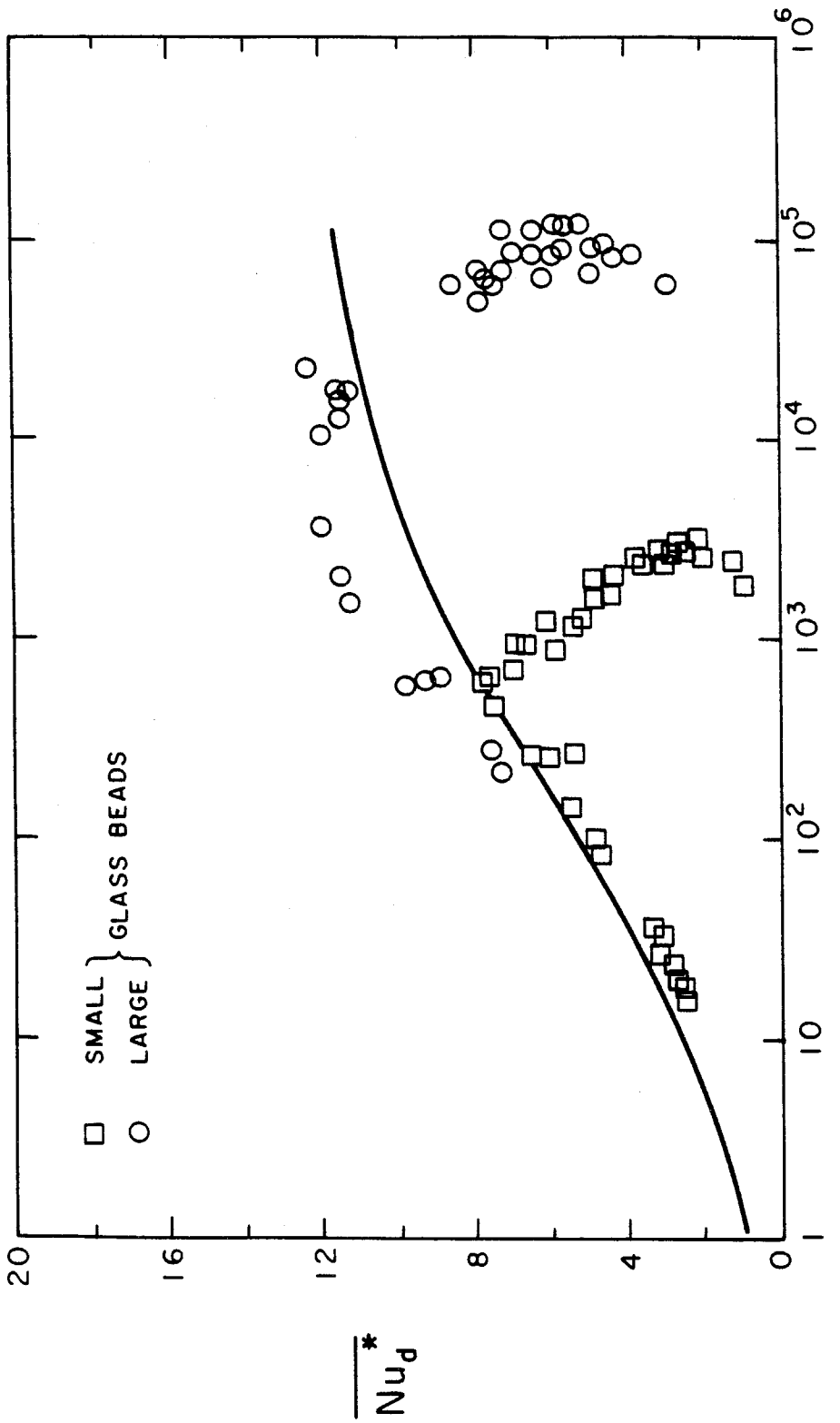

Figure 4.5 The variation of the Nusselt Number, $\overline{Nu_d}^*$, as a function of Peclet Number, Pe_L^* for both sizes of glass beads.

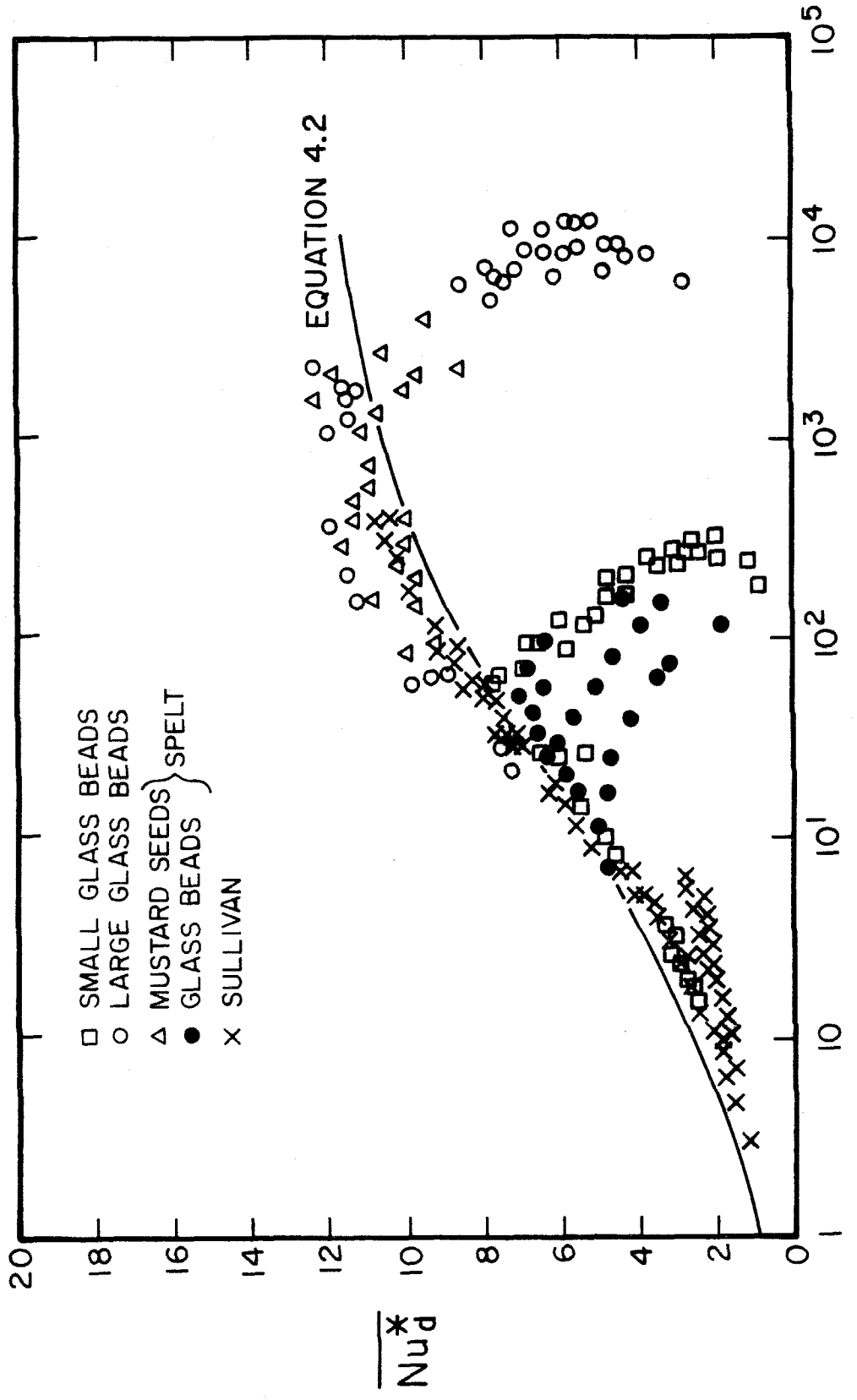

Figure 4.6 The variation of the Nusselt Number, $\overline{Nu}_d^*$, as a function of Peclet Number, Pe_L^*.

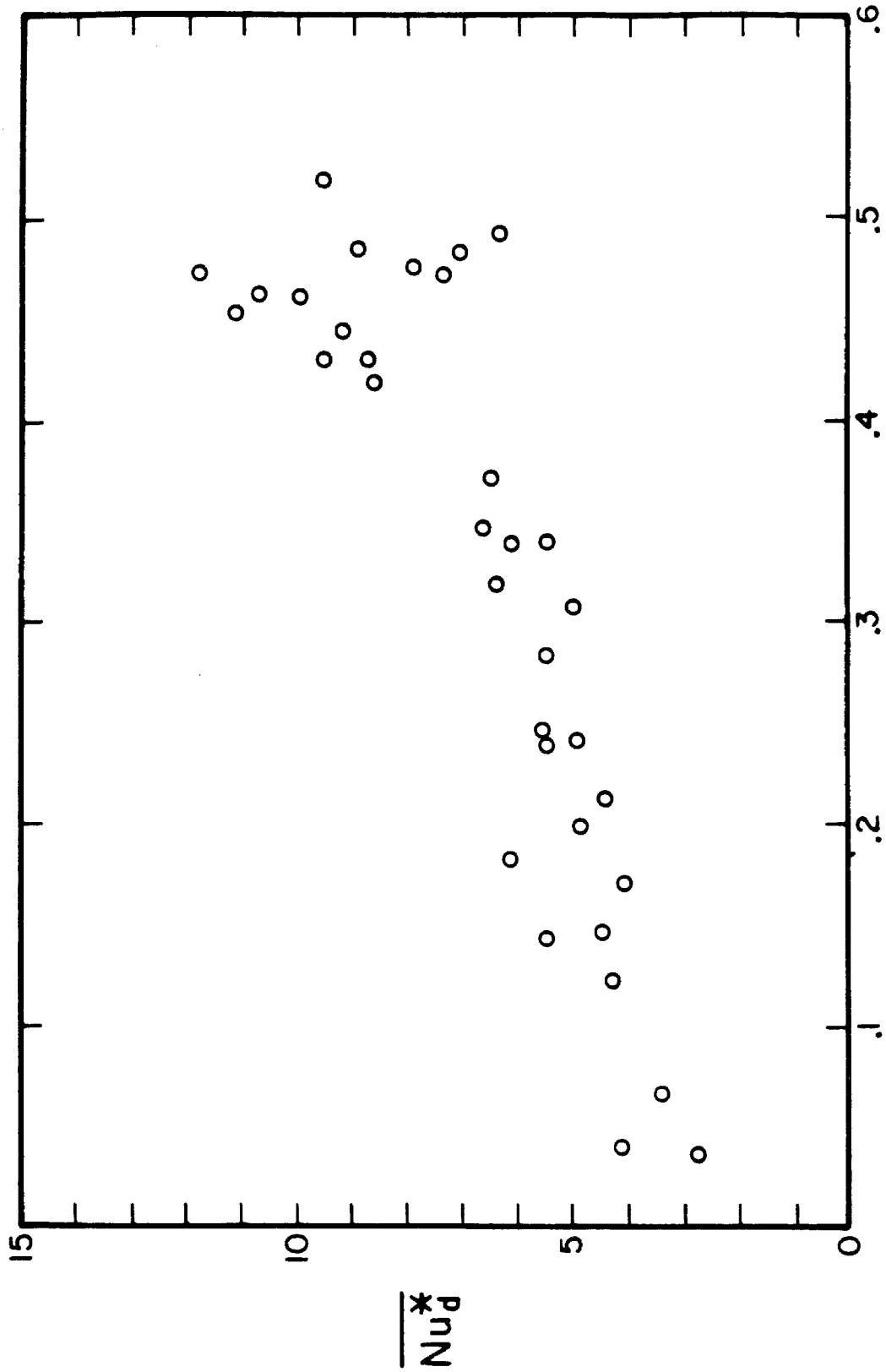

Figure 4.7 The variation of the Nusselt Number, $\overline{Nu_d^*}$, as a function of the solid fraction ν for the large glass beads.

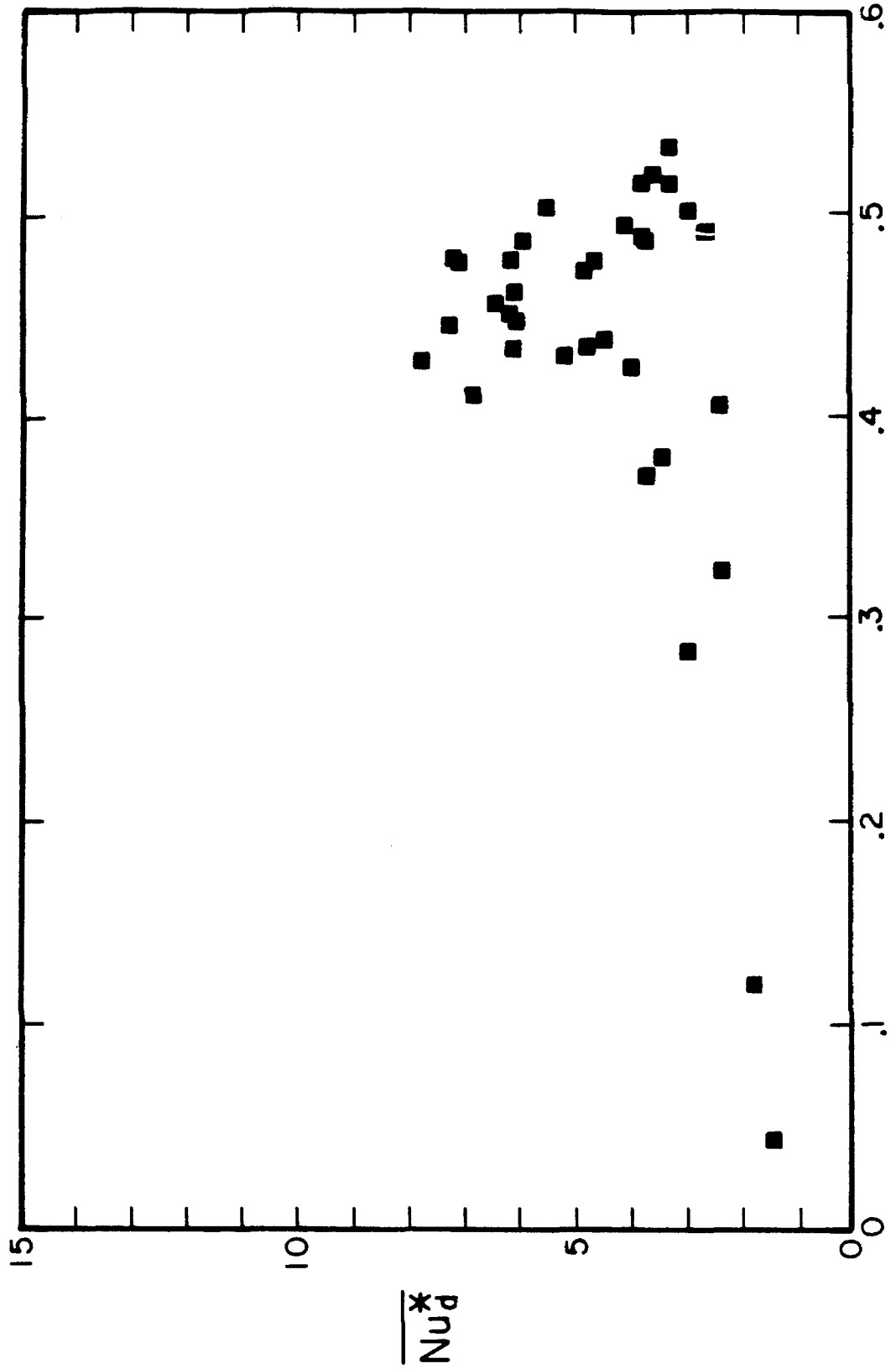

Figure 4.8 The variation of the Nusselt Number, $\overline{Nu}^*_d$, as a function of the solid fraction ν for the small glass beads.

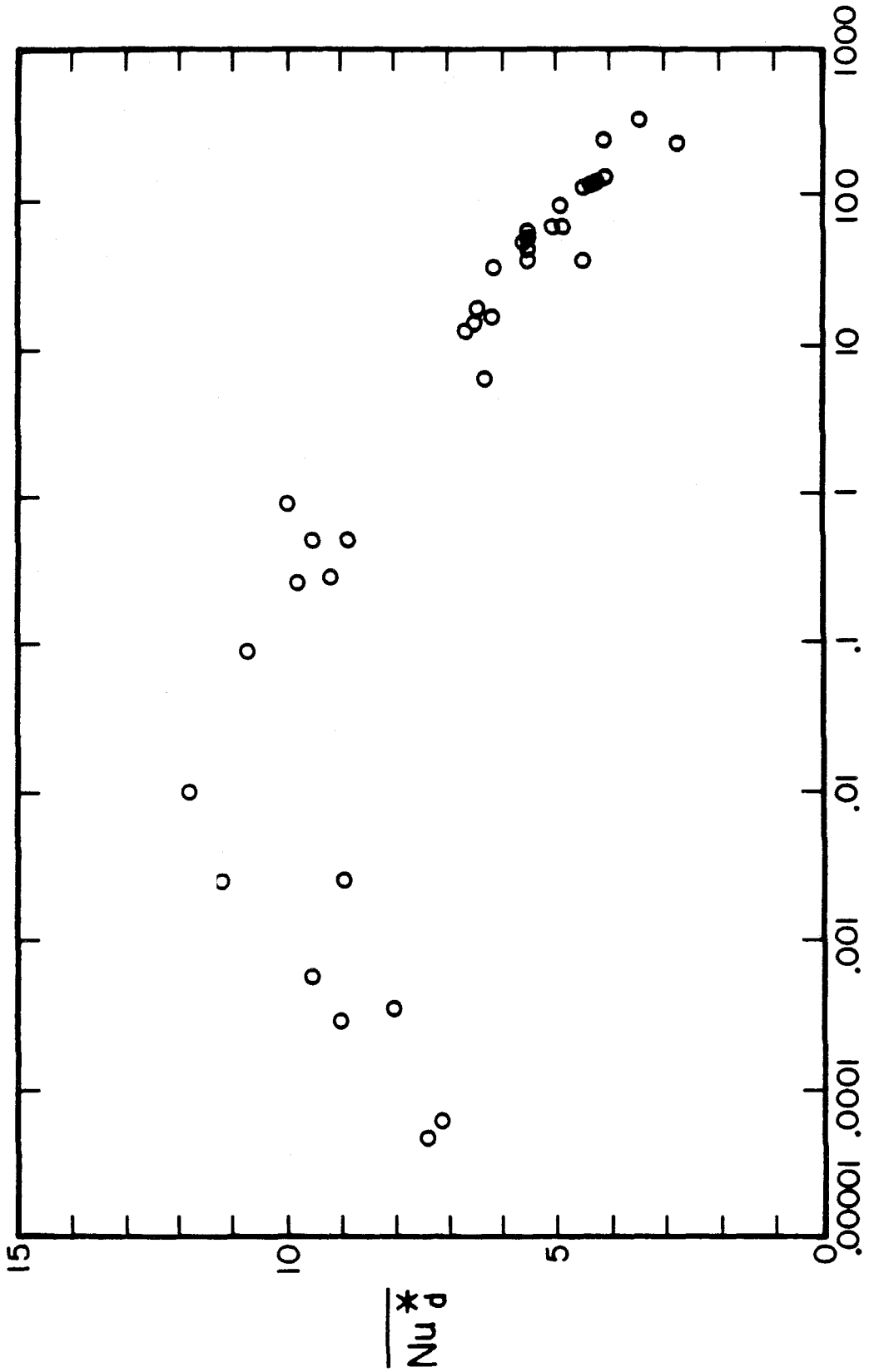

Figure 4.9 The variation of the Nusselt Number, $\overline{Nu_d^*}$, as a function of densinometric Froude Number, $Fr^{*2}_{\nu/\nu_c} = Fr^{*2}(\nu_c/\nu)$, for the large glass beads.

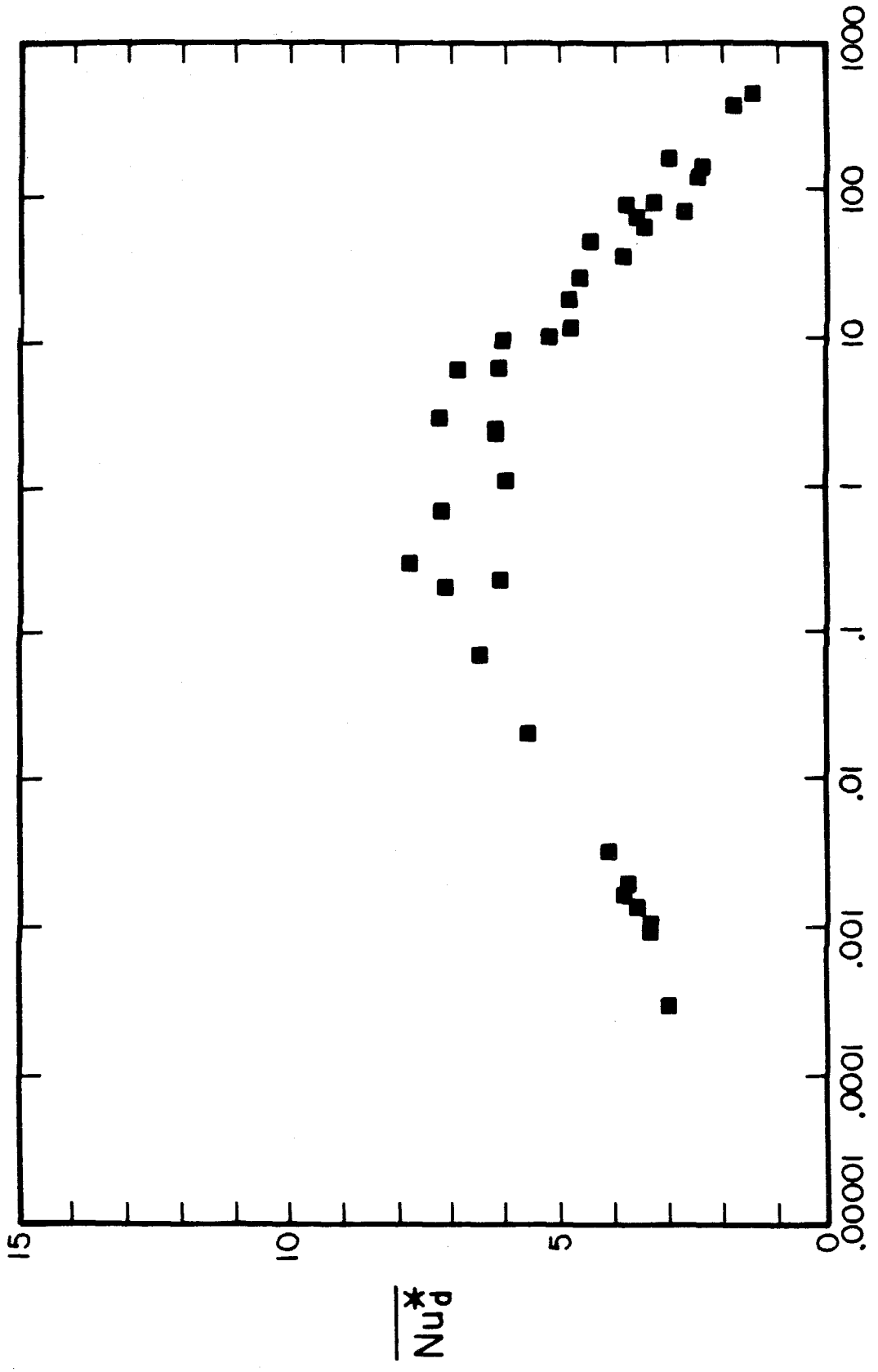

Figure 4.10 The variation of the Nusselt Number, $\overline{Nu_d^*}$, as a function of densinometric Froude Number, $Fr^{*2}_{\nu/\nu_c} = Fr^{*2}(\nu_c/\nu)$, for the small glass beads.

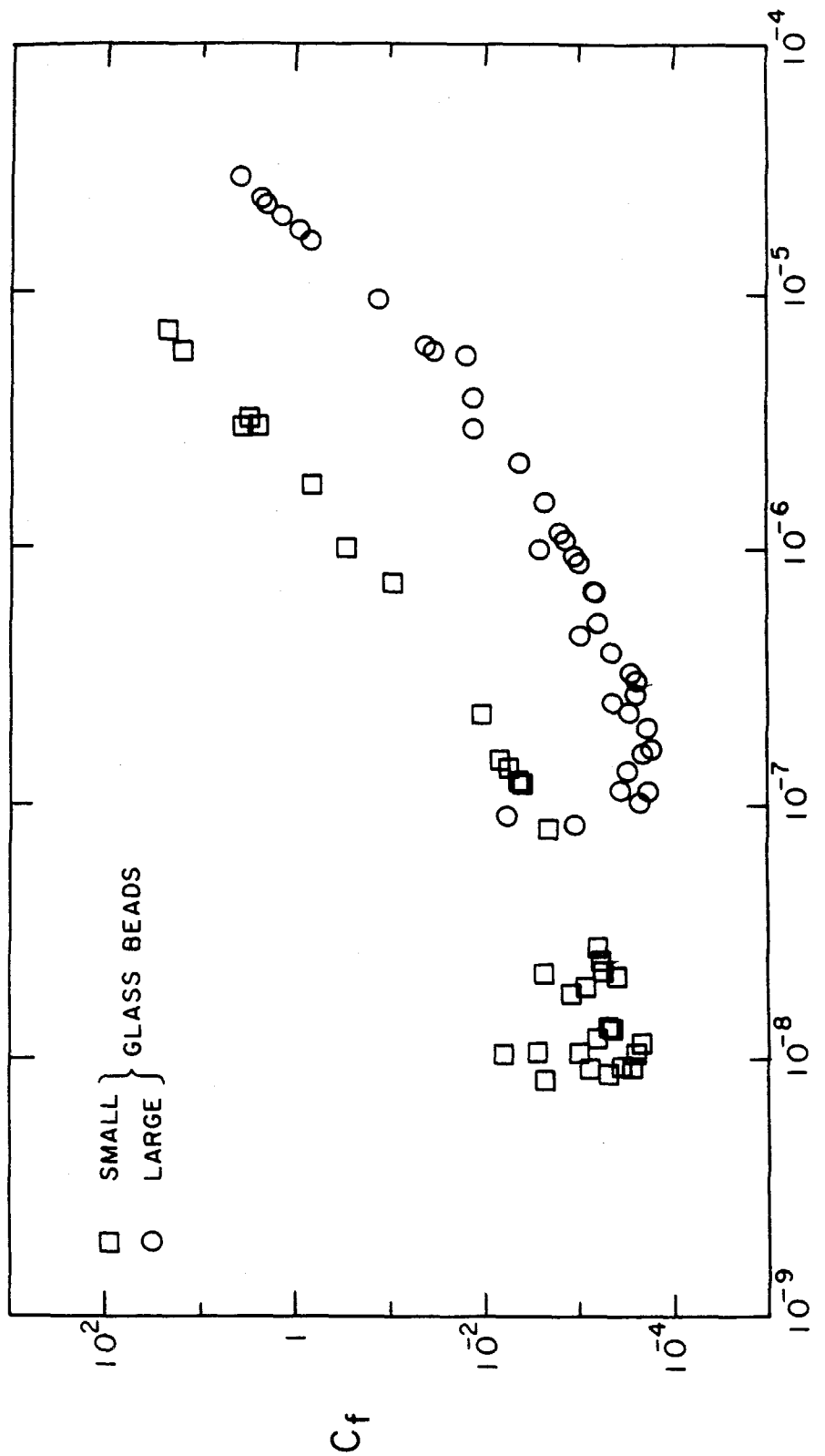

Figure 4.11 The variation of the Stanton Number, St, as a function of friction factor, C_f, for both sizes of glass beads.

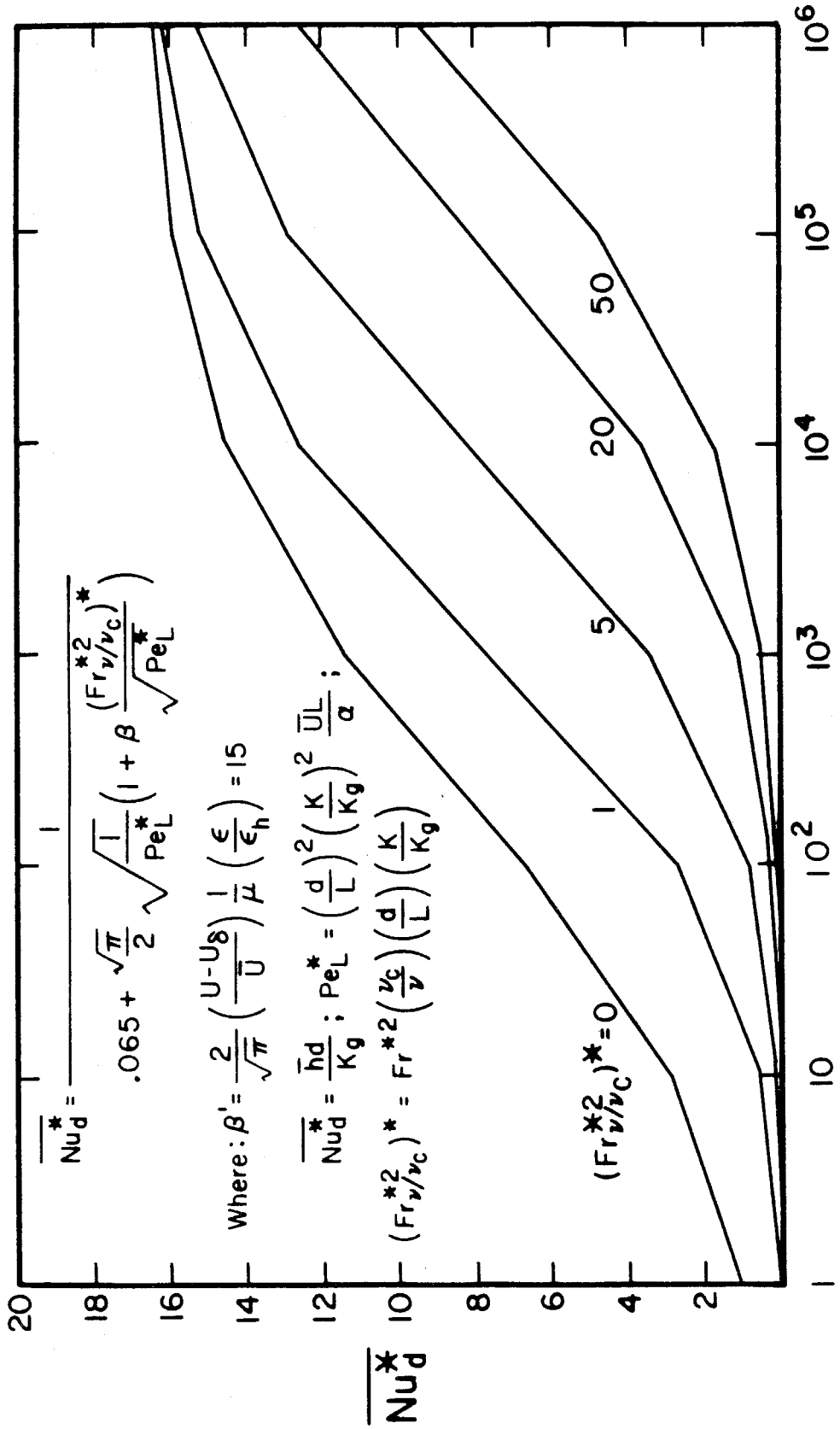

Figure 4.12 Predicted values of the Nusselt Number, $\overline{Nu_d^*}$, as a function of Peclet Number, Pe_L^*, for various Froude Numbers, $(Fr^{*2}_{\nu/\nu_c})^*$ from equation 4.3.

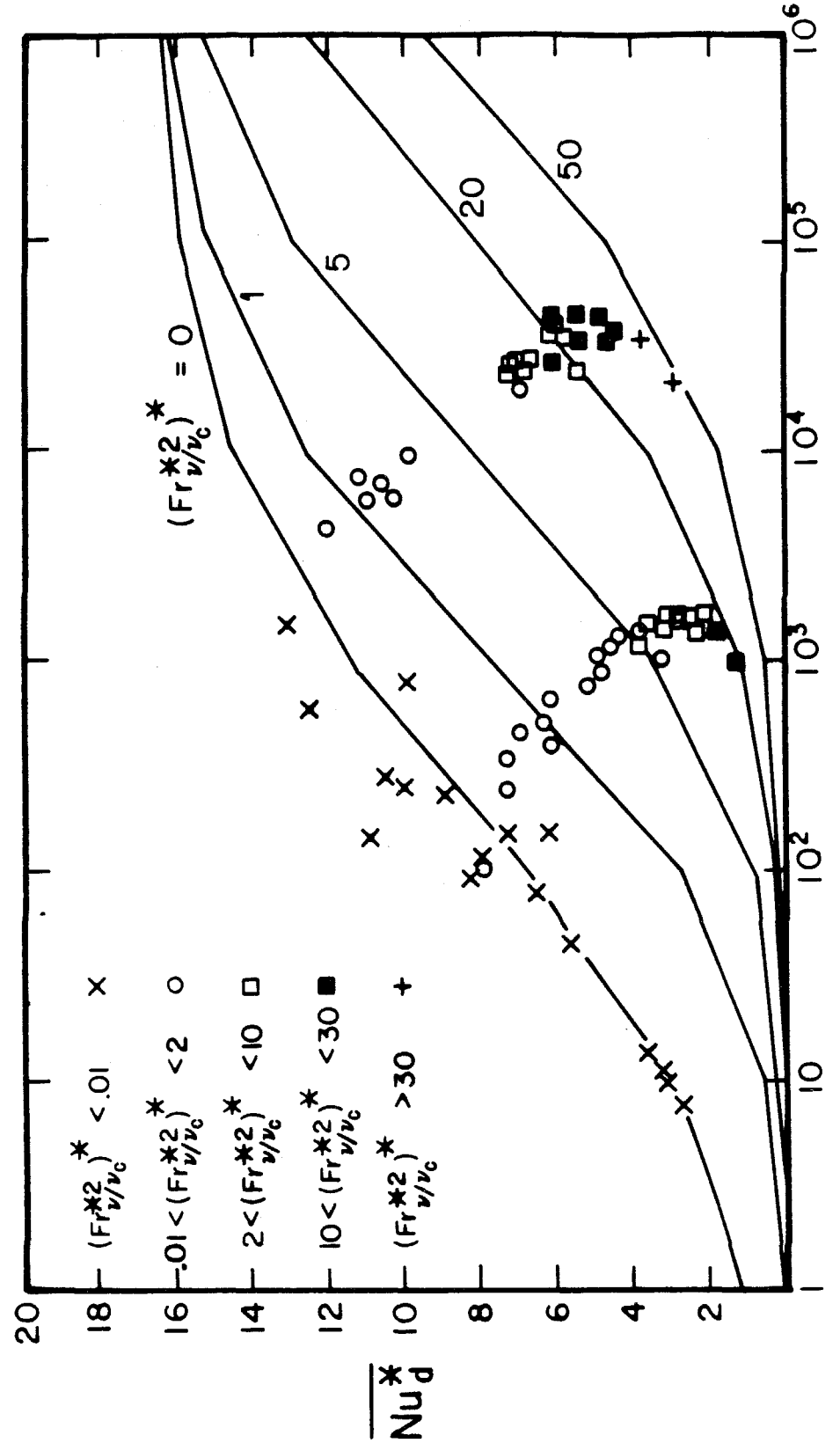

Figure 4.13 Predicted values of the Nusselt Number, $\overline{Nu_d^*}$, as a function of Peclet Number, Pe_L^*, for various Froude Numbers, $(Fr^{*2}_{\nu/\nu_c})^*$ with the experimental values from the present investigation.

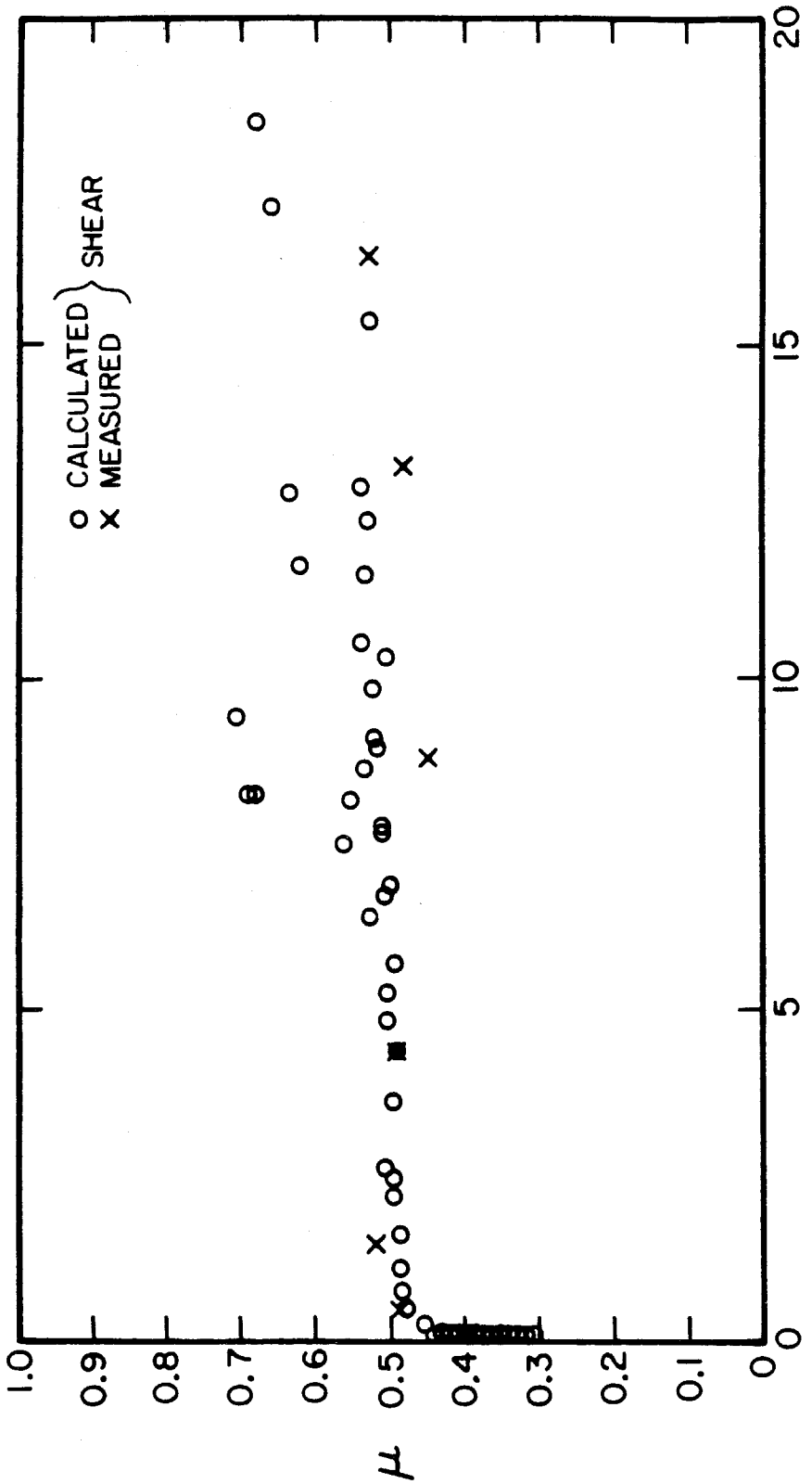

Figure A.1 Comparison of calculated values of the friction coefficient, μ, and the measured friction coefficient as a function of the Froude Number. (All points are polyethylene pellets.)

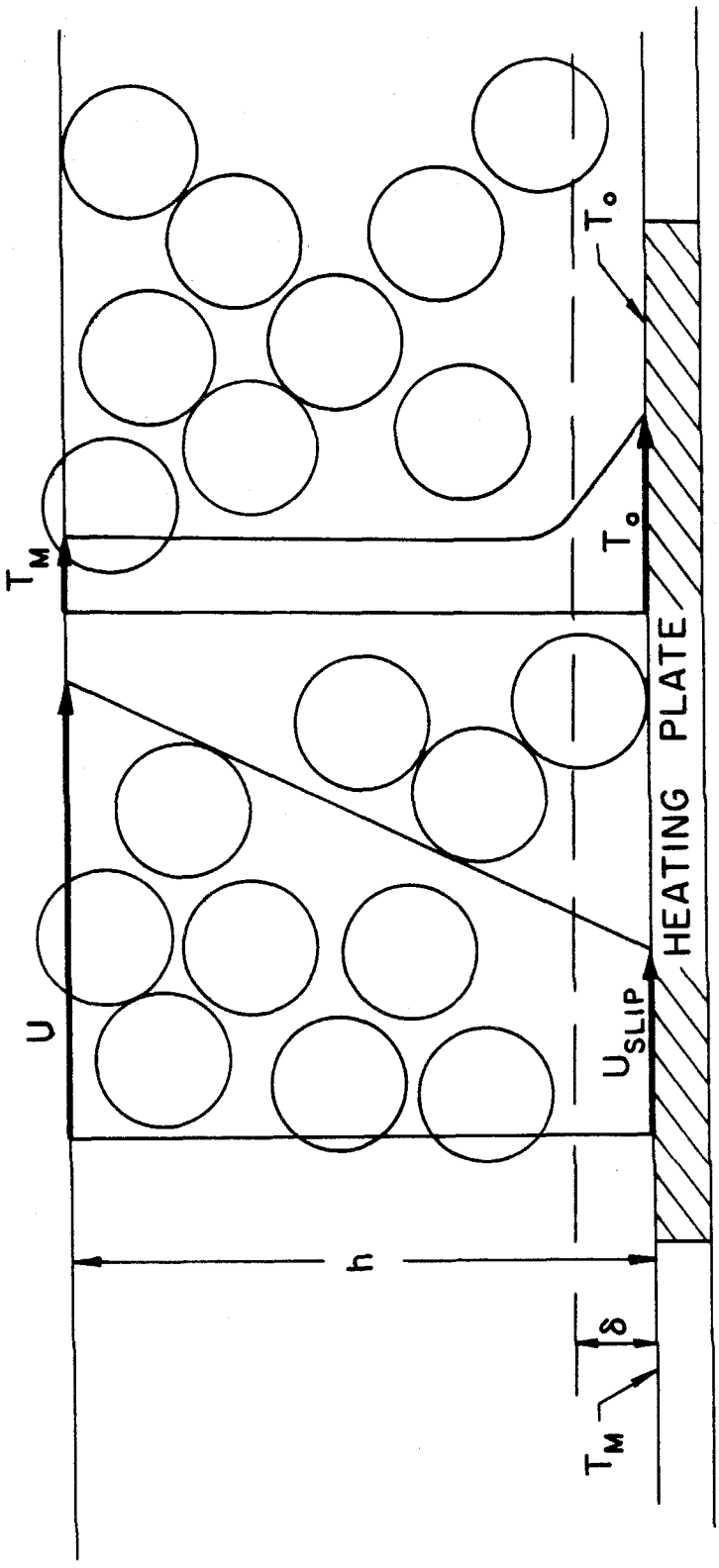

Figure B.1 Schematic of Heat Transfer Process